LA-UR-17-31177
Approved for public release; distribution is unlimited.

Title: A Comparison of Monte Carlo and Deterministic Solvers for keff and Sensitivity Calculations

Author(s): Haeck, Wim
Parsons, Donald Kent
White, Morgan Curtis
Saller, Thomas
Favorite, Jeffrey A.

Intended for: Report

Issued: 2017-12-12

A Comparison of Monte Carlo and Deterministic Solvers for keff and Sensitivity Calculations

W. Haeck, D. K. Parsons, M. C. White, T. G. Saller and J. A. Favorite
Los Alamos National Laboratory, Los Alamos, NM, 87545, USA

December 1, 2017

Contents

Chapter 1

Introduction

Verification and validation of our solutions for calculating the neutron reactivity for nuclear materials is a key issue to address for many applications, including criticality safety, research reactors, power reactors, and nuclear security. Neutronics codes solve variations of the Boltzmann transport equation. The two main variants are Monte Carlo versus deterministic solutions, e.g. the MCNP [1] versus PARTISN [2] codes, respectively. There have been many studies over the decades that examined the accuracy of such solvers and the general conclusion is that when the problems are well-posed, either solver can produce accurate results. However, the devil is always in the details.

The current study examines the issue of self-shielding and the stress it puts on deterministic solvers. Most Monte Carlo neutronics codes use continuous-energy descriptions of the neutron interaction data that are not subject to this effect. The issue of self-shielding occurs because of the discretisation of data used by the deterministic solutions. Multigroup data used in these solvers are the average cross section and scattering parameters over an energy range. Resonances in cross sections can occur that change the likelihood of interaction by one to three orders of magnitude over a small energy range. Self-shielding is the numerical effect that the average cross section in groups with strong resonances can be strongly affected as neutrons within that material are preferentially absorbed or scattered out of the resonance energies. This affects both the average cross section and the scattering matrix.

A prototype of the PARTISN code includes a new implementation of the Bodarenko based method [3] for handling self-shielding [4]. This study compares the results for MCNP, PARTISN using no self-shielding treatment, and PARTISN using the new implementation of the Bondarenko method. For this comparison, MCNP provides the most accurate solution given a set of nuclear data. The MCNP result compared to experiment result represents how well a given suite of evaluated nuclear data performs. Given proper multigroup data, the PARTISN results should converge to the MCNP solution so that a comparison of the PARTISN to the MCNP results will show where the self-shielding treatment is needed and how well it performs. The suite of benchmarks used in this study start with bare high-enriched uranium-235 metal systems and then adds different reflector materials that ramp up the need for self-shielding treatments (starting with beryllium moving through graphite up to uranium and finally iron).

In addition to this study on the impact of self-shielding, this report also provides a comparison between sensitivity profiles calculated using Monte Carlo and deterministic solvers. MCNP has had such a capability for quite some time now but recently the SENSMG tool [5] was developed to provide these quantities by using the PARTISN code as well. SENSMG is a tool for comput-

ing first-order sensitivities of neutron reaction rates and reaction-rate ratios through Generalized Perturbation Theory (GPT).

Chapter 2

Benchmark overview

Five benchmarks from the International Criticality Safety Benchmark Evaluation Project (ICSBEP) handbook have been selected for this work. In what follows we will only refer to these benchmarks using their ICSBEP designation.

2.1 Spherical benchmarks

The selected spherical benchmarks are HEU-MET-FAST-001 (GODIVA, one case), HEU-MET-FAST-032 (four cases), HEU-MET-FAST-041 (six cases) and HEU-MET-FAST-085 (six cases). All benchmarks are HEU spheres; with the exception of HEU-MET-FAST-001, all benchmarks have an external reflector. An overview of the main characteristics of these benchmarks as well as the benchmark effective multiplication value are given in Table 2.1.

As can be seen in Table 2.1, the U235 enrichment is about the same in all cases (being roughly 94 w%). It should be noted that some of the HEU used to construct the cores used in these various benchmarks is actually the same. All experiments (with the exception of GODIVA) were part of the experiments performed at LANL's COMET Universal Assembly Machine. The difference in enrichment between the various benchmarks is mainly due to adjustment of the original experimental results of some of these benchmarks (HEU-MET-FAST-041 and HEU-MET-FAST-085) to a standard HEU concentration of 93.5 w% and HEU density of 18.8 g/cm^3.

The selected benchmarks use a wide variety of reflector materials ranging from light materials (Be, C, Cu) to heavier materials (Fe, W, Th and natural uranium). The benchmarks are essentially fast-spectrum benchmarks, but the presence of a reflector material in significant quantity can have such an impact on the system that a self-shielding treatment becomes necessary to obtain an accurate solution. It is for this reason that the selected benchmarks contain configurations with varying reflector thicknesses for some of the reflector materials (e.g. HEU-MET-FAST-032 for natural uranium, HEU-MET-FAST-041 for beryllium and graphite, and HEU-MET-FAST-085 for copper).

We can observe this when looking at the neutron spectra of some of these benchmark cases given in Figures 2.1 to 2.4. The spectrum for HEU-MET-FAST-001 (the bare GODIVA sphere) is a fast fission neutron spectrum with a negligible epithermal and thermal energy tail. Self-shielding the uranium cross section resonances should (obviously) have little to no effect because very few neutrons will get to the resonance energy range (below 2.25 keV for U235). A similar situation can be expected for

the configurations of HEU-MET-FAST-032 (HEU core with natural uranium reflectors).

The case of HEU-MET-FAST-041 is different. In these cases, the beryllium and graphite reflector in these configuration in spectra that have low energy tails that are more important compared to the previous cases, as a function of the reflector thickness. HEU-MET-FAST-041-002 and HEU-MET-FAST-041-006 are respectively the thickest beryllium and graphite reflectors. For these cases, the presence of the uranium resonances can clearly be observed in the HEU neutron spectrum. For these cases, it will be the self-shielding on uranium that will become important.

The last set of benchmarks (HEU-MET-FAST-085) represents heavy reflector materials which provide little to no moderation, as can be observed in the neutron spectra. Although the neutron spectra are very similar to the ones observed for HEU-MET-FAST-001, self-shielding should still be important in most of the HEU-MET-FAST-085 cases due to the resonances in the reflector materials instead of those of uranium (as was the case for HEU-MET-FAST-041). Copper isotopes have resonances below 100 keV. For iron this is below 900 keV, which is right at the most important part of the spectrum. As a result, a large impact of self-shielding the reflector material cross sections can be expected. The only case where one would expect little influence of self-shielding is HEU-MET-FAST-085-005 with Th232 because the resonances for this nuclide are for much lower energies (similar to uranium).

Table 2.1: Overview of benchmark characteristics.

Benchmark name	HEU core		Reflector		Experimental data	
	U235 [w%]	Radius [cm]	Material	Thickness [cm]	Value	Sigma
HEU-MET-FAST-001-001	93.71	8.7407	None	0	1.00000	0.00100
HEU-MET-FAST-032-001	94	6.32598	natU	9.9822	1.00000	0.00160
HEU-MET-FAST-032-002	94	6.38531	natU	8.9408	1.00000	0.00270
HEU-MET-FAST-032-003	94	6.97659	natU	4.42468	1.00000	0.00170
HEU-MET-FAST-032-004	94	7.75520	natU	1.73482	1.00000	0.00170
HEU-MET-FAST-041-001	93.5	6.73197	Be	4.699	1.00130	0.00300
HEU-MET-FAST-041-002	93.5	5.64241	Be	11.7856	1.00220	0.00430
HEU-MET-FAST-041-003	93.5	7.38298	C	5.08	1.00600	0.00290
HEU-MET-FAST-041-004	93.5	6.91306	C	10.16	1.00600	0.00250
HEU-MET-FAST-041-005	93.5	6.66647	C	15.24	1.00600	0.00310
HEU-MET-FAST-041-006	93.5	6.41839	C	20.32	1.00600	0.00450
HEU-MET-FAST-085-001	93.5	7.150268	Cu	5.0292	0.99980	0.00290
HEU-MET-FAST-085-002	93.5	6.593366	Cu	10.56132	0.99970	0.00310
HEU-MET-FAST-085-003	93.5	7.108868	Fe	10.16	0.99950	0.00460
HEU-MET-FAST-085-004	93.5	7.173361	Ni-Cu-Zn	4.7752	0.99960	0.00290
HEU-MET-FAST-085-005	93.5	7.798674	Th	12.39607	0.99950	0.00240
HEU-MET-FAST-085-006	93.5	6.889272	W	5.08	0.99970	0.00290

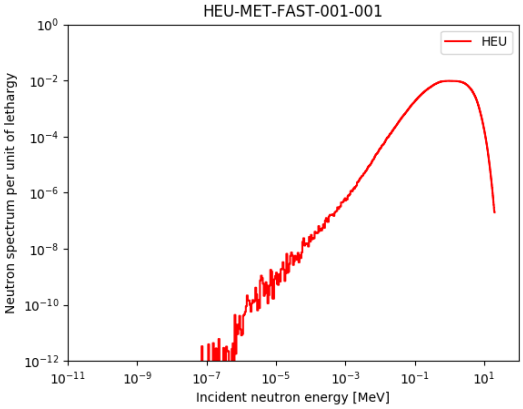

Figure 2.1: The neutron spectrum for HEU-MET-FAST-001.

2.2 Cylindrical benchmarks

The selected cylindrical benchmark is HEU-COMP-INTER-003 (seven cases). All cases in this benchmark are stacked cylindrical UH3 cans surrounded by an axial and radial reflector. An overview of the main characteristics of these cases as well as the benchmark effective multiplication value are given in Table 2.2.

As can be seen in Table 2.1, the U235 enrichment is similar to the enrichment in the spherical benchmarks (being roughly 92 w%). The HEU-COMP-INTER-003 use three different reflector materials (depleted uranium, beryllium and iron). The first four cases are thick reflector cases (with a thickness of about 7.4 cm) while the last three cases are thin reflector cases (with a thickness of about 2.3 to 2.4 cm).

The benchmarks are essentially intermediate spectrum benchmarks with an important lower energy population. The spectra given in figures 2.5 and 2.6 are very similar to some of the spectra observed for HEU-MET-FAST-041, the only difference being that the UH3 and the reflector spectra are now the same (contrary to the HEU core spectra in HEU-MET-FAST-041 which differed from the corresponding relfecotr spectra). As such, it can be expected that a self-shielding treatment will be required for these cases to obtain an accurate solution.

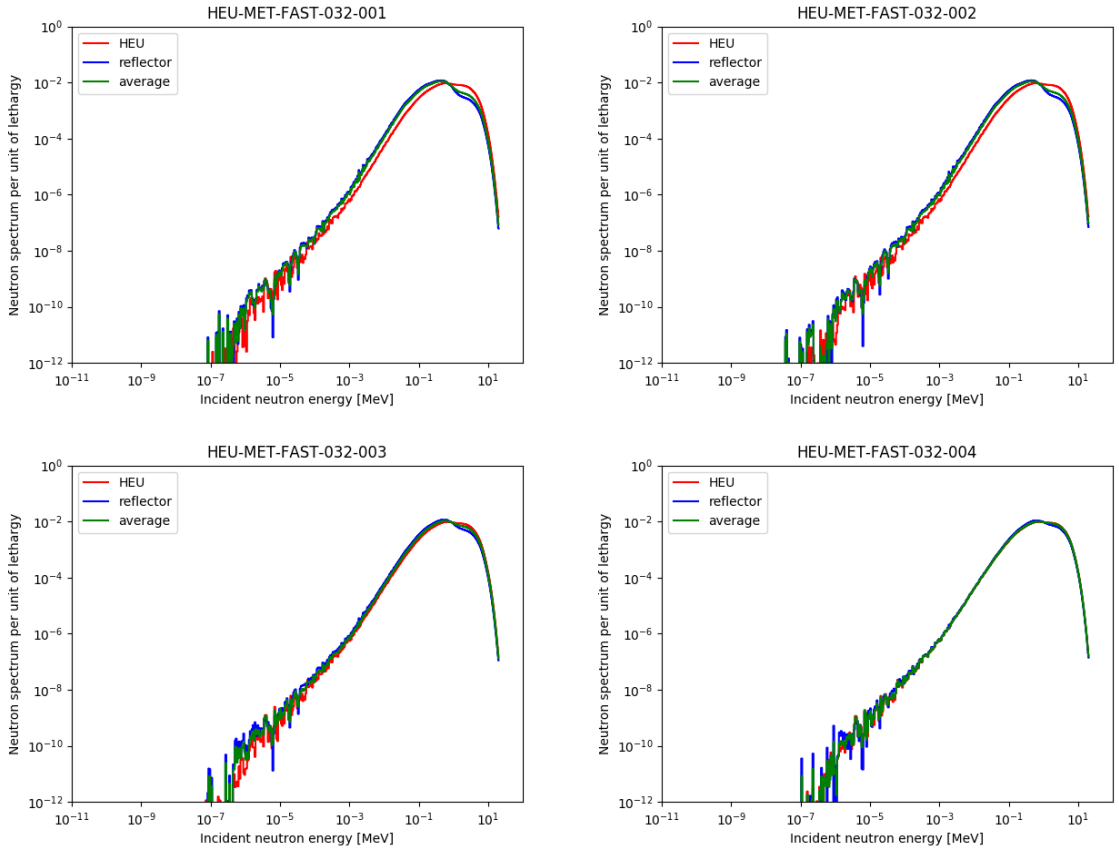

Figure 2.2: The neutron spectra for the HEU-MET-FAST-032 cases.

Table 2.2: Overview of benchmark characteristics.

Benchmark name	HEU core		Reflector		Experimental data	
	U235 [w%]	Radius [cm]	Material	Thickness [cm]	Value	Sigma
HEU-COMP-INTER-003-001	92	7.5050	depU	7.4396	1.00000	0.00570
HEU-COMP-INTER-003-002	92	7.5050	Be, depU	7.4396	1.00000	0.00610
HEU-COMP-INTER-003-003	92	7.5050	Be, depU	7.4396	1.00000	0.00560
HEU-COMP-INTER-003-004	92	7.5050	Fe, depU	7.4396	1.00000	0.00550
HEU-COMP-INTER-003-005	92	7.5050	Be	2.3419	1.00000	0.00470
HEU-COMP-INTER-003-006	92	7.5050	depU	2.3597	1.00000	0.00470
HEU-COMP-INTER-003-007	92	7.5050	depU	2.3597	1.00000	0.00500

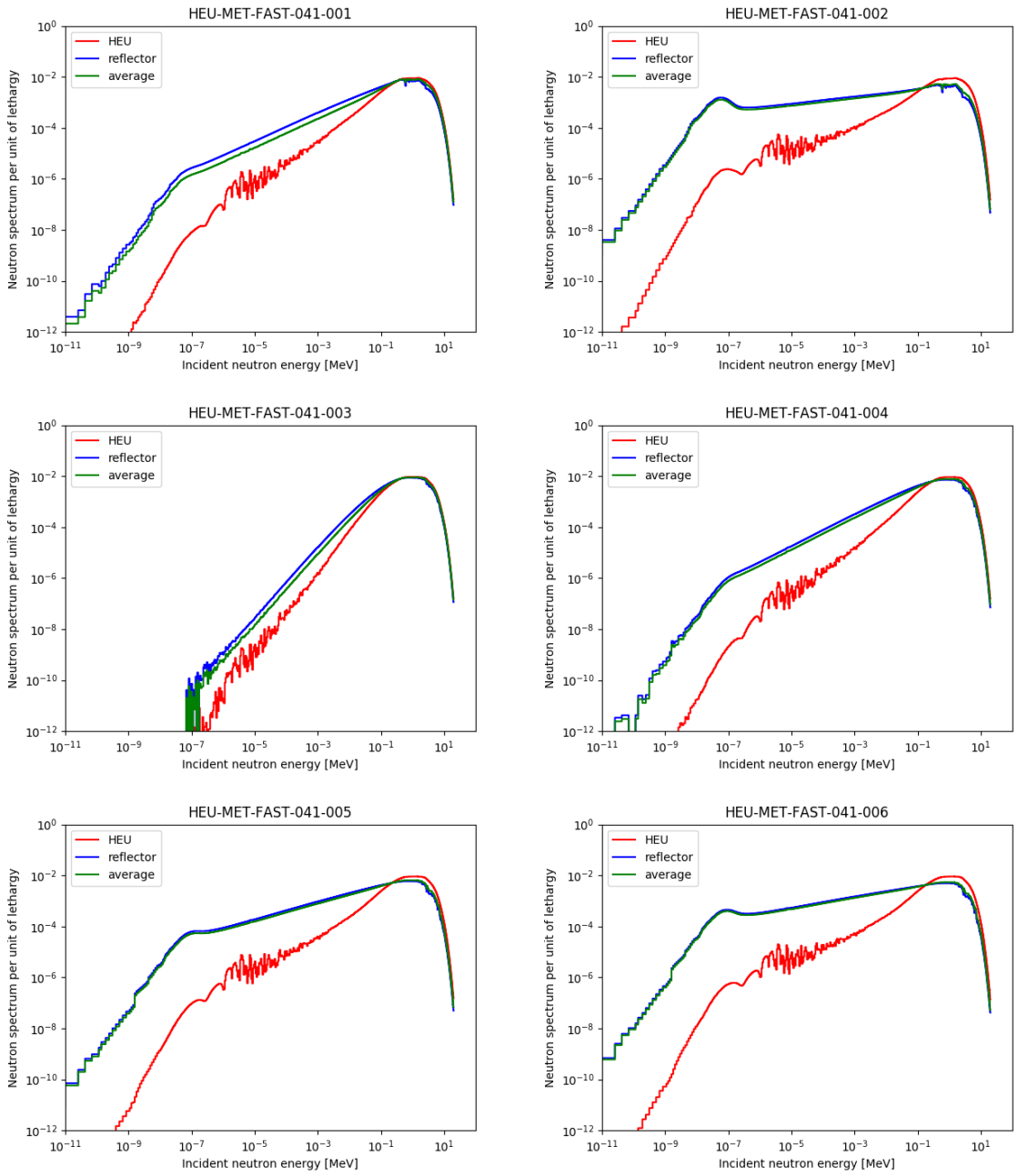

Figure 2.3: The neutron spectra for the HEU-MET-FAST-041 cases.

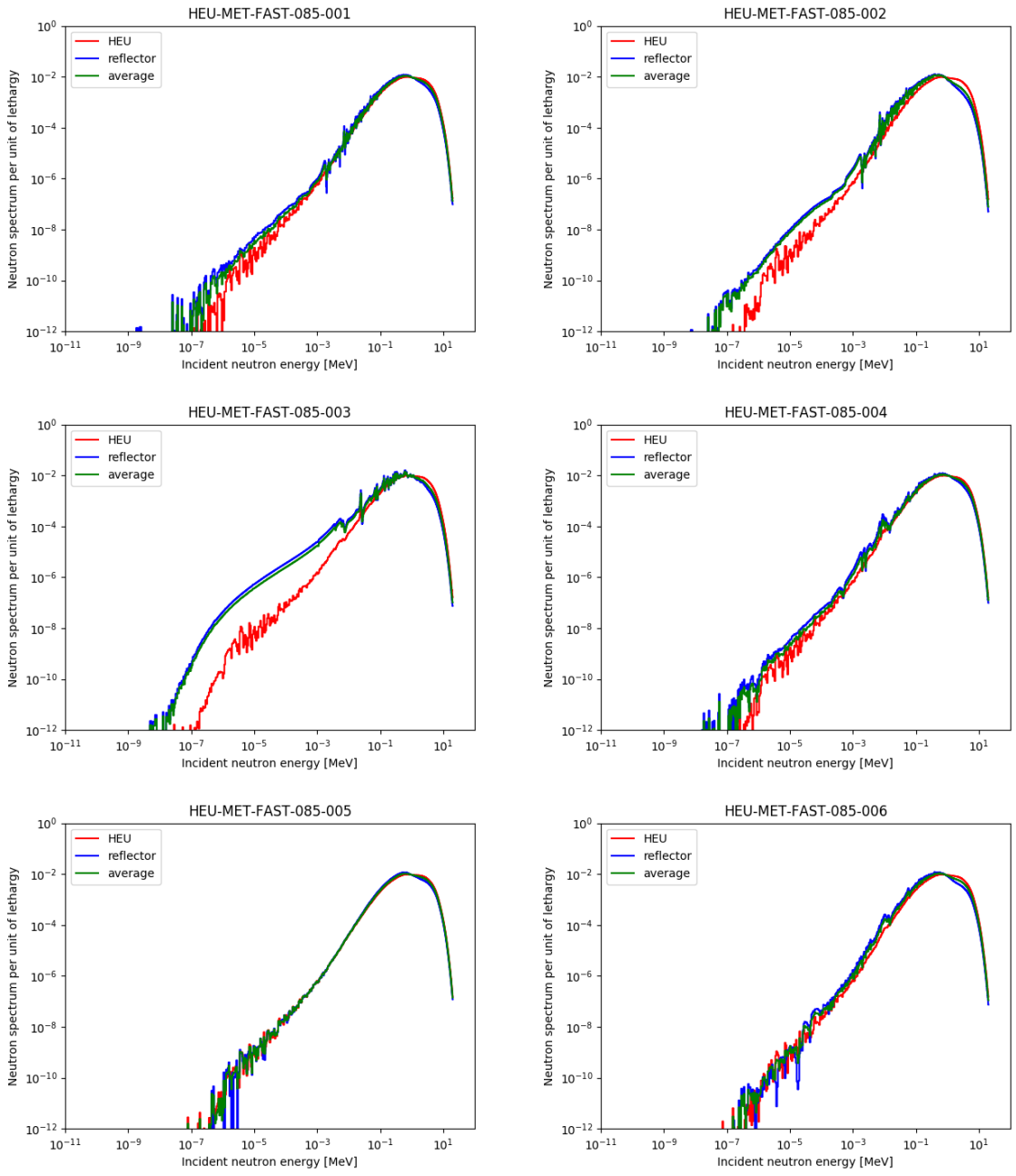

Figure 2.4: The neutron spectra for the HEU-MET-FAST-085 cases.

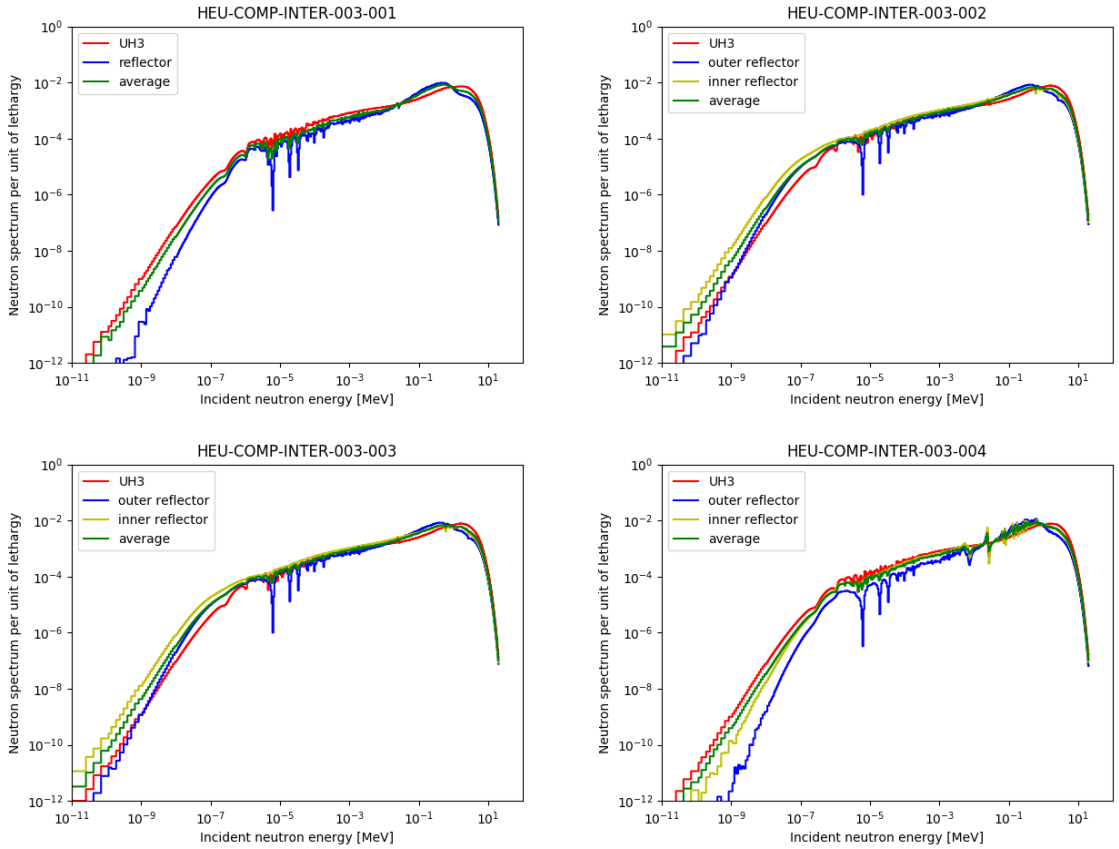

Figure 2.5: The neutron spectra for the thick reflector HEU-COMP-INTER-003 cases.

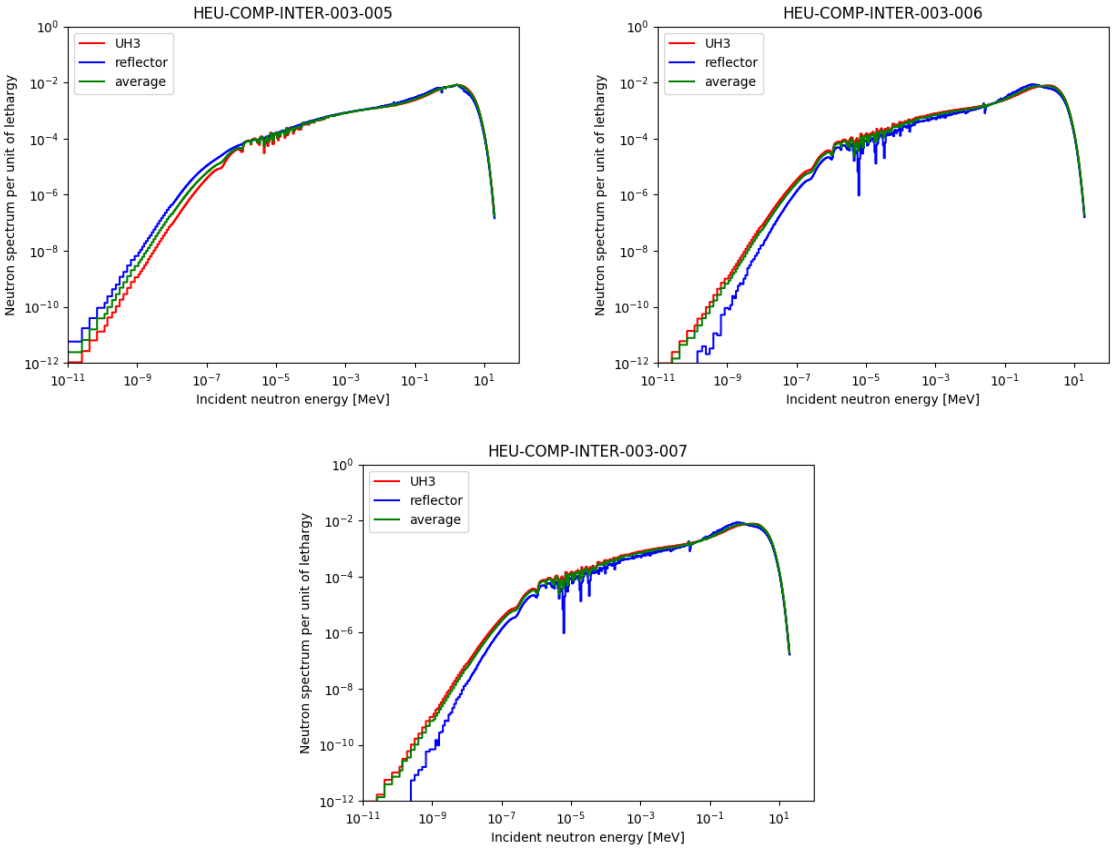

Figure 2.6: The neutron spectra for the thin reflector HEU-COMP-INTER-003 cases.

Chapter 3

Calculation overview

All Monte Carlo calculations were performed using MCNP 6.2 with the official continuous energy ENDF/B-VII.1 nuclear data library at 293.6 K (ZAID extension 80c). The number of particles per cycle for each case was set to 100000 for a total of 25 inactive and 50000 active kcode cycles. As a result, all effective multiplication factor values are reported within a statistical precision of 1 pcm (one sigma) which is 10 times more than the standard precision normally used for benchmarking purposes. This was done to reduce the statistical noise in the calculated spectra and sensitivity profiles.

All PARTISN calculations were performed using PARTISN 8.27.14 using the official 618 group ENDF/B-VII.1 nuclear data library (mt71x) without self-shielding. The SN order used in all calculations was 64 and scattering used a P3 expansion. The convergence criterion was set to 1e-5.

All SENSMG calculations also used PARTISN 8.27.14 with the same library and calculation parameters, with the exception of the convergence criterion (1e-6 was used) and the number of inner and outer iterations (the SENSMG defaults are larger than the PARTISN defaults). In all calculations except for HEU-MET-FAST-001-001, source acceleration was switched off due to convergence issues. As a calculation check, the effective multiplication factor results reported by SENSMG were compared to the individual PARTISN calculations. All values are in agreement.

No SENSMG and only some PARTISN input decks were available at the beginning of this work. For the available PARTISN input decks, inconsistencies were found between these input decks and the reference MCNP input decks. As a result, new PARTISN and SENSMG input decks were constructed using the reference benchmark input decks for MCNP as a basis to insure consistency between the various codes.

Chapter 4

Results: effective multiplication factors

The results for the effective multiplication factor for the MCNP and PARTISN calculations are given in Table 4.1. A graphical representation of these results is given in Figure 4.1. The grey points and the error bars are the experimental effective multiplication values for each benchmark case. The error bars on this graph represent the 99% confidence range (three sigma). The red points represent the result obtained with MCNP. No error bars are shown for these results as they would not be visible (all results were calculated within at least 10 pcm one sigma). The blue and green curve show the PARTISN results with and without self-shielded cross sections.

The results obtained with MCNP are nicely within 3 sigma from the experimental values. The unself-shielded PARTISN results follow the MCNP results quite well with the exception of some of the heavy reflector materials in HEU-MET-FAST-085, being copper (cases 1 and 2), iron (case 3) and Ni-Cu-Zn (case 4), and most of the HEU-COMP-INTER-003 cases.

As indicated earlier, we see the impact of the self-shielding treatment where one would expect them when looking at the neutron spectra. HEU-MET-FAST-001 and HEU-MET-FAST-032 (which contain only uranium) do not change considerably (when applying self-shielding, the multiplication factor drops by about 10 to 20 pcm). Even though the PARTISN results without self-shielding are already well in line with MCNP, the inclusion of self-shielding tends to slightly improve the agreement.

For the light reflector material cases of HEU-MET-FAST-041, the effect for the beryllium cases depends strongly upon the reflector thickness. Between both beryllium cases, there is about one to two orders of magnitude difference in the neutron population in the uranium resonance range (as can be seen in Figure 2.3). As a result, the self-shielding of uranium has a significantly larger impact in the case of HEU-MET-FAST-041-002 compared to HEU-MET-FAST-041-001. It is exactly for this reason that the result for PARTISN without self-shielding for HEU-MET-FAST-041-001 is already so close to the MCNP result. For the carbon reflector cases, the impact is less visible as with beryllium (mainly because the beryllium cases are more thermalised than the carbon cases).

The most important impact of the self-shielding treatment can be observed for HEU-MET-FAST-085 and HEU-COMP-INTER-003. When applying Bondarenko self-shielded cross sections to the PARTISN calculations, we observe a significant improvement in the problematic cases for HEU-MET-FAST-085 (the copper, iron and Ni-Cu-Zn cases). While not obtaining a perfect agreement with MCNP, the effective multiplication values for these cases are now within 3 sigma of the experimental value. The other two cases of HEU-MET-FAST-085 are Th232 for which we see no effect (as expected) and tungsten for which the self-shielding correction now gives us a result that is perfectly in line

with MCNP.

The more thermalised spectra of the HEU-COMP-INTER-003 cases lead to significant differences with the MCNP values when no self-shielding is used in PARTISN, as expected. The only exception here would be HEU-COMP-INTER-003-004 which has the internal iron reflector. When applying self-shielding, the PARTISN values line up quite well with the MCNP values, again as expected. Only for the previously mentioned HEU-COMP-INTER-003-004 case does the difference with MCNP become larger.

Table 4.1: Effective multiplication factor results for the selected benchmarks.

Benchmark name	Experimental data		MCNP6.2		PARTISN 8.27.08	Bondarenko self-shielding
	Value	Sigma	Value	Sigma	Value	Value
HEU-MET-FAST-001-001	1.00000	0.00100	0.99985	0.00001	1.00011	1.00001
HEU-MET-FAST-032-001	1.00000	0.00160	1.00414	0.00001	1.00508	1.00481
HEU-MET-FAST-032-002	1.00000	0.00270	1.00468	0.00001	1.00570	1.00540
HEU-MET-FAST-032-003	1.00000	0.00170	1.00010	0.00001	1.00109	1.00081
HEU-MET-FAST-032-004	1.00000	0.00170	1.00089	0.00001	1.00148	1.00134
HEU-MET-FAST-041-001	1.00130	0.00300	1.00691	0.00001	1.00711	1.00672
HEU-MET-FAST-041-002	1.00220	0.00430	1.00514	0.00001	1.00405	1.00529
HEU-MET-FAST-041-003	1.00600	0.00290	1.00240	0.00001	1.00296	1.00215
HEU-MET-FAST-041-004	1.00600	0.00250	1.00720	0.00001	1.00793	1.00689
HEU-MET-FAST-041-005	1.00600	0.00310	1.00287	0.00001	1.00336	1.00257
HEU-MET-FAST-041-006	1.00600	0.00450	1.00427	0.00001	1.00442	1.00399
HEU-MET-FAST-085-001	0.99980	0.00290	1.00011	0.00001	1.00522	1.00022
HEU-MET-FAST-085-002	0.99970	0.00310	1.00433	0.00001	1.01305	1.00673
HEU-MET-FAST-085-003	0.99950	0.00460	0.99612	0.00001	1.01588	0.99190
HEU-MET-FAST-085-004	0.99960	0.00290	0.99984	0.00001	1.00324	0.99965
HEU-MET-FAST-085-005	0.99950	0.00240	1.00042	0.00001	1.00083	1.00025
HEU-MET-FAST-085-006	0.99970	0.00290	1.00600	0.00001	1.00695	1.00596
HEU-COMP-INTER-003-001	1.00000	0.00570	1.00605	0.00001	0.99939	1.00727
HEU-COMP-INTER-003-002	1.00000	0.00610	1.00564	0.00001	0.99804	1.00590
HEU-COMP-INTER-003-003	1.00000	0.00560	1.00522	0.00001	0.99763	1.00542
HEU-COMP-INTER-003-004	1.00000	0.00550	1.00362	0.00001	1.00248	1.00060
HEU-COMP-INTER-003-005	1.00000	0.00470	0.99804	0.00001	0.99046	0.99652
HEU-COMP-INTER-003-006	1.00000	0.00470	0.99642	0.00001	0.99198	0.99564
HEU-COMP-INTER-003-007	1.00000	0.00500	0.99604	0.00001	0.99171	0.99518

Figure 4.2 gives the effective multiplication factor as a function of the reflector thickness for four materials (beryllium, carbon, copper and uranium). These four materials are the only reflector materials to appear more than once in our selected benchmarks. For the beryllium results in this graph, the double reflector cases using depleted uranium and beryllium from HEU-COMP-INTER-003 were omitted. For the uranium results in this graph, depleted uranium and natural uranium

results were combined while dual reflector cases from HEU-COMP-INTER-003 were omitted. Due to the low number of available results, it is difficult to draw conclusions or determine trends in the graphs. The only case in which we can suspect a trend is the case for uranium in which we can observe what looks like an upward trend as a function of reflector thickness.

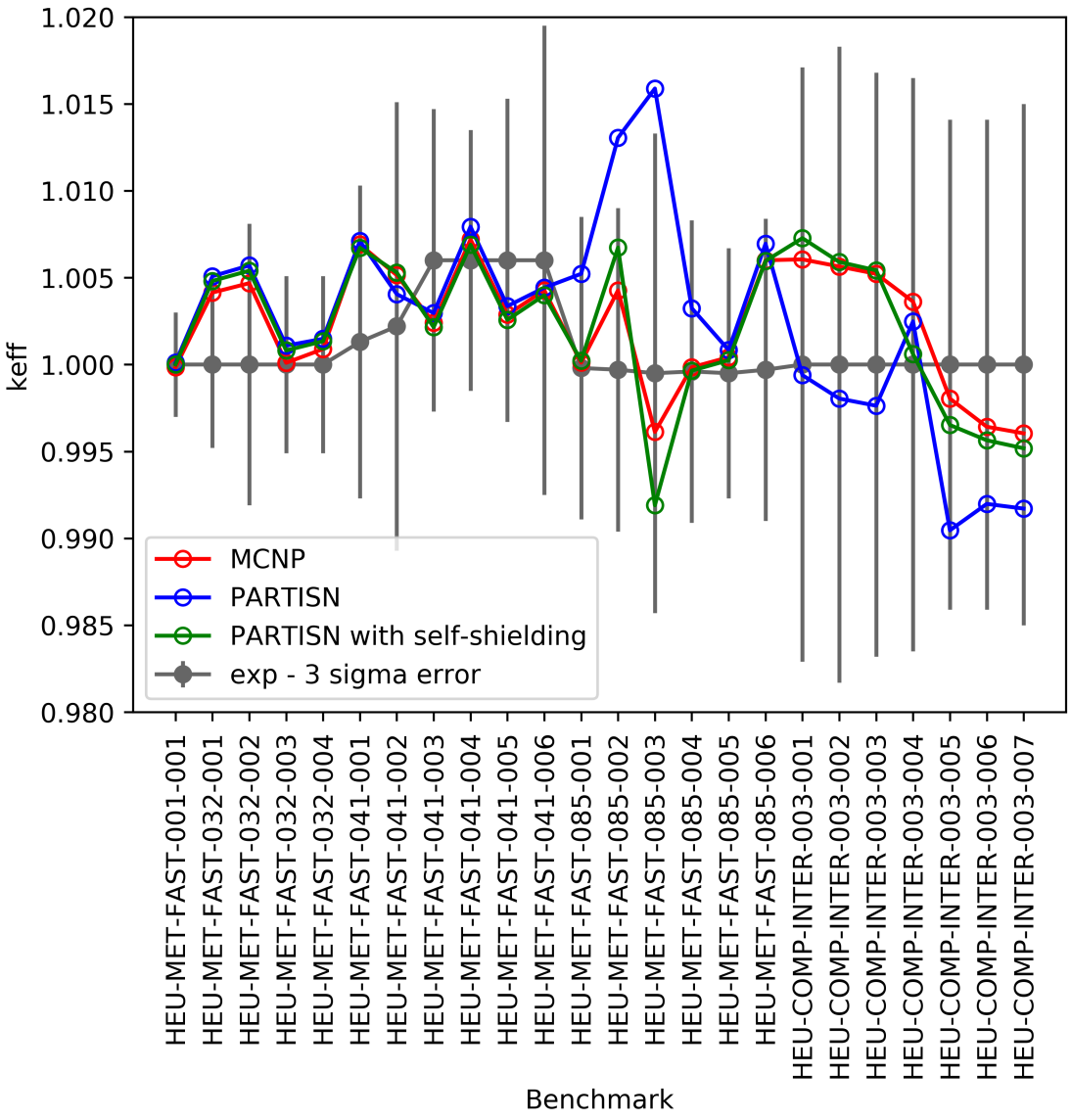

Figure 4.1: Effective multiplication factor results.

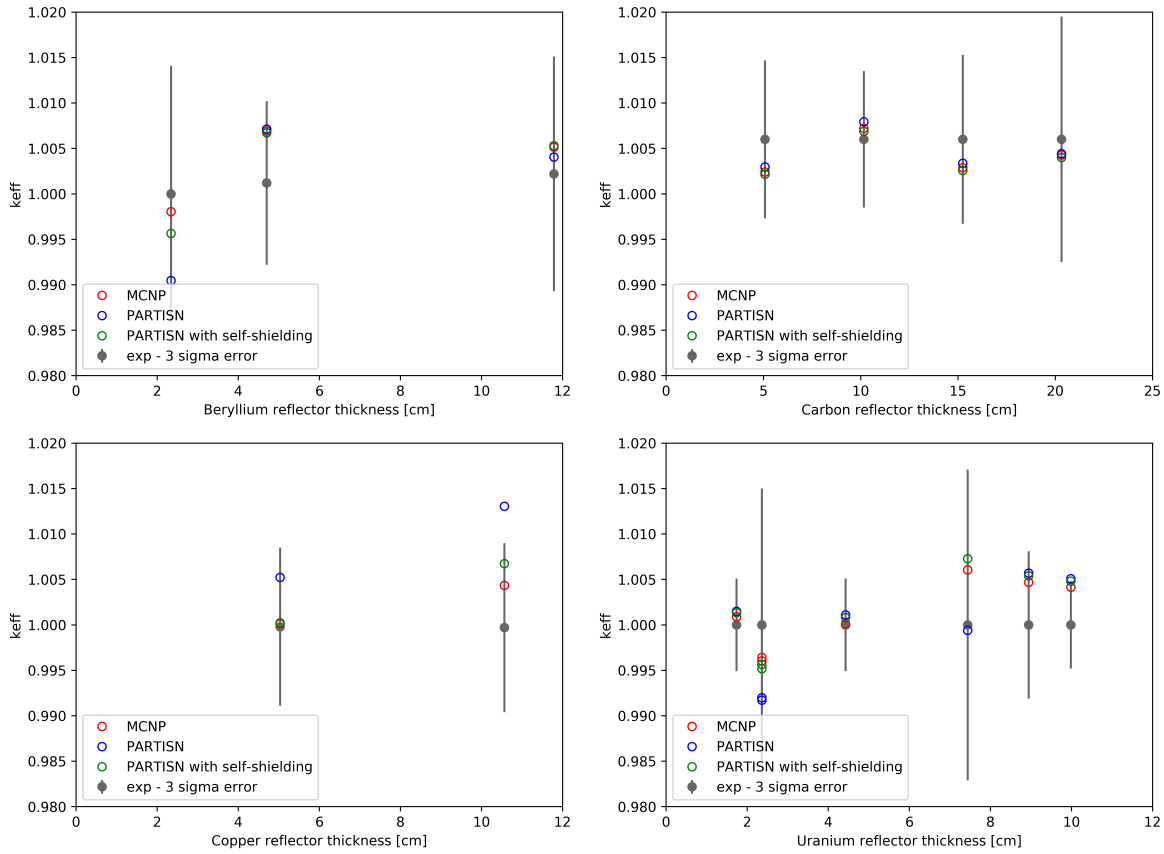

Figure 4.2: Effective multiplication factor results as function of reflector thickness for beryllium (top left), carbon (top right), copper (bottom left) and uranium (both depleted and natural, bottom right).

Chapter 5

Results: sensitivity profiles

The MCNP sensitivity profiles and the ones calculated using SENSMG are given in the following sections for the reactions that can be easily compared: capture, fission, nubar and the fission neutron spectrum. Only non zero sensitivity profiles are given. The red curves are for MCNP and the blue curves for SENSMG.

As expected, knowing that the selected benchmarks are all high enriched U235 benchmarks, the most important contributors for the sensitivity are (in order): U235 total nu, the U235 fission cross section and the U235 fission spectrum. We can also observe that the sensitivity profiles obtained through SENSMG correspond very well with the ones obtained with MCNP. The sensitivity profiles for the fission spectra calculated by MCNP appear to exhibit some noise, but the agreement with the SENSMG calculated profile is excellent. It should be noted that to obtain this level of agreement, MCNP calculations with 100 times more particles than are normally used for benchmark purposes were required.

It is interesting to note that even though the spherical benchmarks selected for this study were only fast-spectrum benchmarks, some sensitivity profiles show a non zero sensitivity in the thermal energy range. Good examples of this are the beryllium capture and U235 capture and total fission nu profiles in the beryllium reflected cases of HEU-MET-FAST-041. As could be seen in the Figures given in chapter 2, the spectra show the presence of a significant amount of thermalised neutrons, which is also visible in the sensitivity profiles.

The profiles differ significantly with reflector thickness. This is particularly true for beryllium capture. For the thick reflector, we observe a sensitivity to beryllium capture about three orders of magnitude larger than for the thin reflector, and only for neutron energies below 1 eV. The actual sensitivity is still quite low compared to the U235 sensitivities but even those exhibit a non zero sensitivity for the lower energy ranges. For the thick beryllium reflector case of HEU-MET-FAST-041-002, the sensitivity for the U235 total fission nu in the thermal energy range is about one tenth of what we observe at 1 MeV. For the thin reflector in HEU-MET-FAST-041-001, it is zero.

Another qualitative remark that can be made with respect to the profiles is that there appear to be some small differences for the profiles calculated by MCNP and SENSMG below 10 keV. For HEU-MET-FAST-041-001, this could be attributed to remaining statistical noise in the MCNP calculated profiles but this is definitely not the case for HEU-MET-FAST-041-002. The influence of the self-shielding correction in the cross sections for these two cases was only visible for HEU-MET-FAST-041-002. Knowing that the SENSMG calculations were performed using PARTISN without the self-

shielding treatment, the differences we observe in the HEU-MET-FAST-041-002 profiles at lower energies might be related to this fact.

This suspicion is confirmed when we look at the sensitivity profiles for the iron reflected HEU sphere from HEU-MET-FAST-085-003. While the profiles still agree very well, there does appear to be a small but noticeable difference between the SENSMG and MCNP results in the fast energy region. Cross section self-shielding appears to have a significantly smaller impact on the sensitivity profiles compared to the effective multiplication factor, but if the self shielded cross sections could also be used for the calculation of the sensitivity profiles in SENSMG, then we would probably obtain better agreement.

Due to the more thermalised nature of the spectra for HEU-COMP-INTER-003, the sensitivities at lower energies for these cases are a lot more pronounced than in the fast spherical benchmark cases. In some cases such as the U235 fission cross section or the total nu, the sensitivity profiles show two energy regions with significant sensitivity: between 100 keV and 10 MeV (which we also saw for the fast spherical benchmarks) but also between 1 eV and 1 keV. And in the case of U235 total nu, it is this last region that is the most important from a sensitivity point of view.

With HEU-COMP-INTER-003, there is the U236 fission spectrum for which MCNP and SENSMG do not seem to agree at all, which is strange seeing that both codes actually agree on the fission spectrum sensitivities for the other uranium isotopes. Futher investigation will be required to explain this difference (this might potentially indicate a difference in data between the continuous energy and multi-group libraries).

During the course of this benchmark study, SENSMG was corrected due to differences observed in initial fission spectrum sensitivity profiles. To obtain agreement, we needed to run PARTISN in SENSMG with the fissdata option set to 2 (the default and recommended value being 0, the fission matrix). When setting fissdata to 0, the fission spectrum profiles calculated by SENSMG no longer corresponded with MCNP, as can be seen in Figure 5.1. This problem has been corrected since then and the fission spectrum sensitivities with the fissdata option set to 0 now agree very well (with the exception of the above mentioned U236).

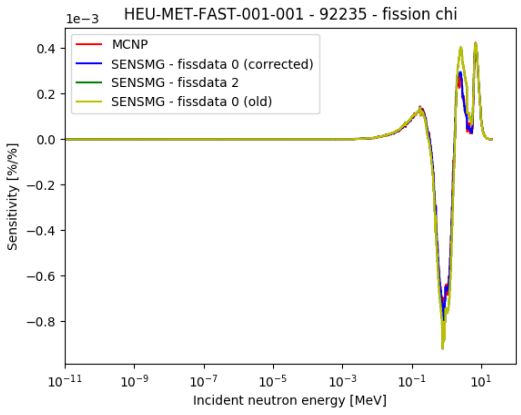

Figure 5.1: Sensitivity profiles for the U235 fission spectrum in HEU-MET-FAST-001-001 using the PARTISN fissdata 0 (default option) and fissdata 2.

5.1 HEU-MET-FAST-001-001

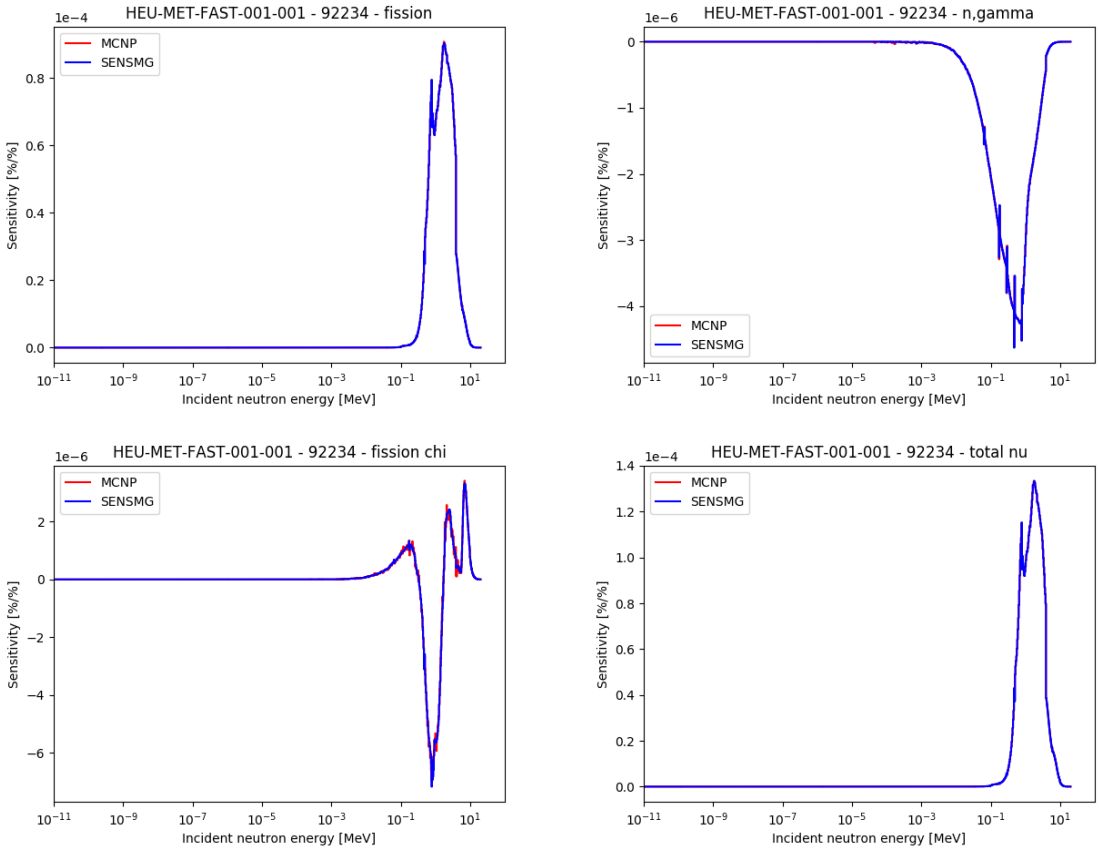

Figure 5.2: Sensitivity profiles for U234 in HEU-MET-FAST-001-001.

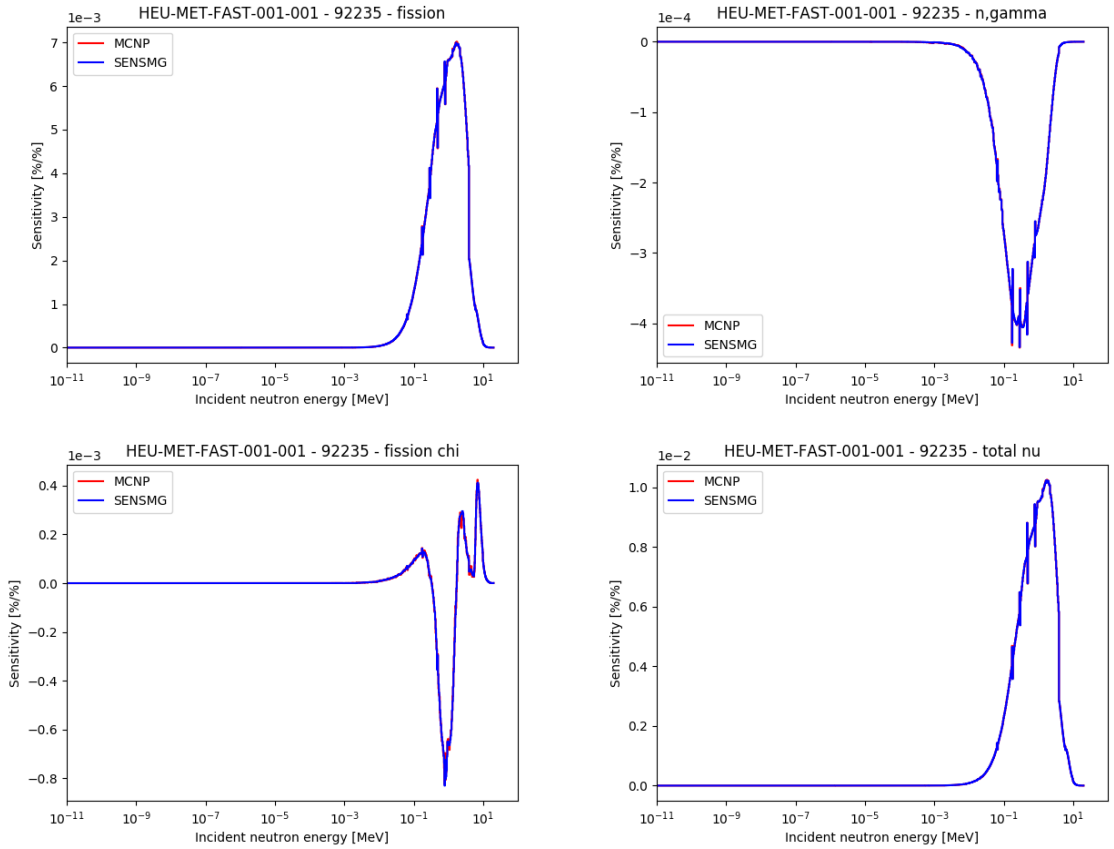

Figure 5.3: Sensitivity profiles for U235 in HEU-MET-FAST-001-001.

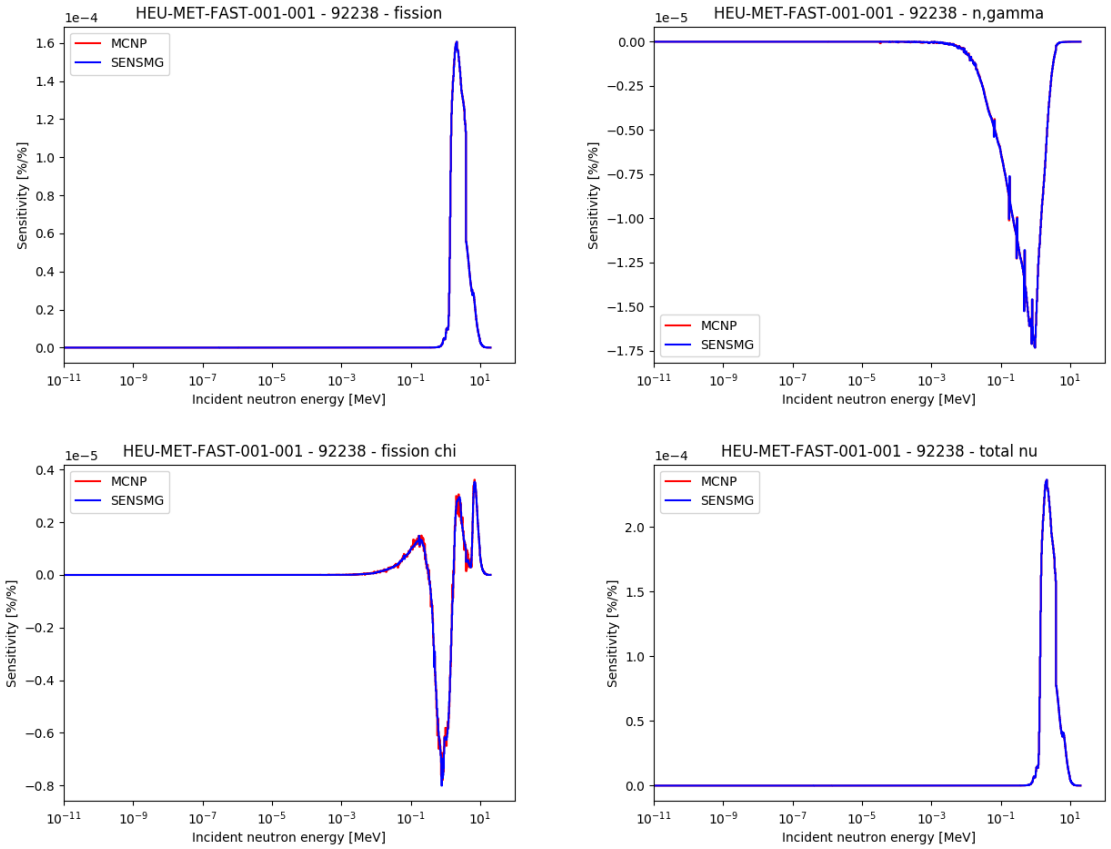

Figure 5.4: Sensitivity profiles for U238 in HEU-MET-FAST-001-001.

5.2 HEU-MET-FAST-032-001

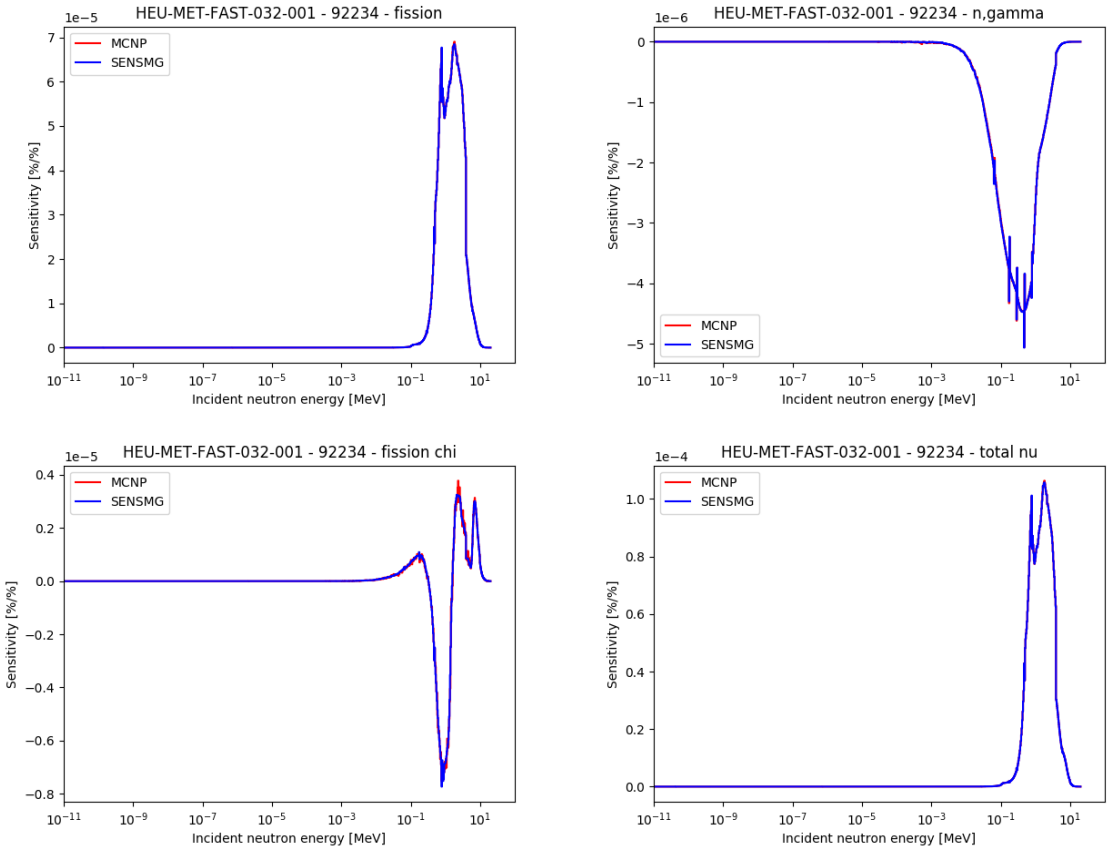

Figure 5.5: Sensitivity profiles for U234 in HEU-MET-FAST-032-001.

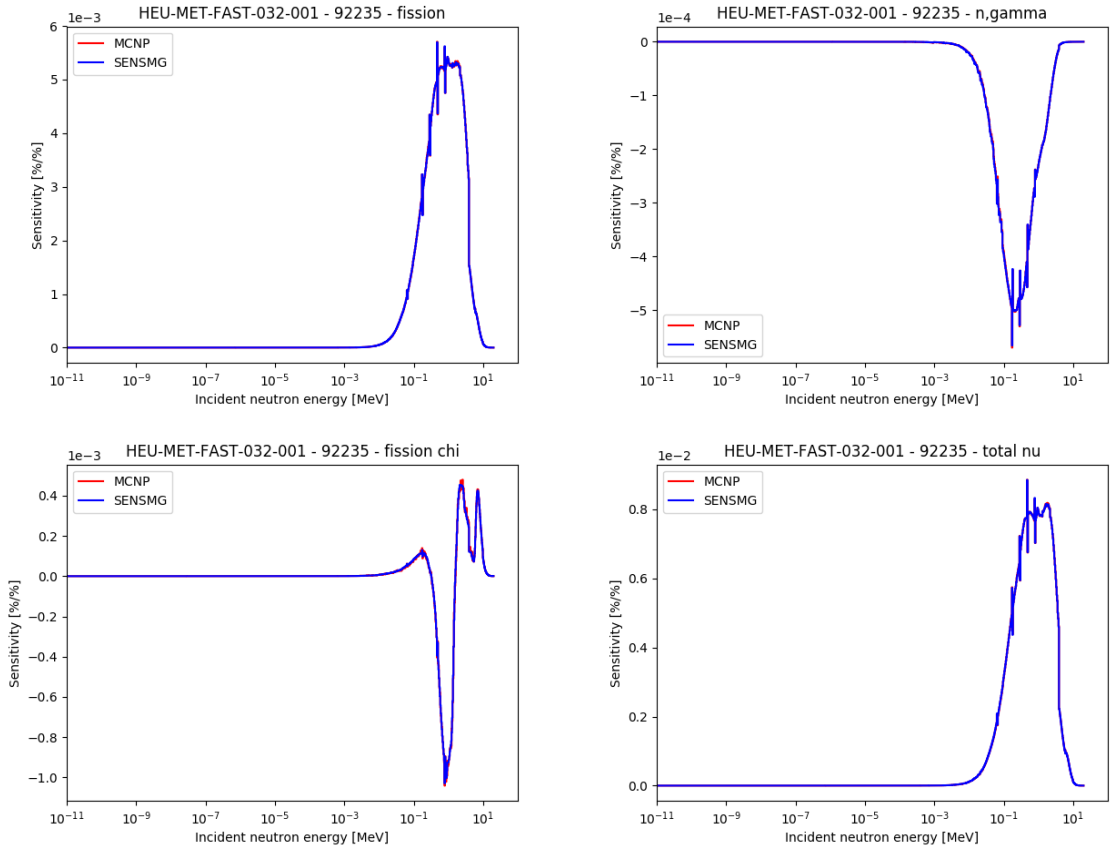

Figure 5.6: Sensitivity profiles for U235 in HEU-MET-FAST-032-001.

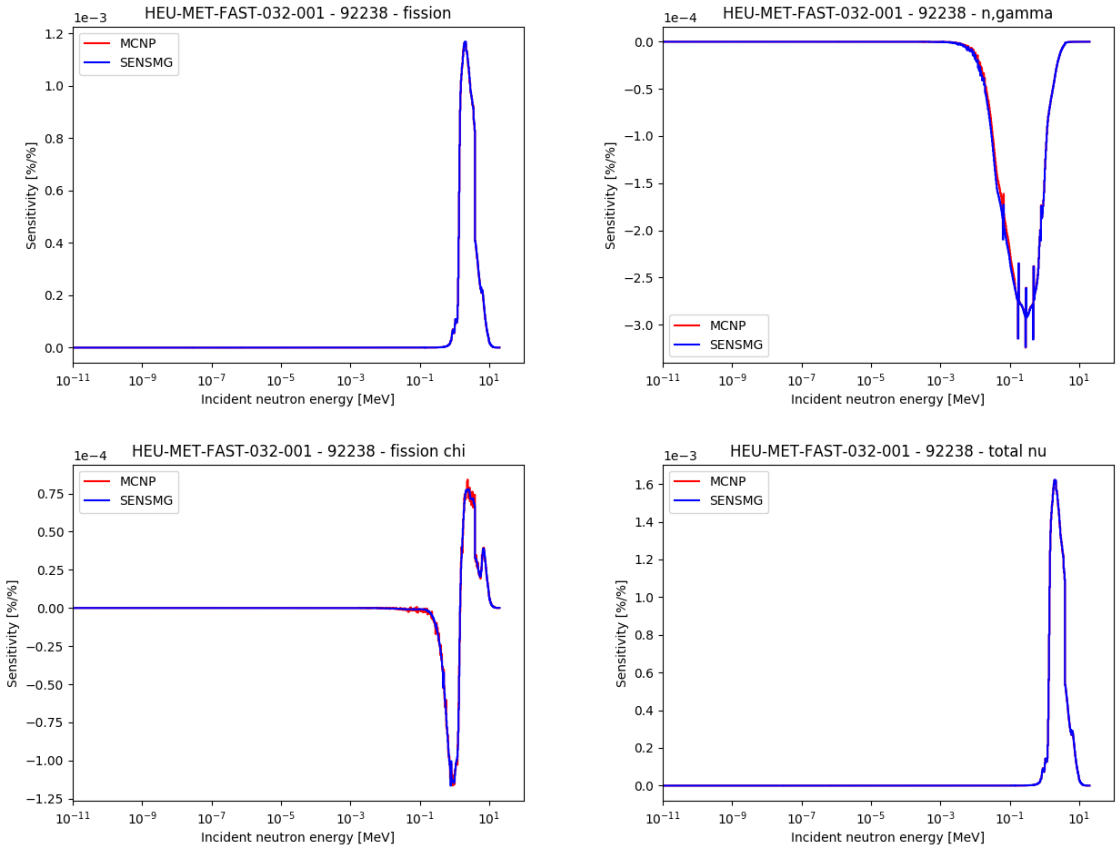

Figure 5.7: Sensitivity profiles for U238 in HEU-MET-FAST-032-001.

5.3 HEU-MET-FAST-032-002

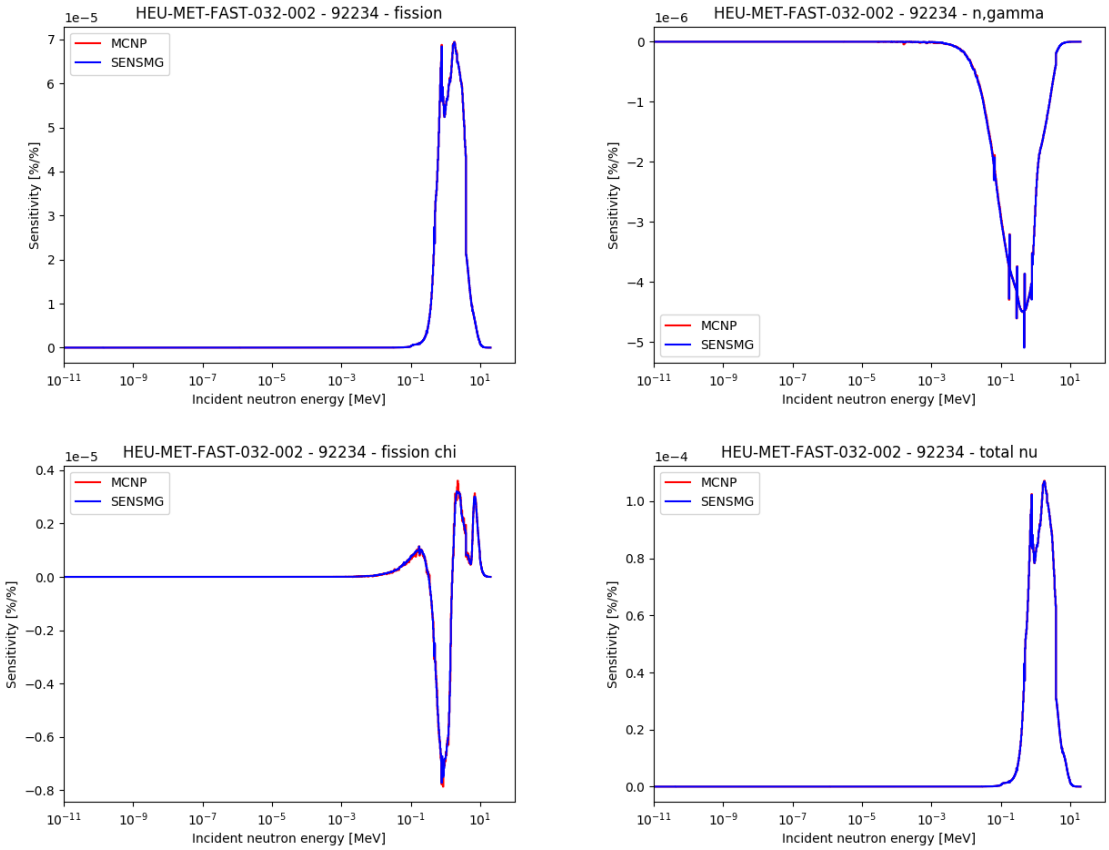

Figure 5.8: Sensitivity profiles for U234 in HEU-MET-FAST-032-002.

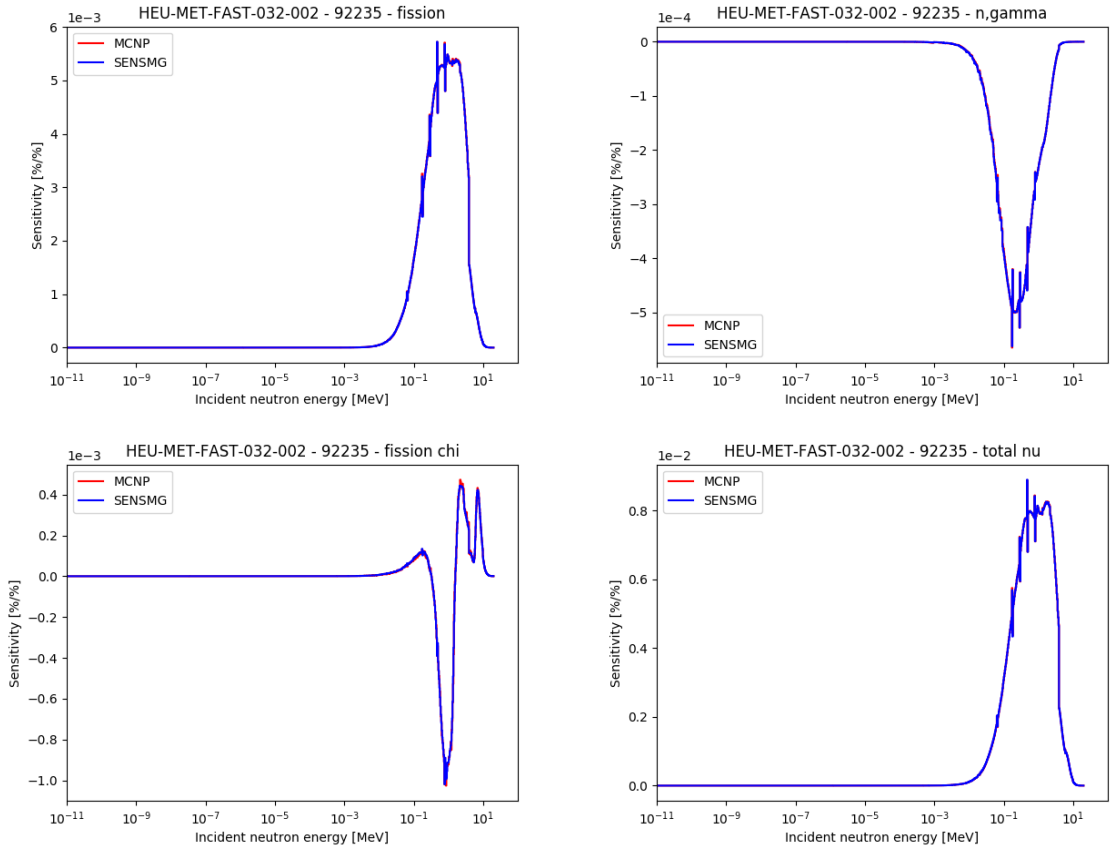

Figure 5.9: Sensitivity profiles for U235 in HEU-MET-FAST-032-002.

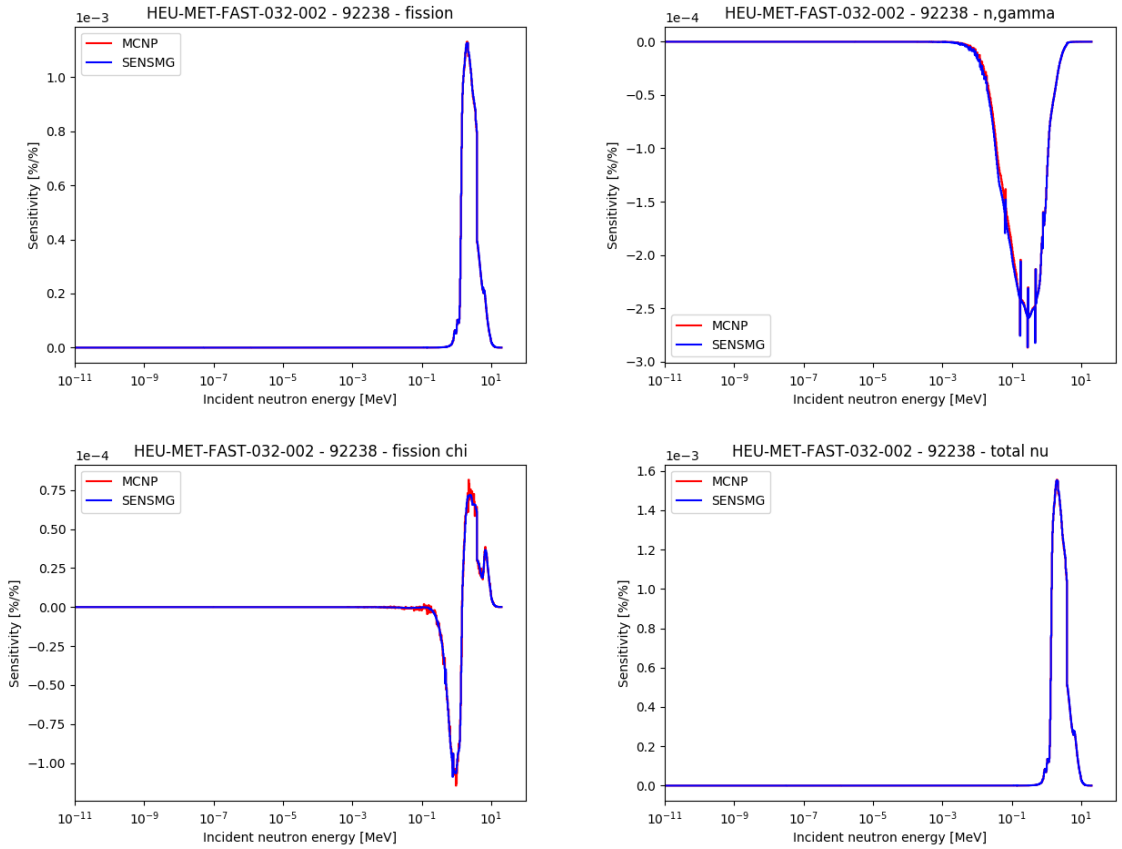

Figure 5.10: Sensitivity profiles for U238 in HEU-MET-FAST-032-002.

5.4 HEU-MET-FAST-032-003

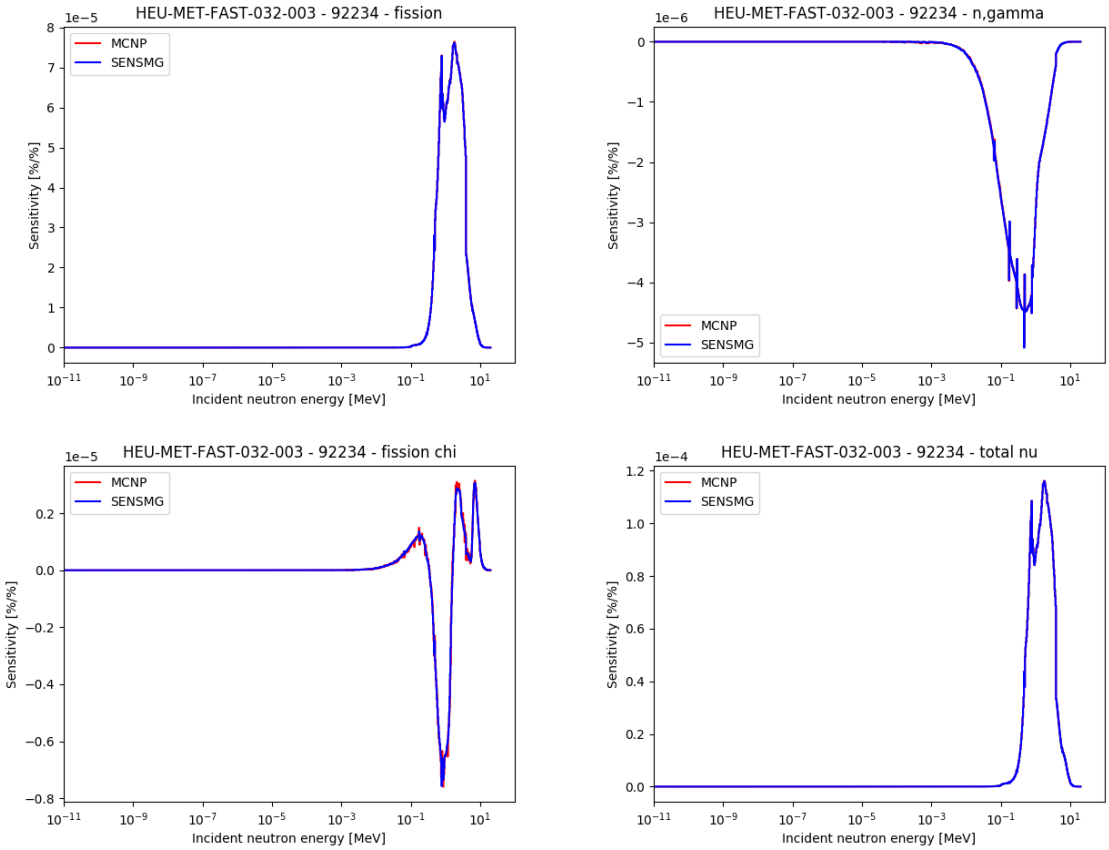

Figure 5.11: Sensitivity profiles for U234 in HEU-MET-FAST-032-003.

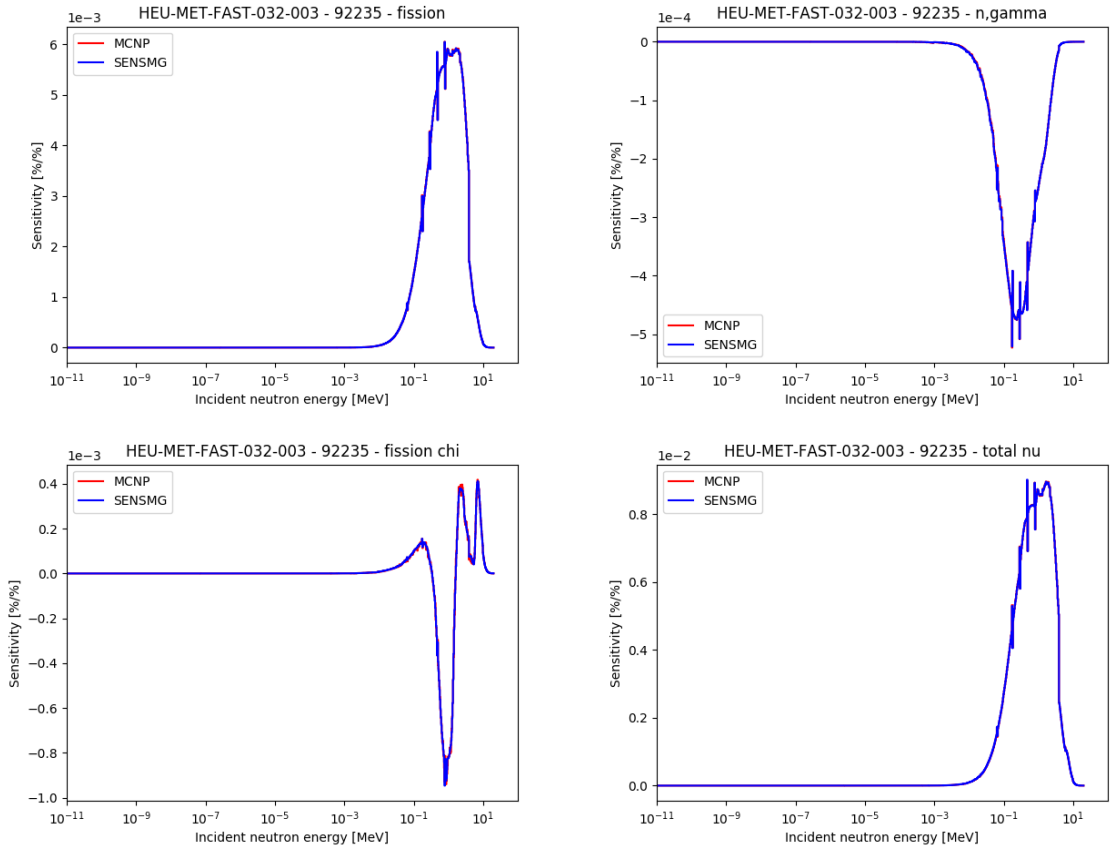

Figure 5.12: Sensitivity profiles for U235 in HEU-MET-FAST-032-003.

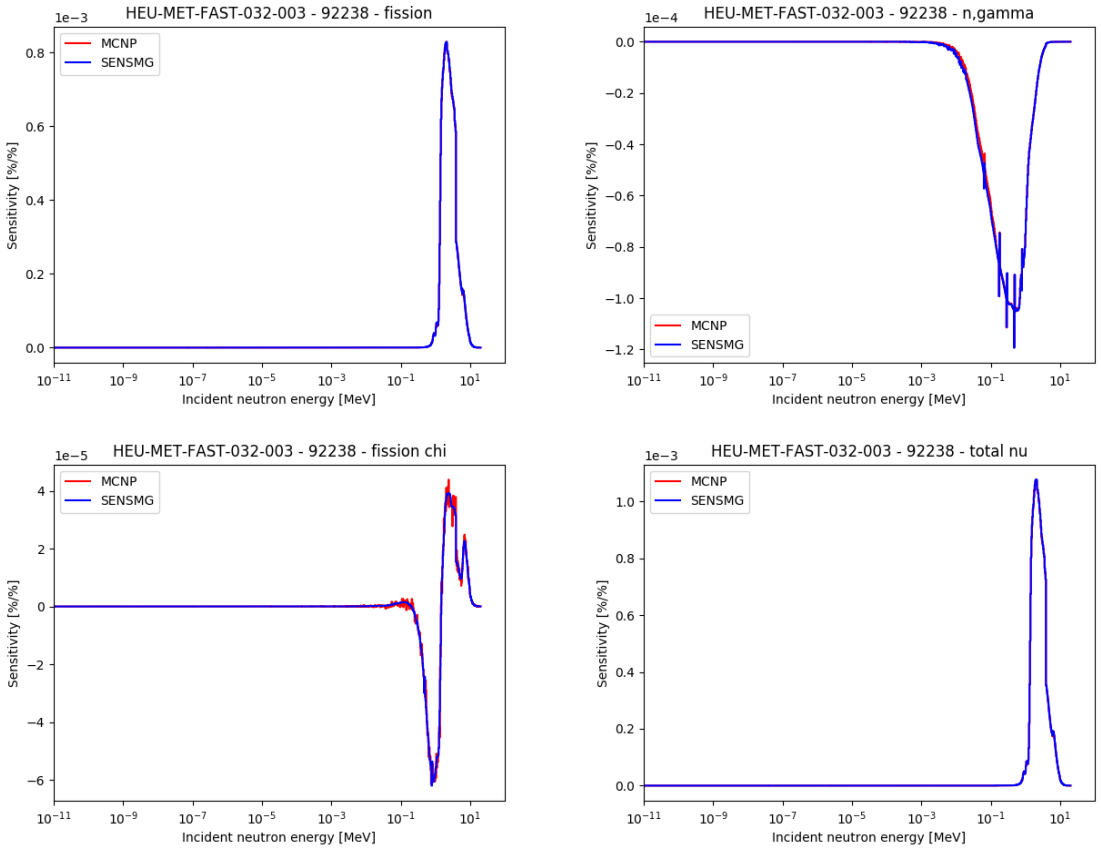

Figure 5.13: Sensitivity profiles for U238 in HEU-MET-FAST-032-003.

5.5 HEU-MET-FAST-032-004

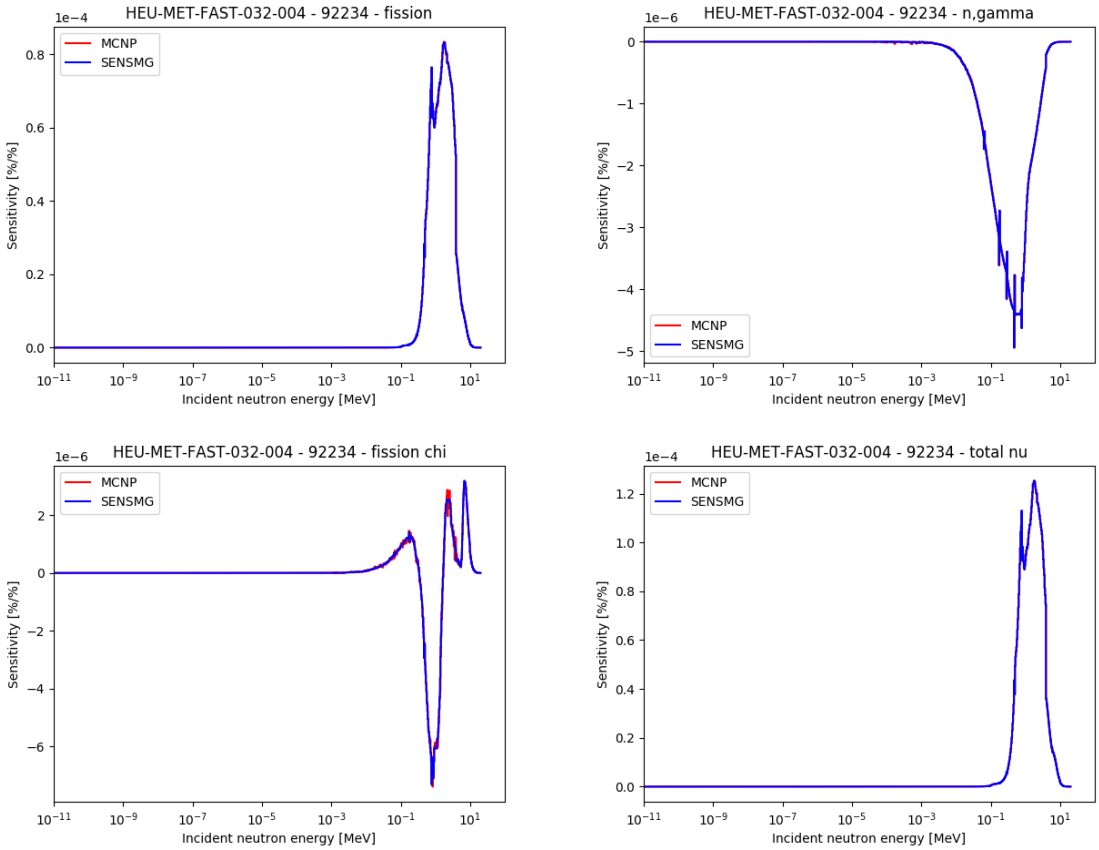

Figure 5.14: Sensitivity profiles for U234 in HEU-MET-FAST-032-004.

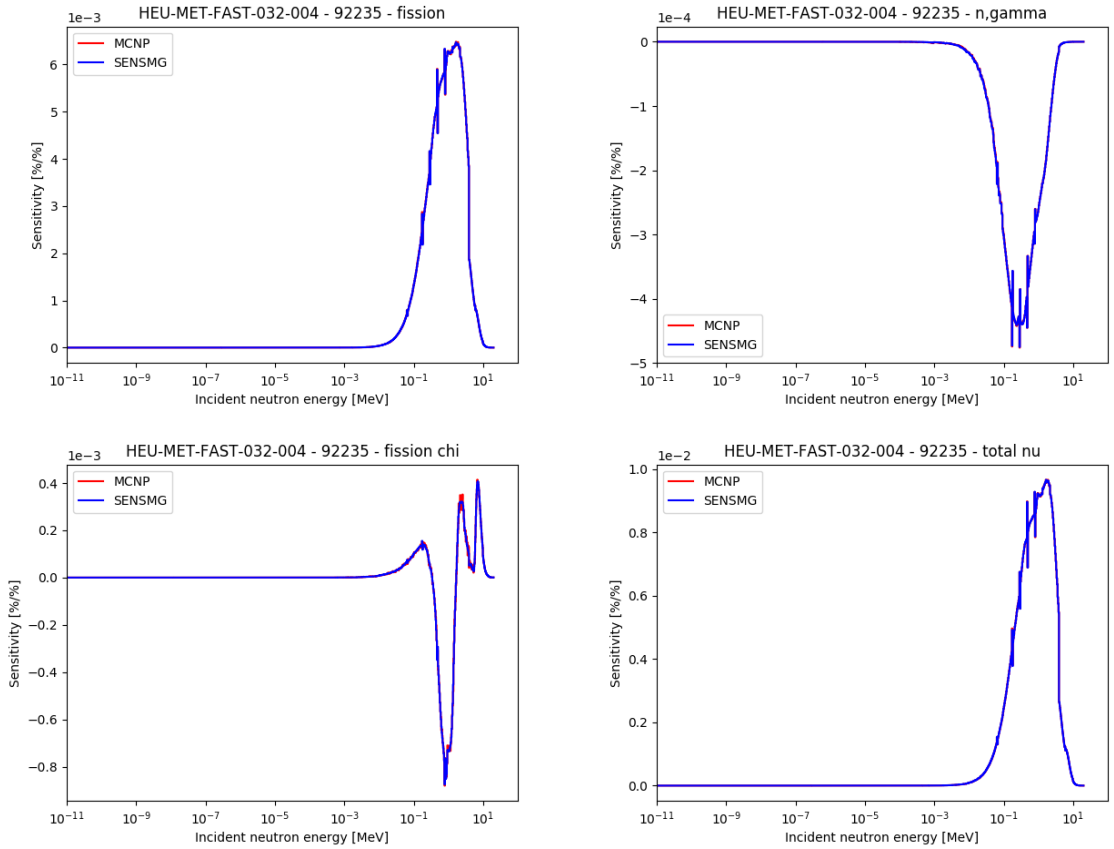

Figure 5.15: Sensitivity profiles for U235 in HEU-MET-FAST-032-004.

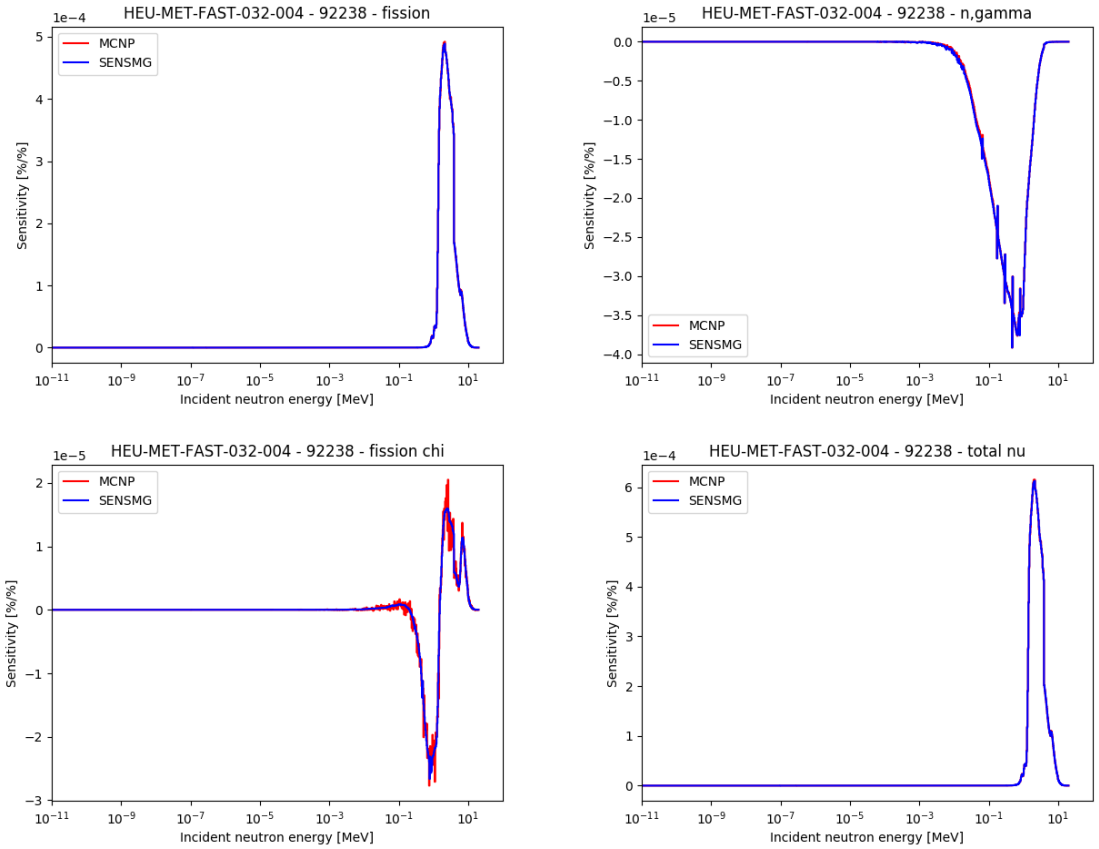

Figure 5.16: Sensitivity profiles for U238 in HEU-MET-FAST-032-004.

5.6 HEU-MET-FAST-041-001

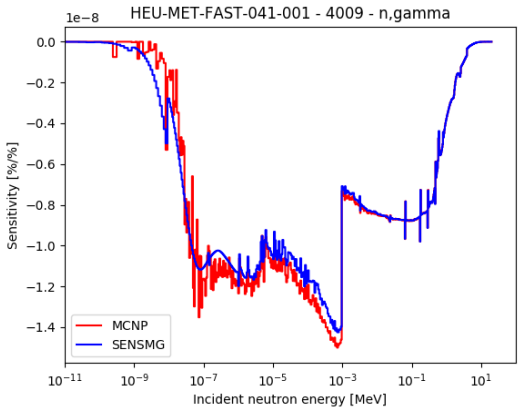

Figure 5.17: Sensitivity profiles for Be9 in HEU-MET-FAST-041-001.

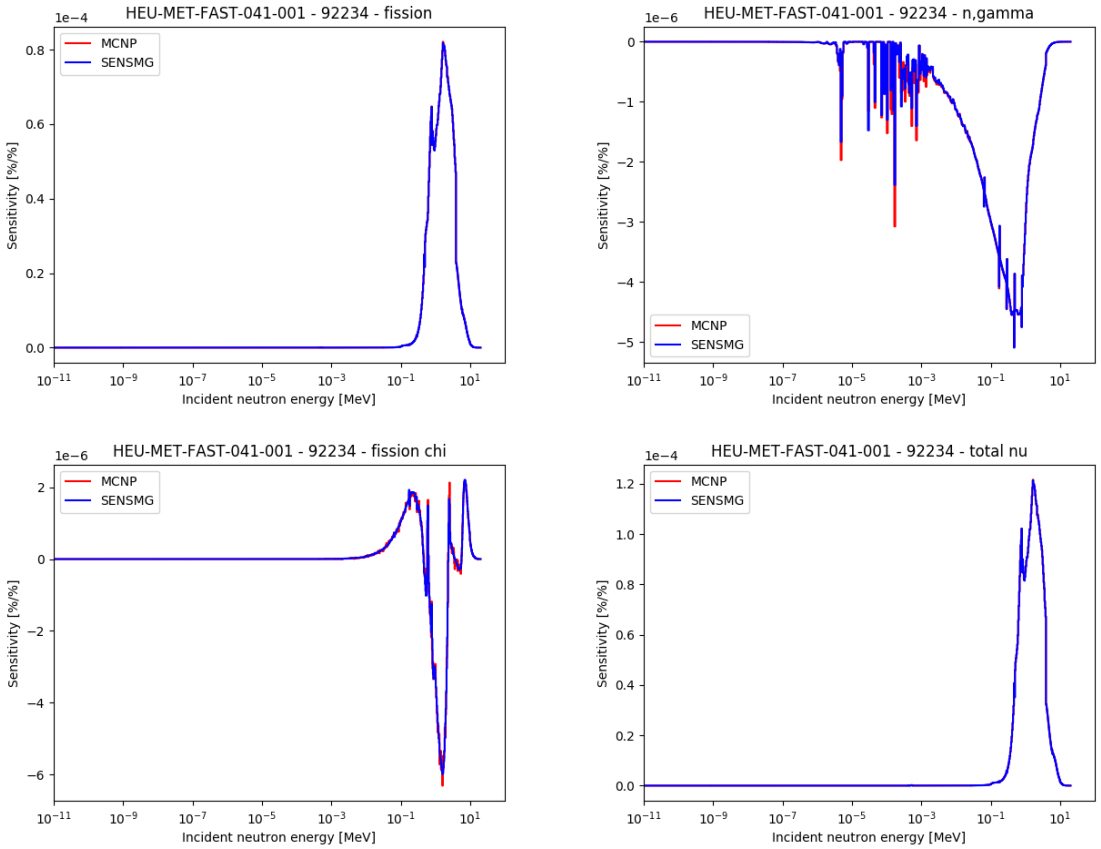

Figure 5.18: Sensitivity profiles for U234 in HEU-MET-FAST-041-001.

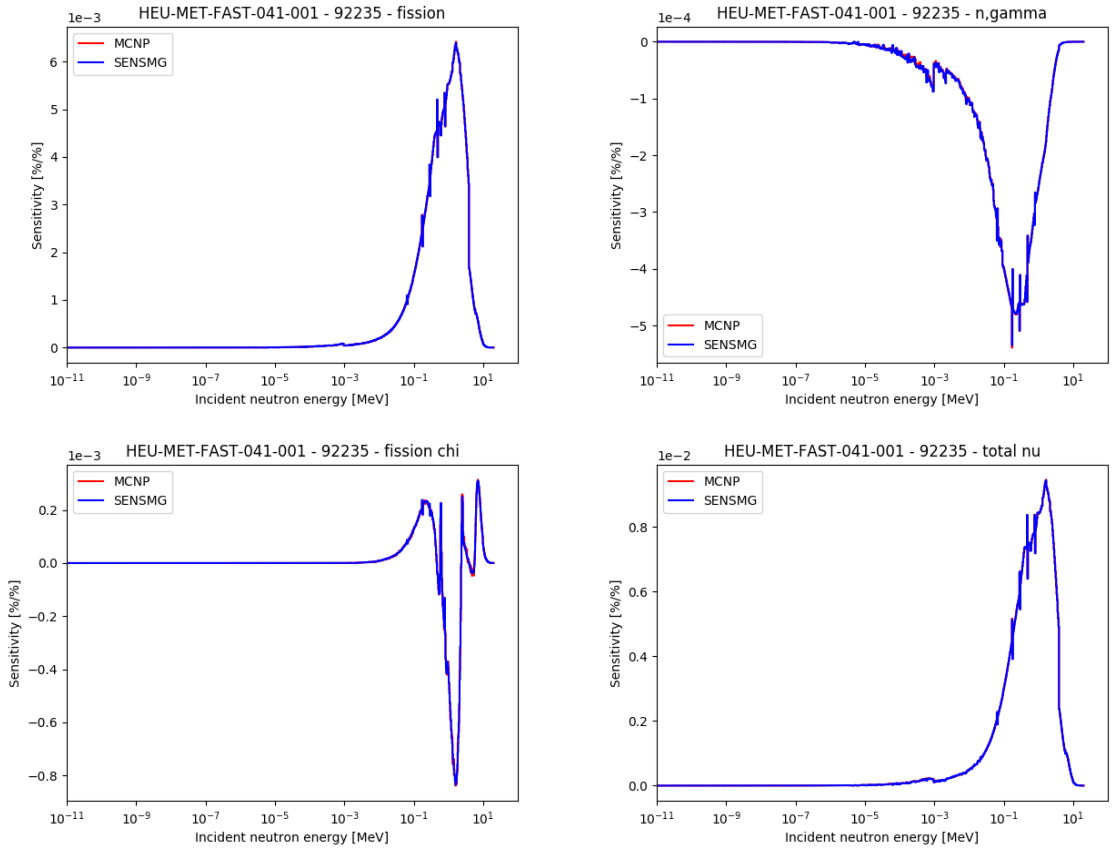

Figure 5.19: Sensitivity profiles for U235 in HEU-MET-FAST-041-001.

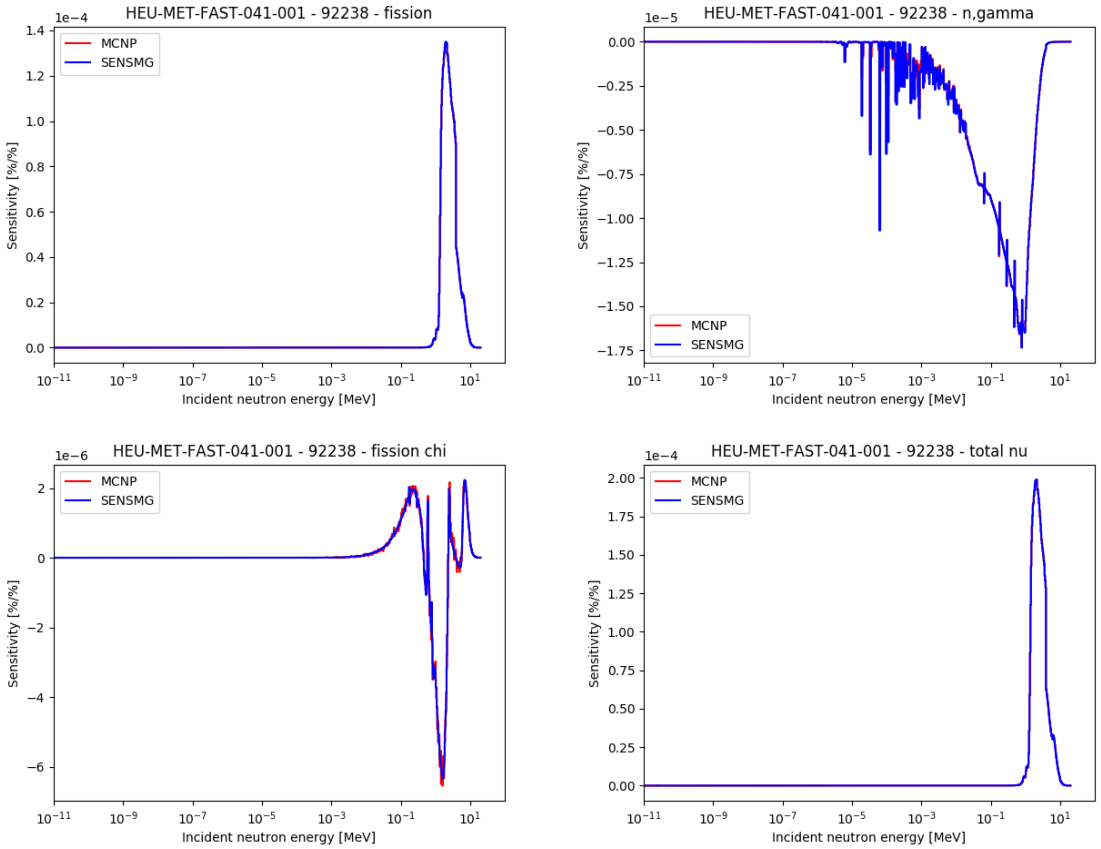

Figure 5.20: Sensitivity profiles for U238 in HEU-MET-FAST-041-001.

5.7 HEU-MET-FAST-041-002

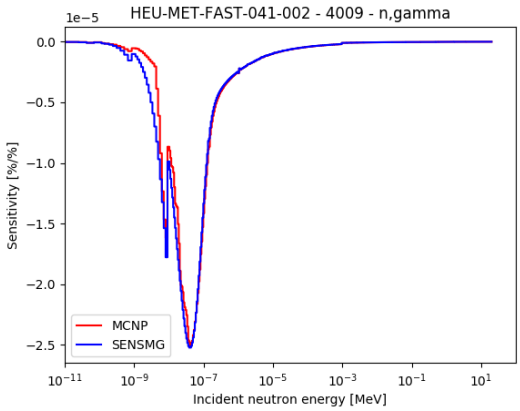

Figure 5.21: Sensitivity profiles for Be9 in HEU-MET-FAST-041-002.

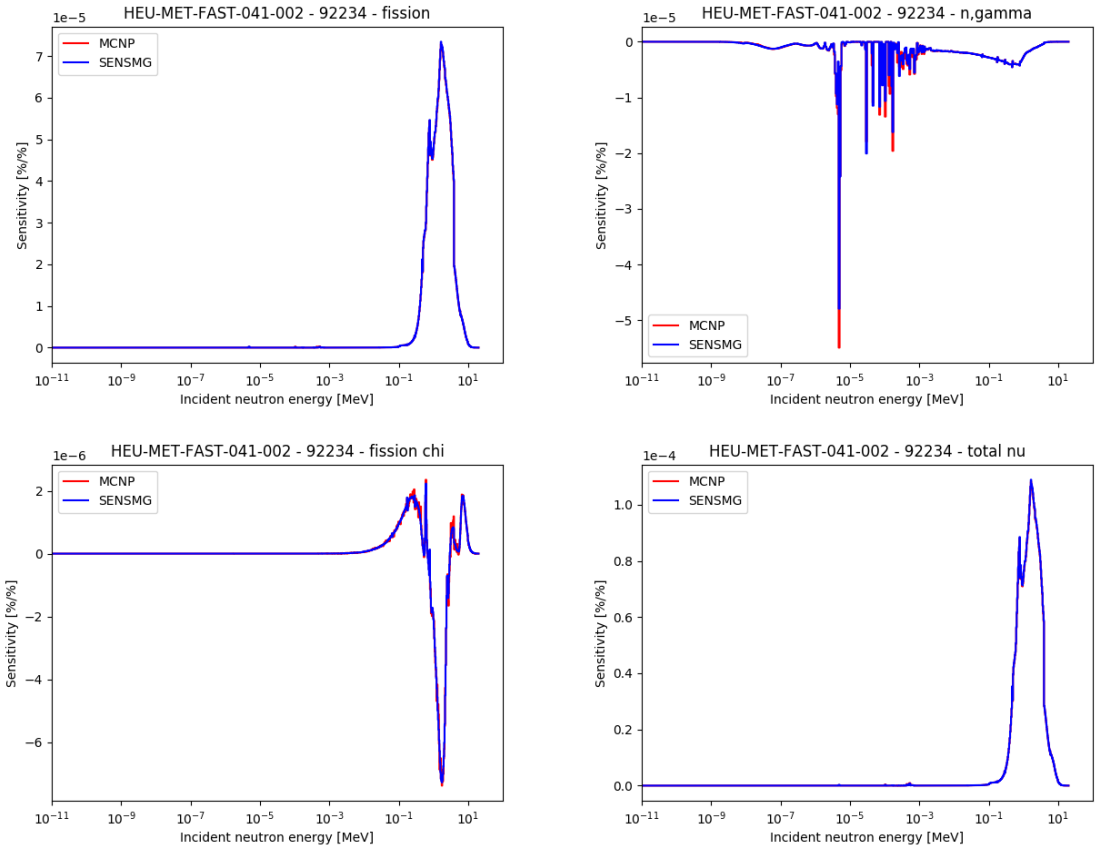

Figure 5.22: Sensitivity profiles for U234 in HEU-MET-FAST-041-002.

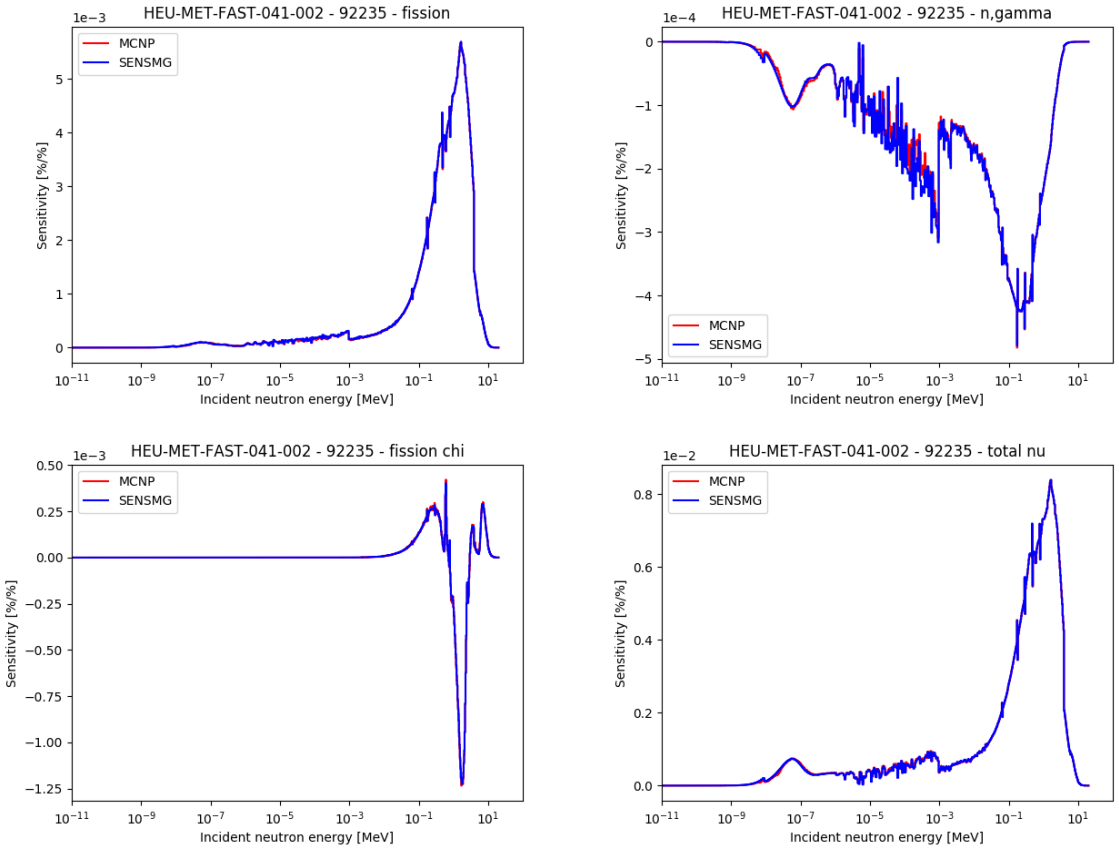

Figure 5.23: Sensitivity profiles for U235 in HEU-MET-FAST-041-002.

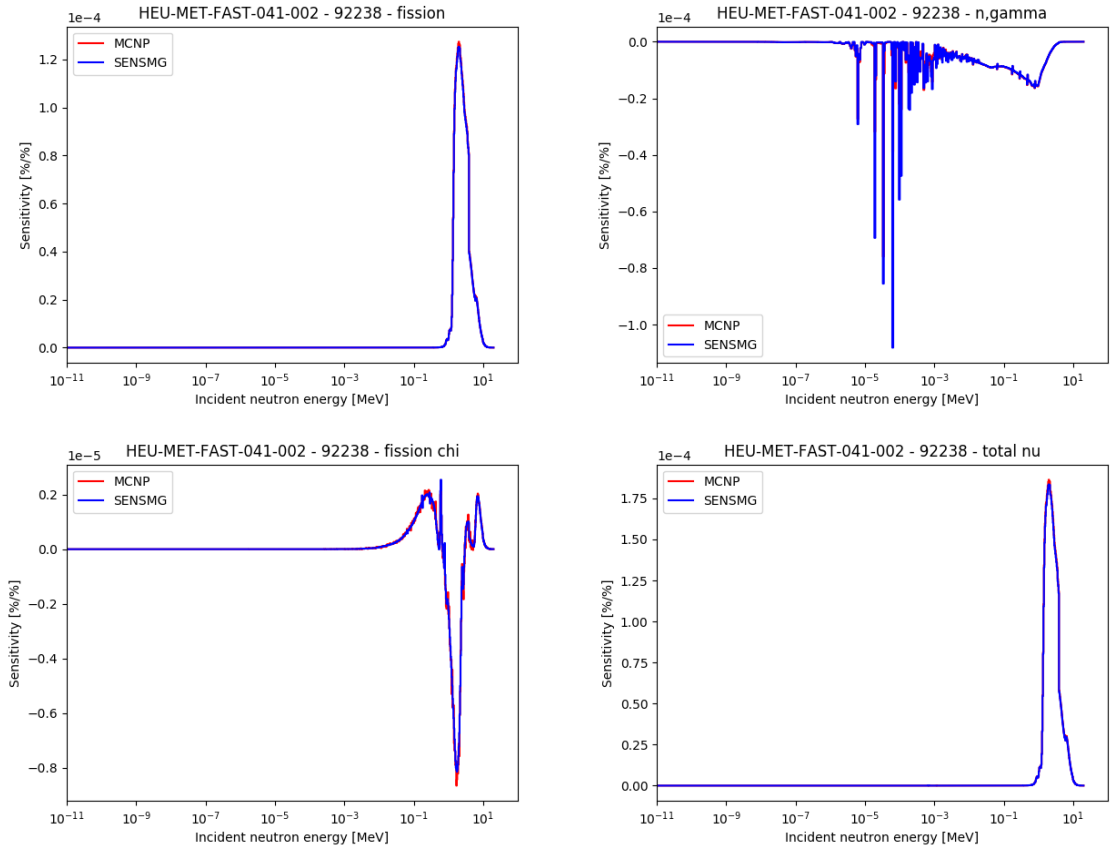

Figure 5.24: Sensitivity profiles for U238 in HEU-MET-FAST-041-002.

5.8 HEU-MET-FAST-041-003

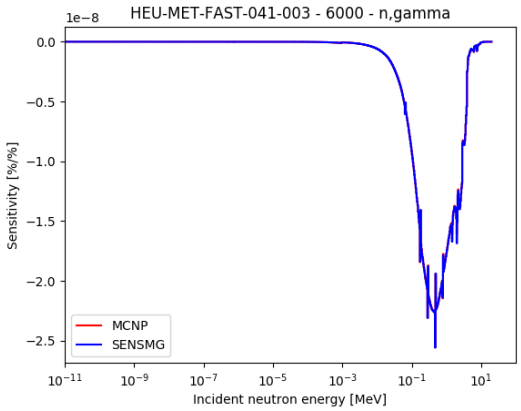

Figure 5.25: Sensitivity profiles for C in HEU-MET-FAST-041-003.

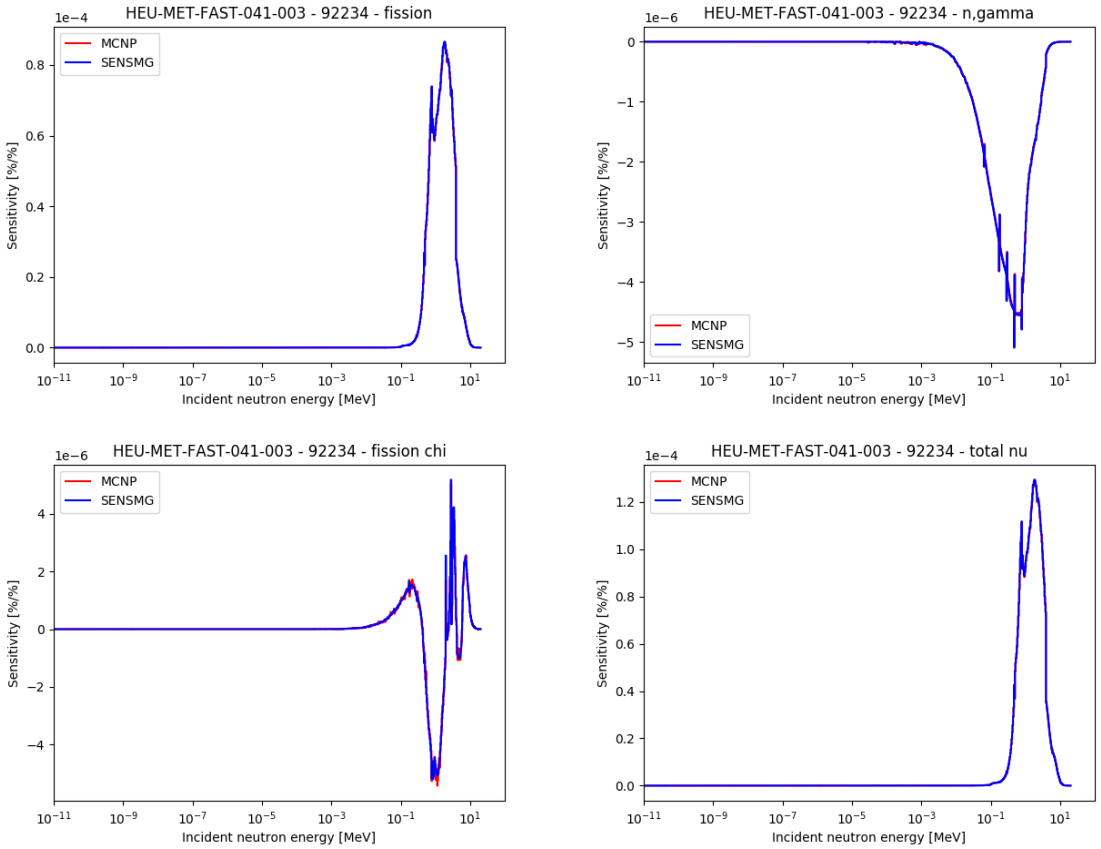

Figure 5.26: Sensitivity profiles for U234 in HEU-MET-FAST-041-003.

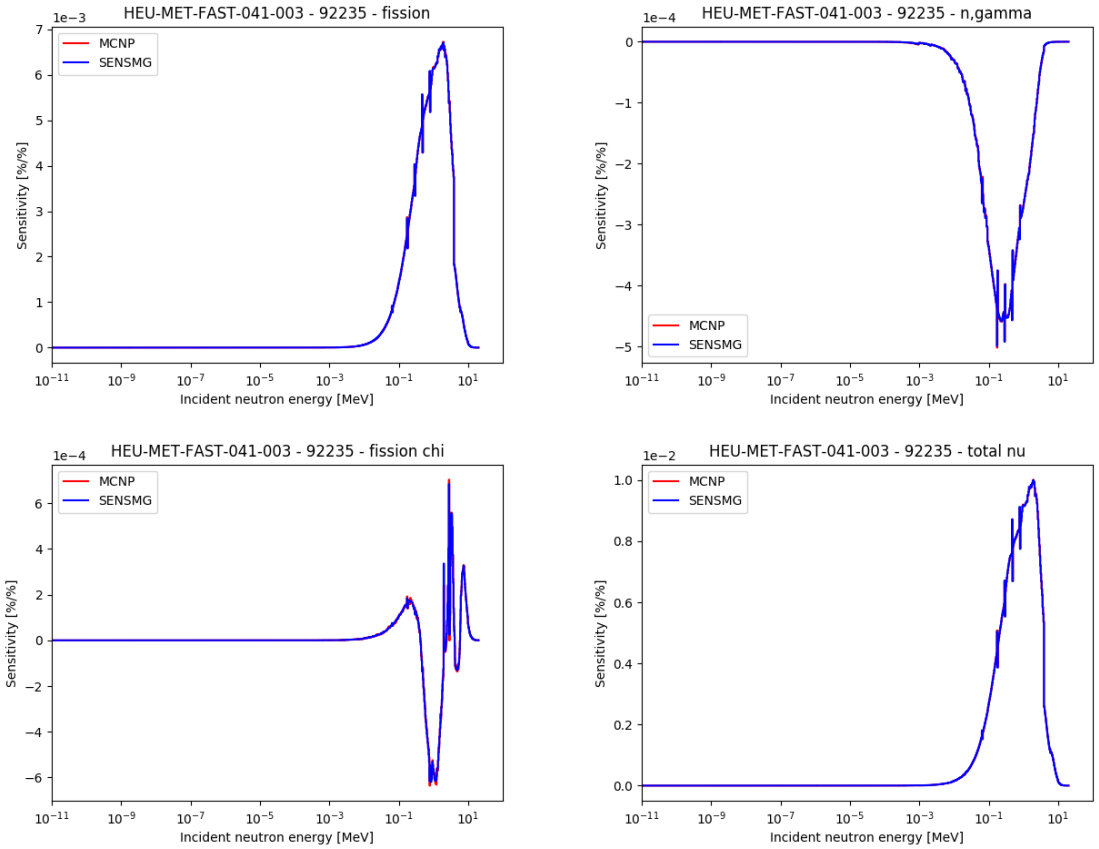

Figure 5.27: Sensitivity profiles for U235 in HEU-MET-FAST-041-003.

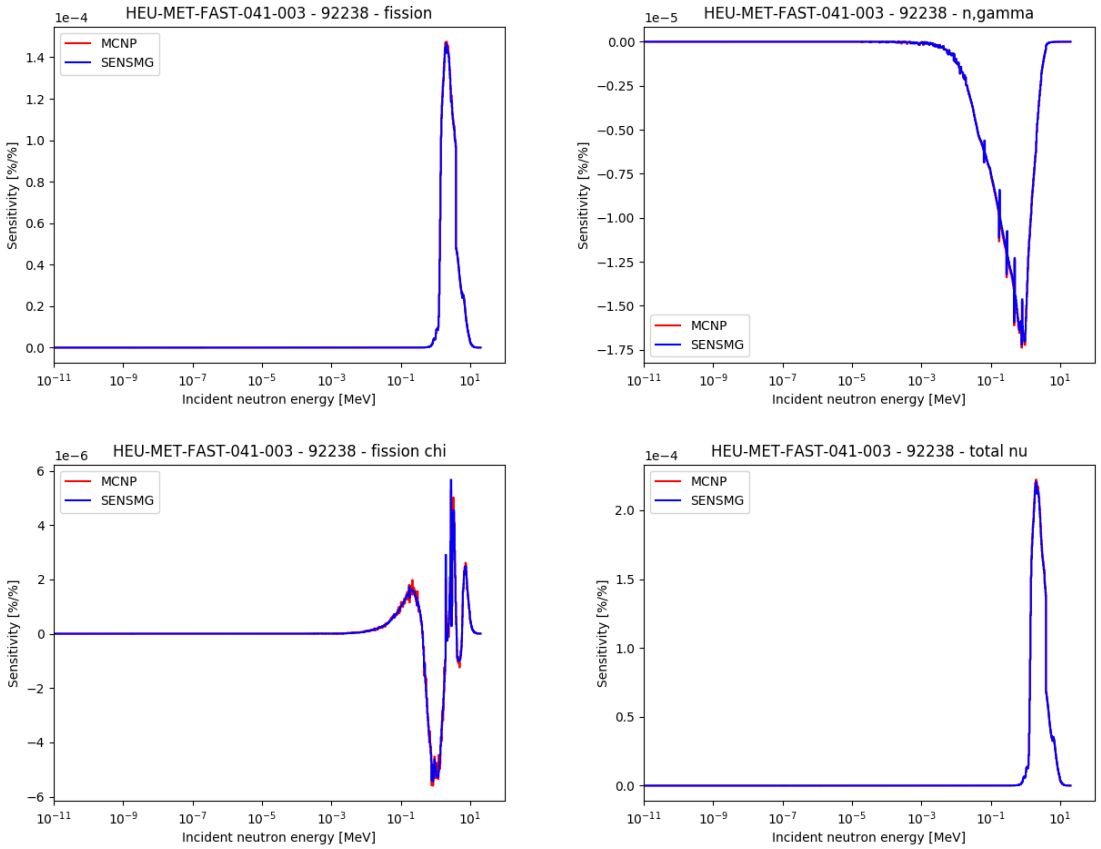

Figure 5.28: Sensitivity profiles for U238 in HEU-MET-FAST-041-003.

5.9 HEU-MET-FAST-041-004

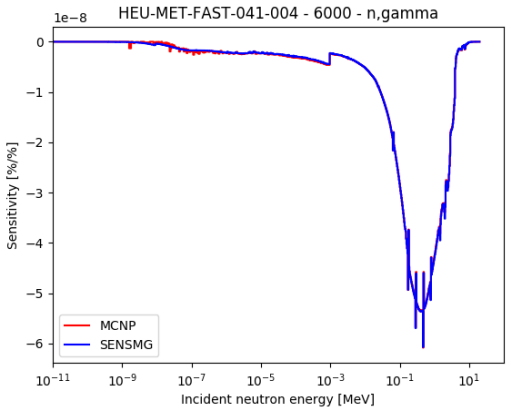

Figure 5.29: Sensitivity profiles for C in HEU-MET-FAST-041-004.

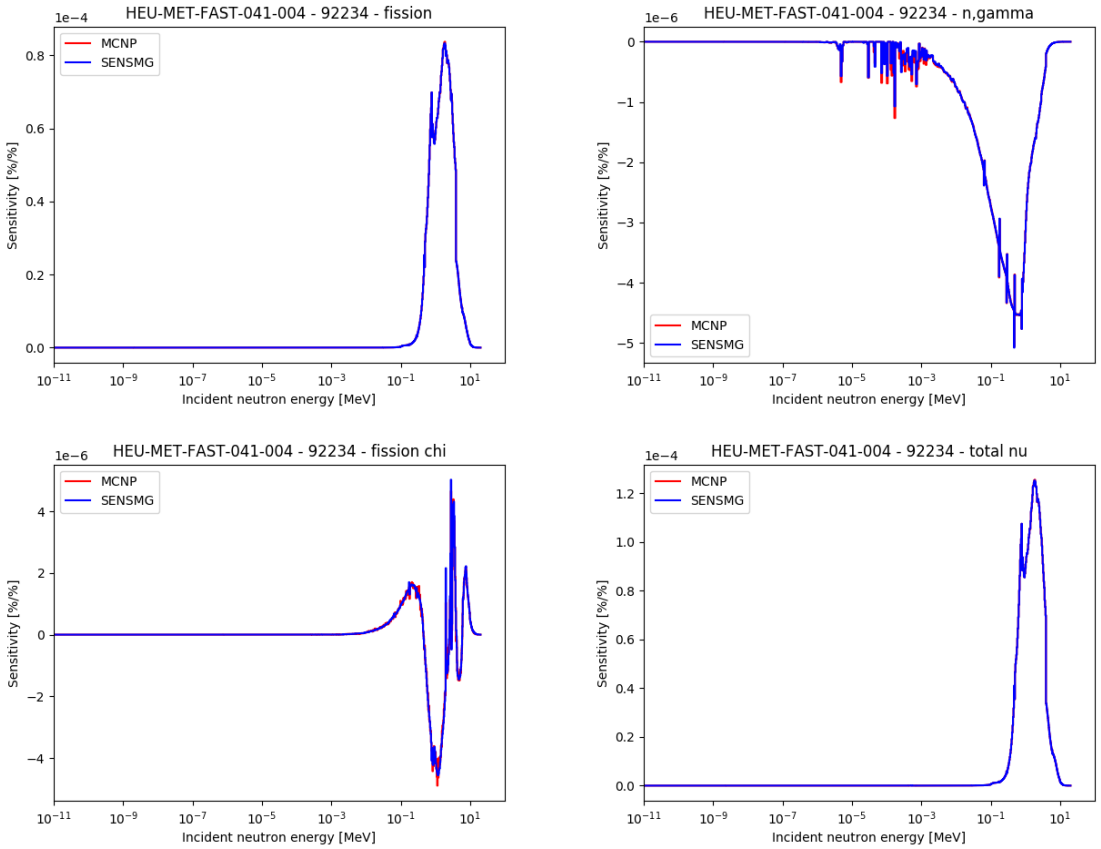

Figure 5.30: Sensitivity profiles for U234 in HEU-MET-FAST-041-004.

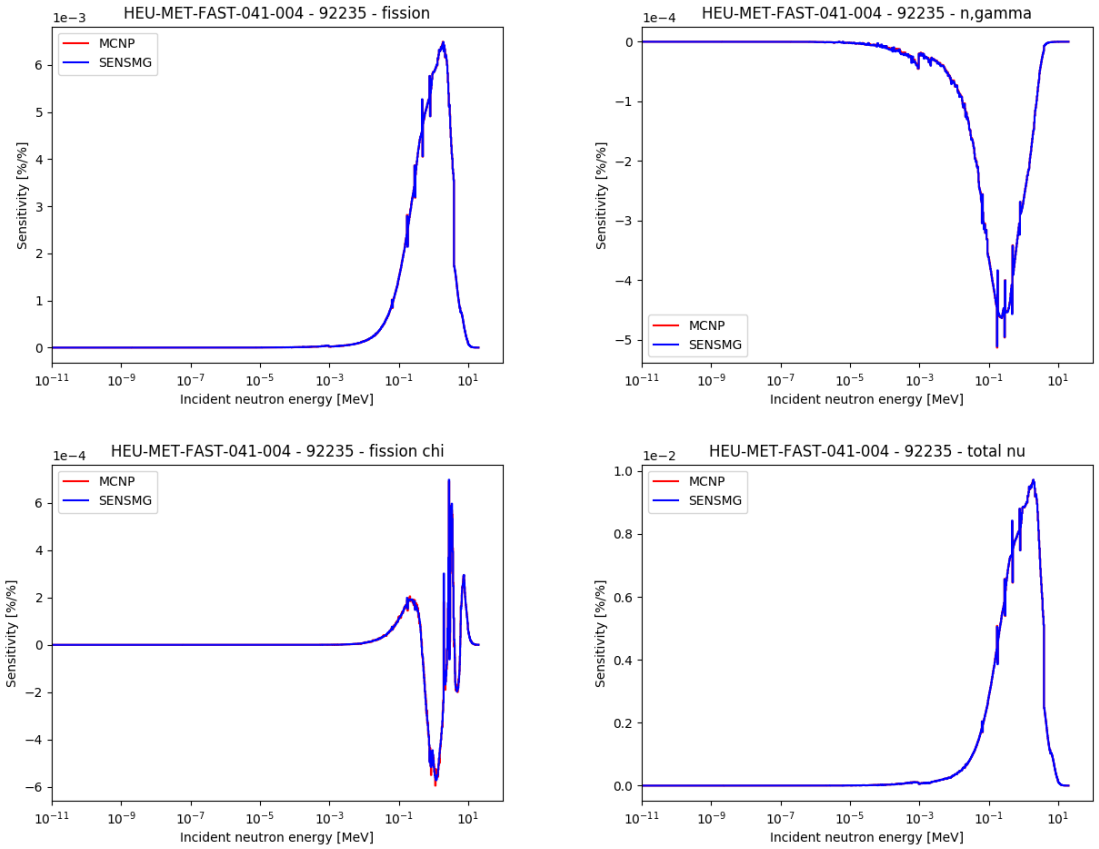

Figure 5.31: Sensitivity profiles for U235 in HEU-MET-FAST-041-004.

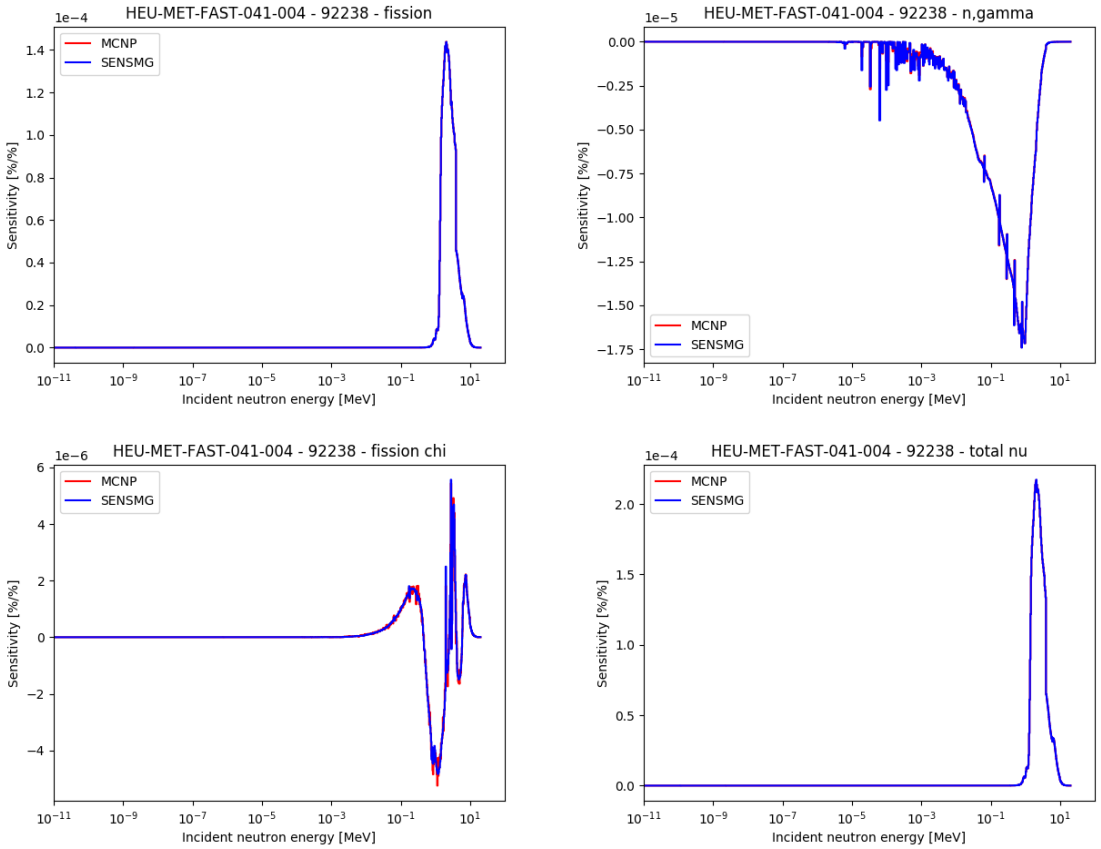

Figure 5.32: Sensitivity profiles for U238 in HEU-MET-FAST-041-004.

5.10 HEU-MET-FAST-041-005

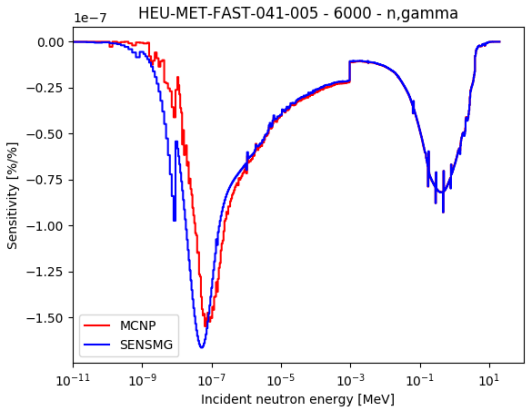

Figure 5.33: Sensitivity profiles for C in HEU-MET-FAST-041-005.

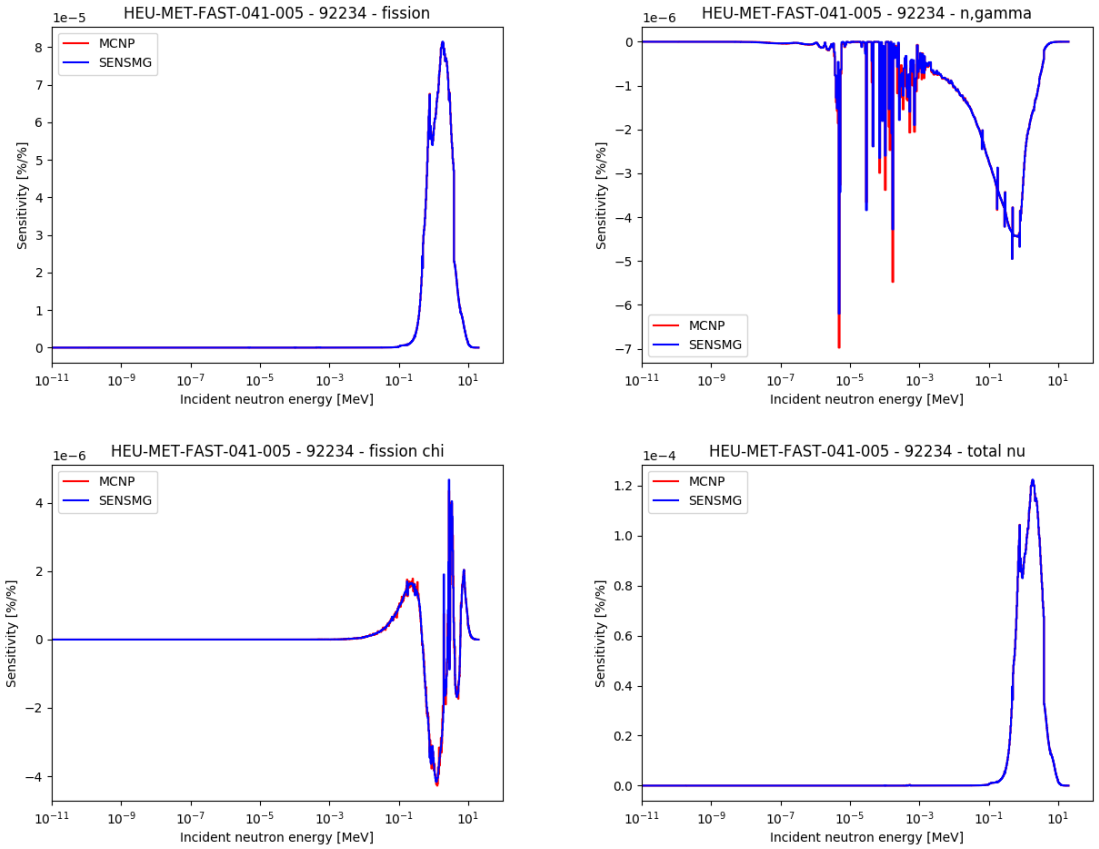

Figure 5.34: Sensitivity profiles for U234 in HEU-MET-FAST-041-005.

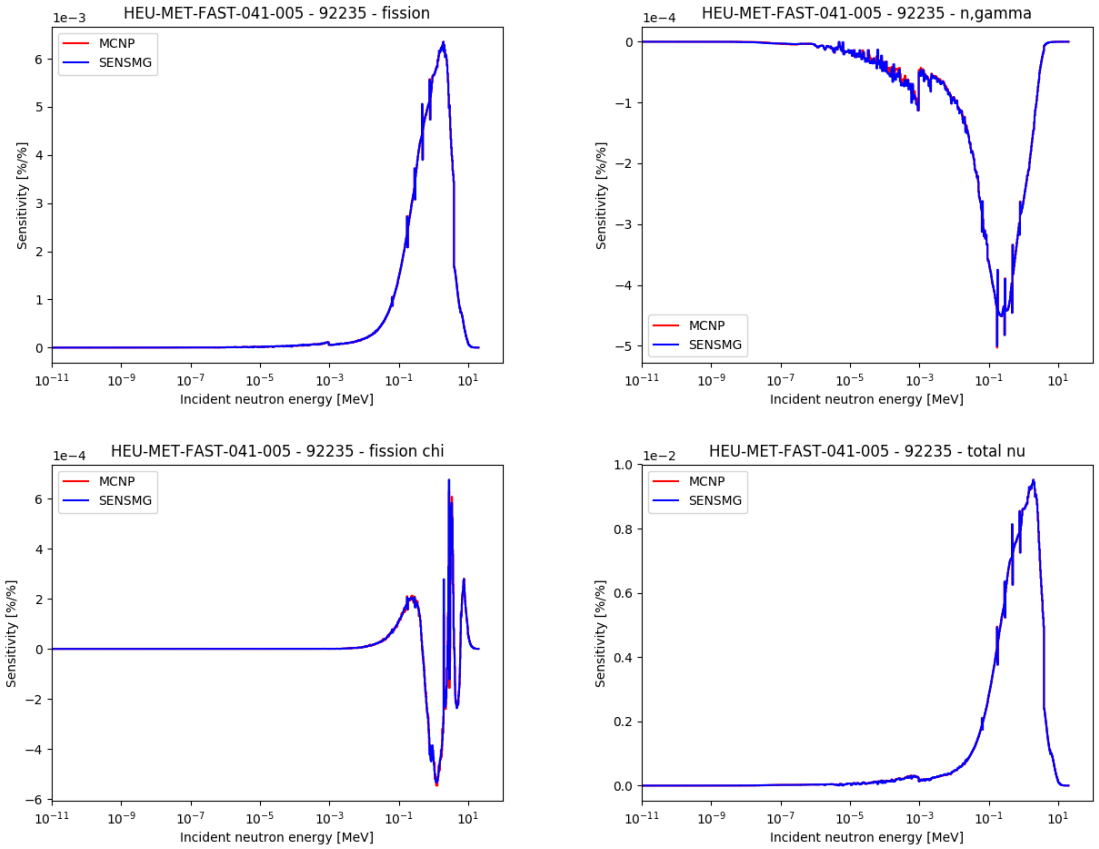

Figure 5.35: Sensitivity profiles for U235 in HEU-MET-FAST-041-005.

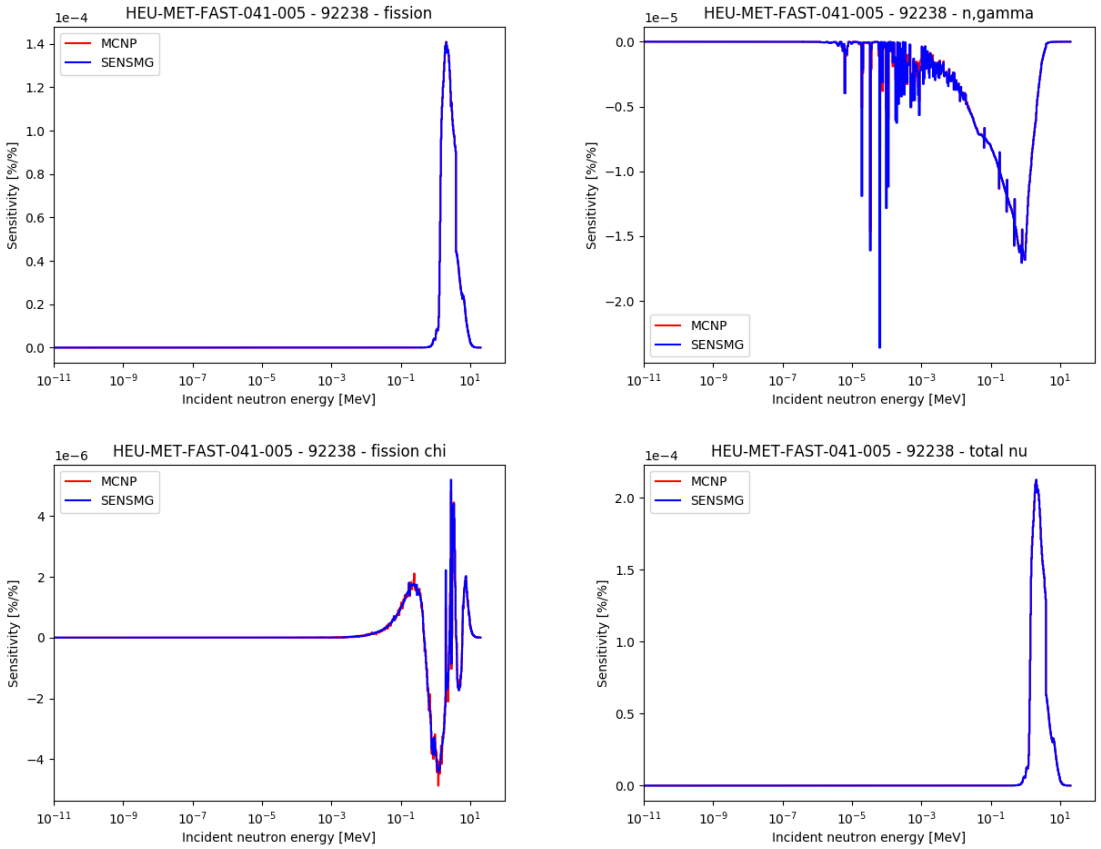

Figure 5.36: Sensitivity profiles for U238 in HEU-MET-FAST-041-005.

5.11 HEU-MET-FAST-041-006

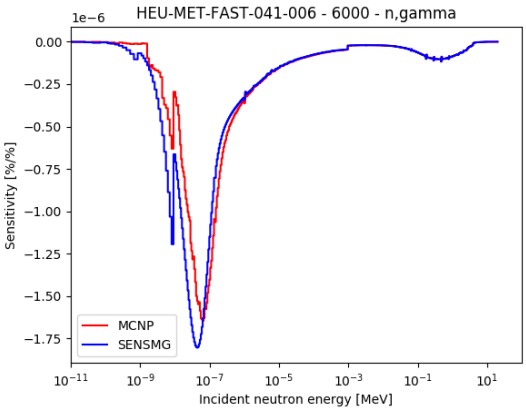

Figure 5.37: Sensitivity profiles for C in HEU-MET-FAST-041-006.

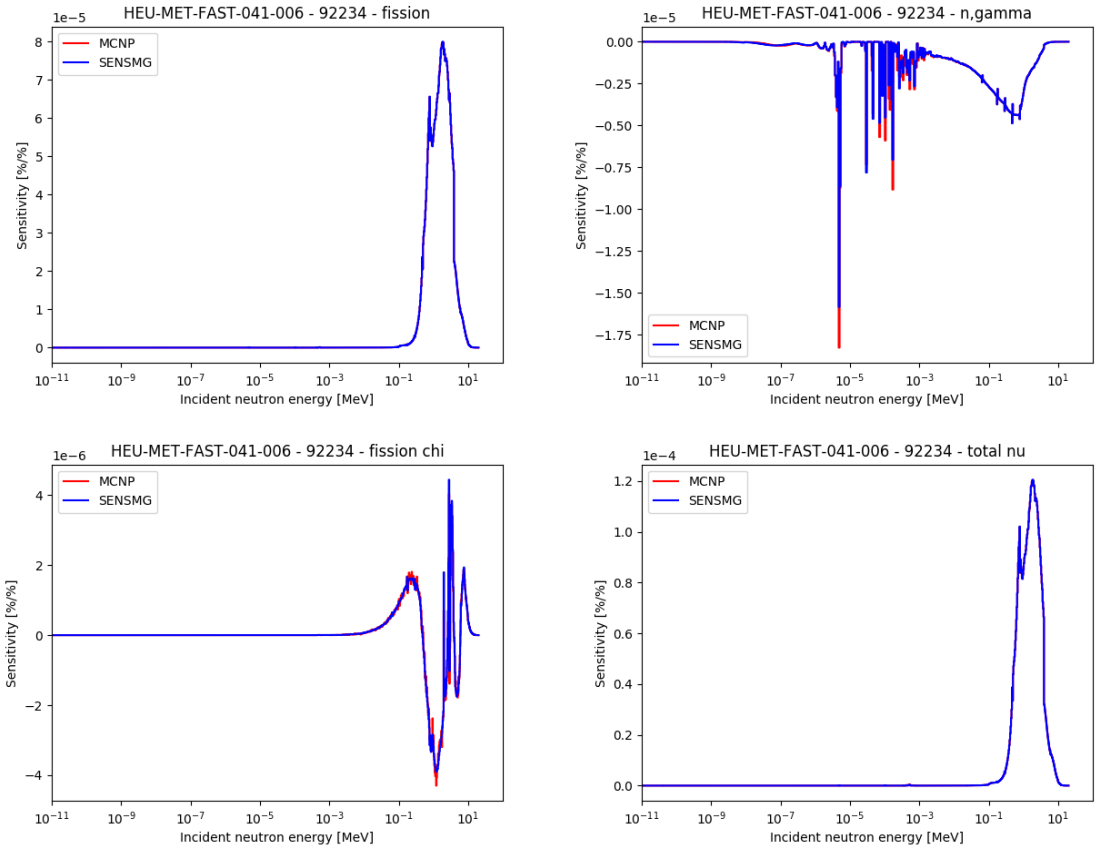

Figure 5.38: Sensitivity profiles for U234 in HEU-MET-FAST-041-006.

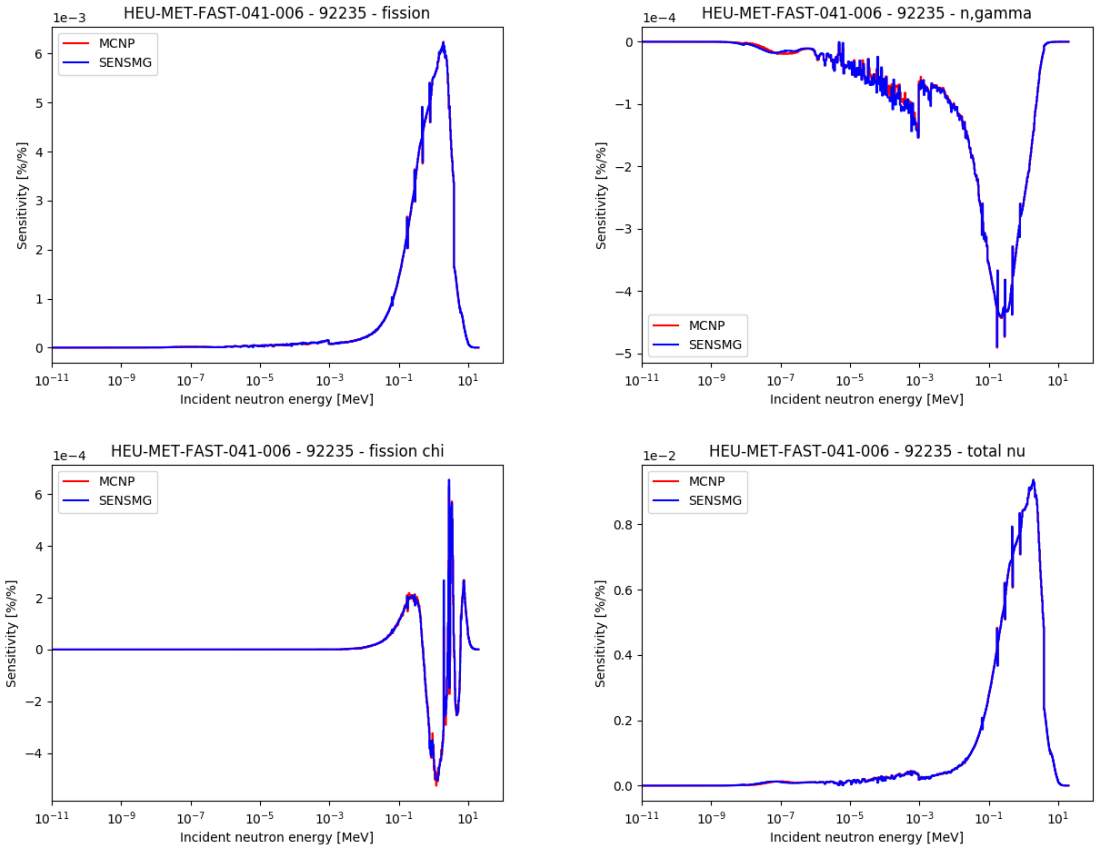

Figure 5.39: Sensitivity profiles for U235 in HEU-MET-FAST-041-006.

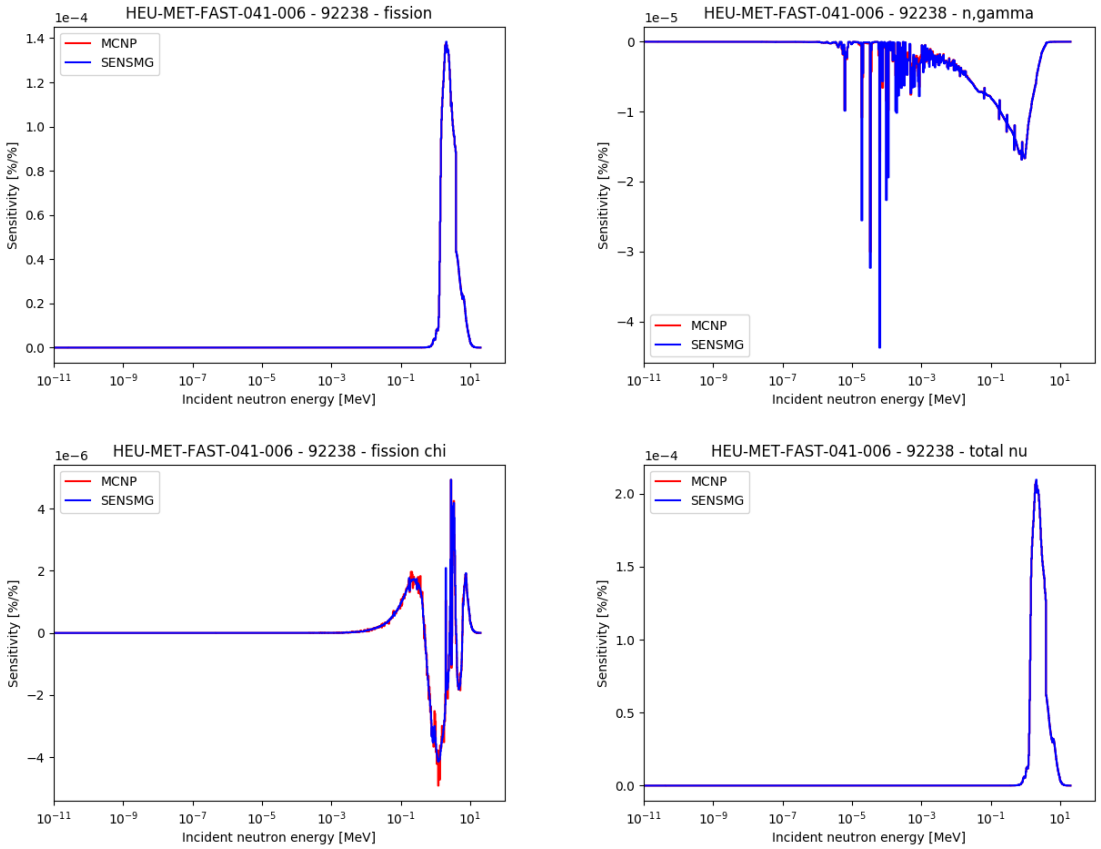

Figure 5.40: Sensitivity profiles for U238 in HEU-MET-FAST-041-006.

5.12 HEU-MET-FAST-085-001

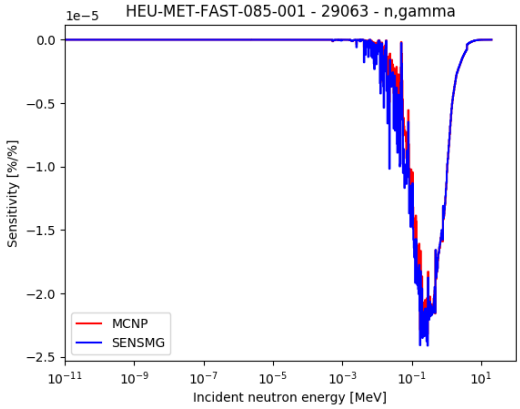

Figure 5.41: Sensitivity profiles for Cu63 in HEU-MET-FAST-085-001.

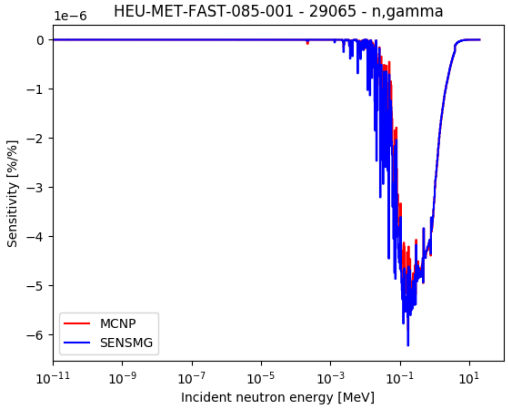

Figure 5.42: Sensitivity profiles for Cu65 in HEU-MET-FAST-085-001.

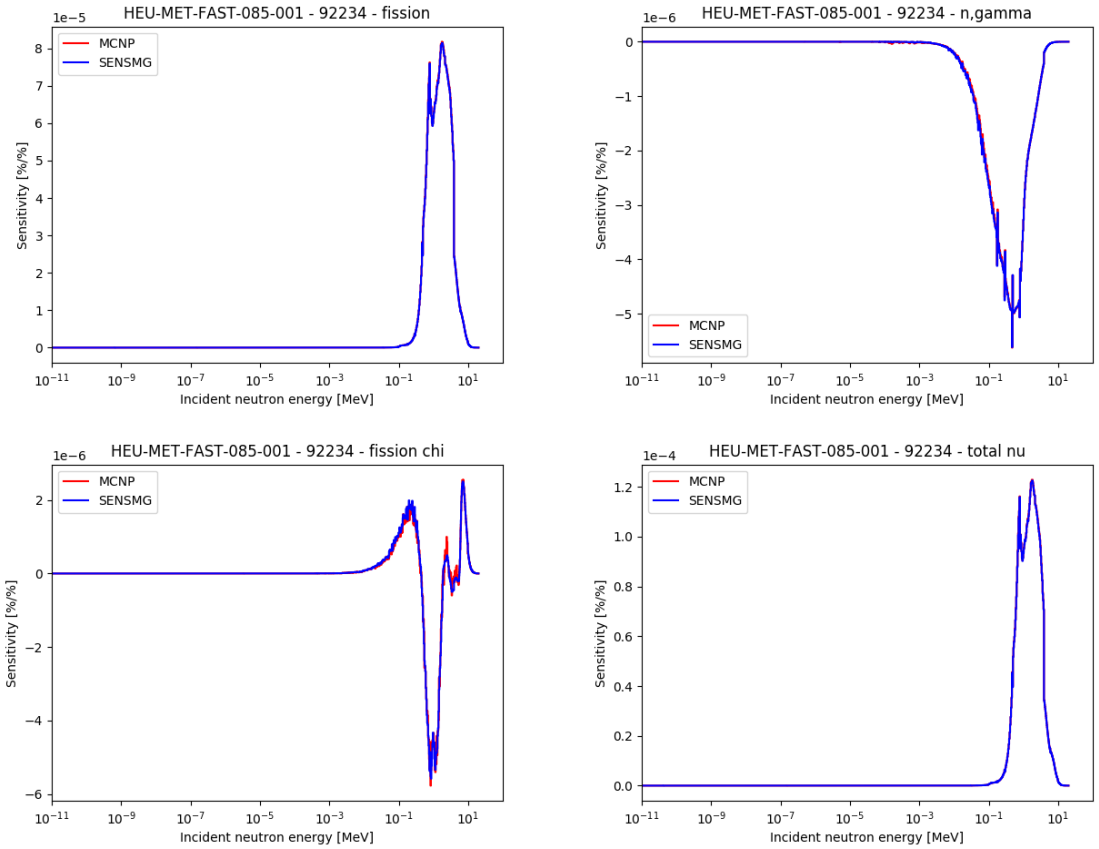

Figure 5.43: Sensitivity profiles for U234 in HEU-MET-FAST-085-001.

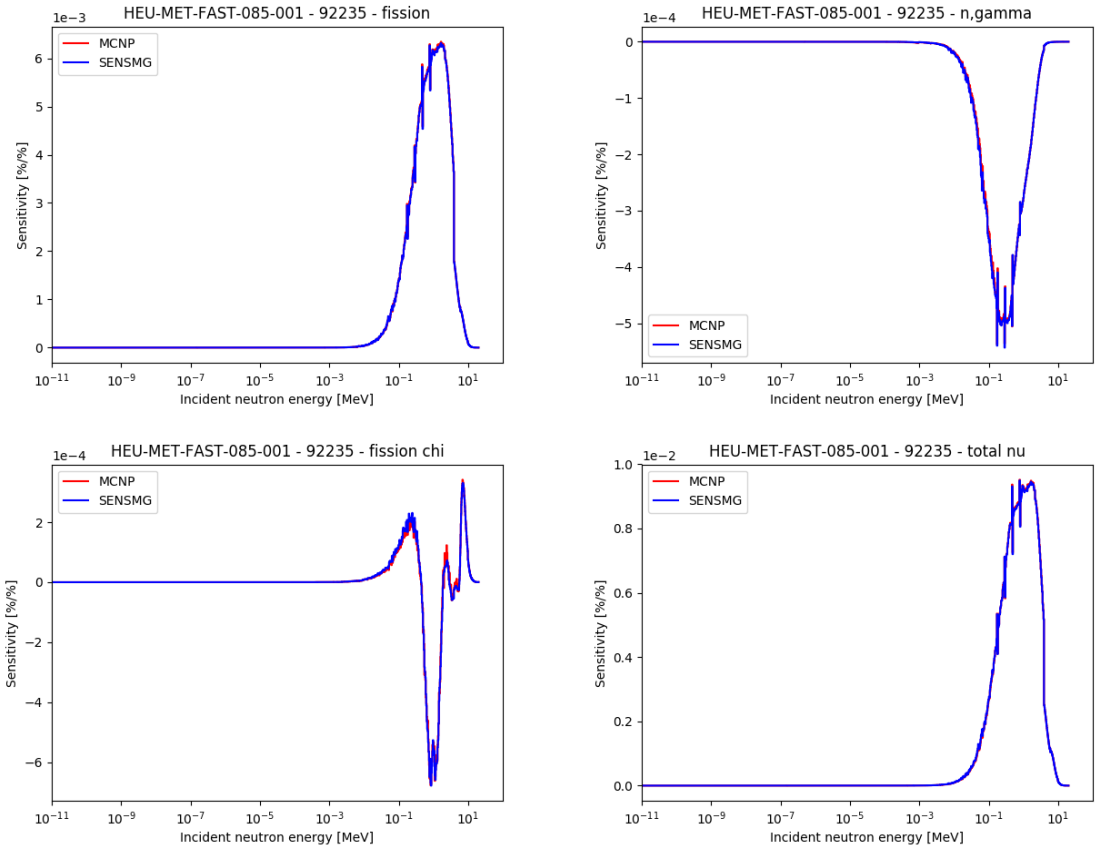

Figure 5.44: Sensitivity profiles for U235 in HEU-MET-FAST-085-001.

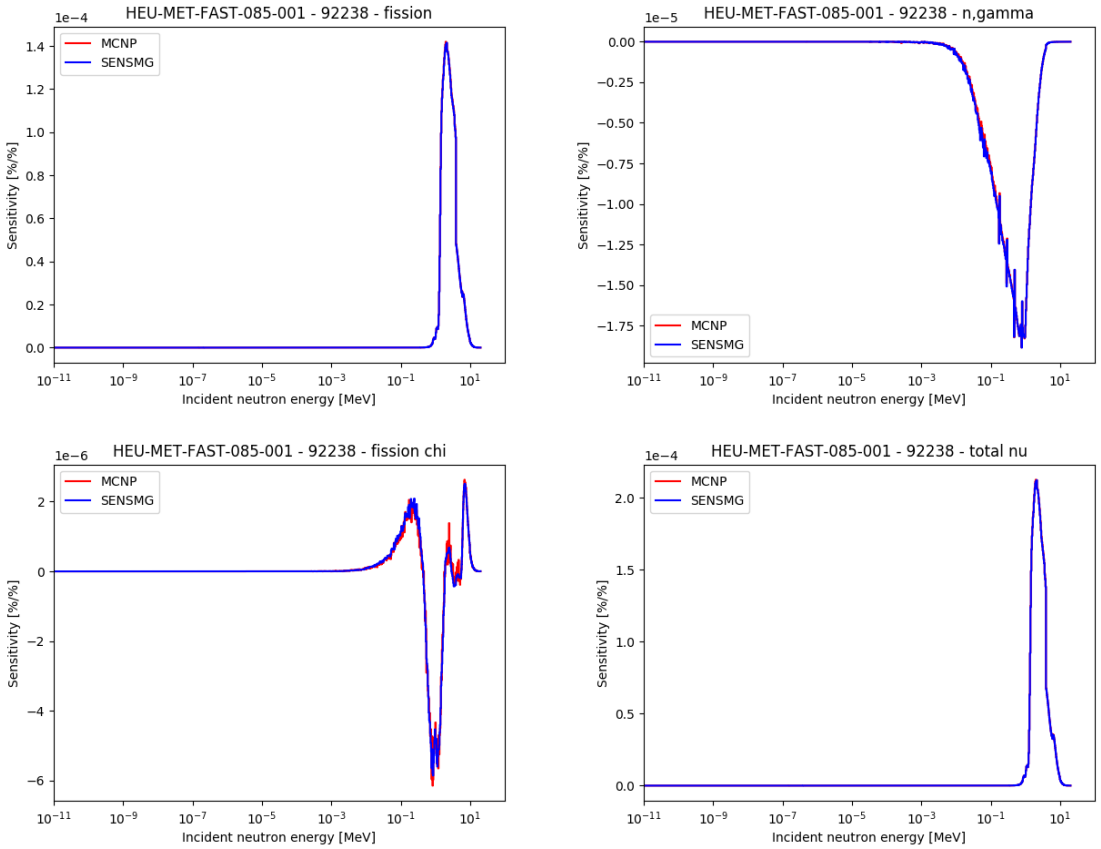

Figure 5.45: Sensitivity profiles for U238 in HEU-MET-FAST-085-001.

5.13 HEU-MET-FAST-085-002

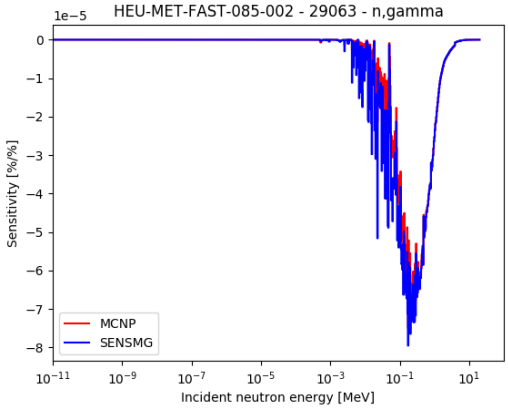

Figure 5.46: Sensitivity profiles for Cu63 in HEU-MET-FAST-085-002.

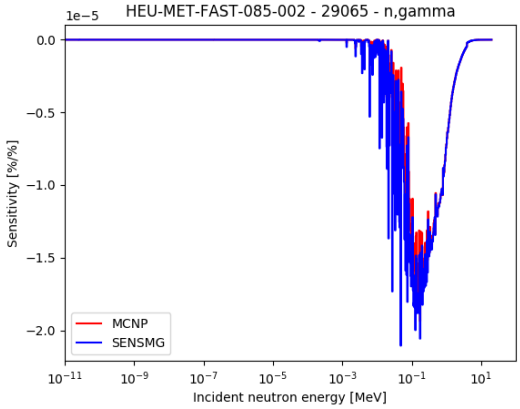

Figure 5.47: Sensitivity profiles for Cu65 in HEU-MET-FAST-085-002.

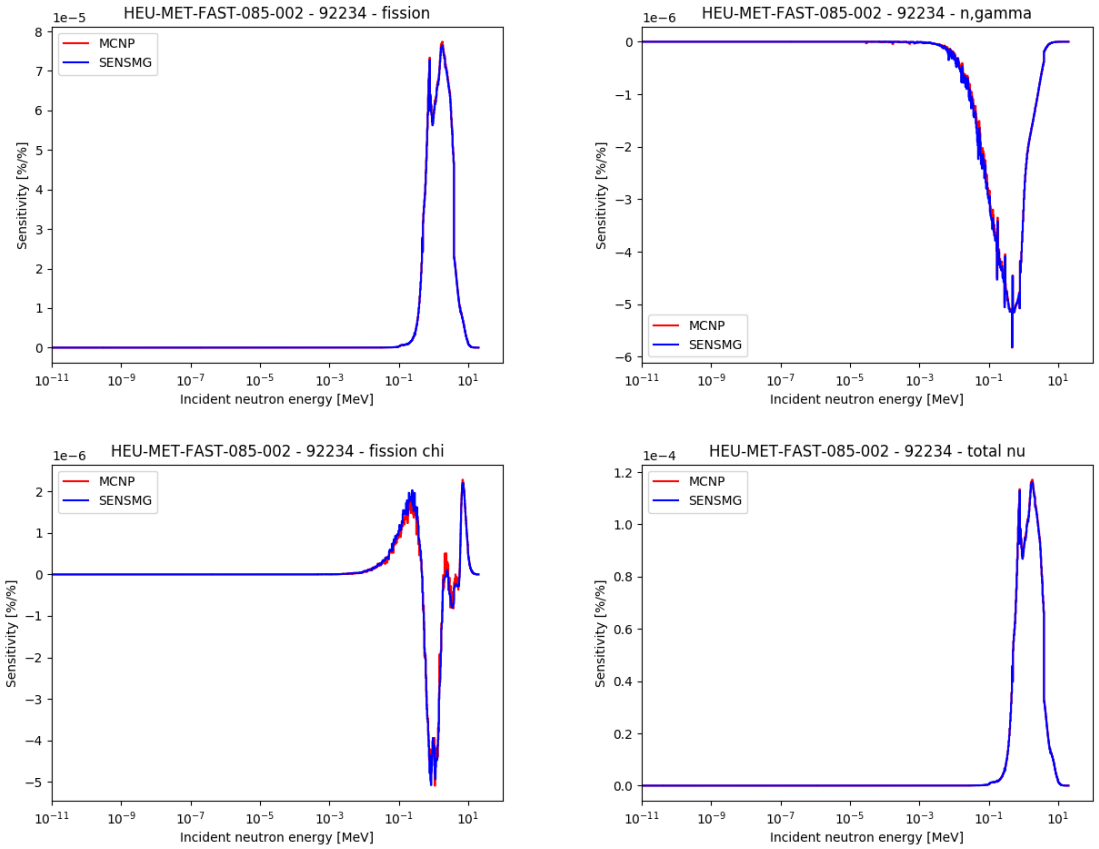

Figure 5.48: Sensitivity profiles for U234 in HEU-MET-FAST-085-002.

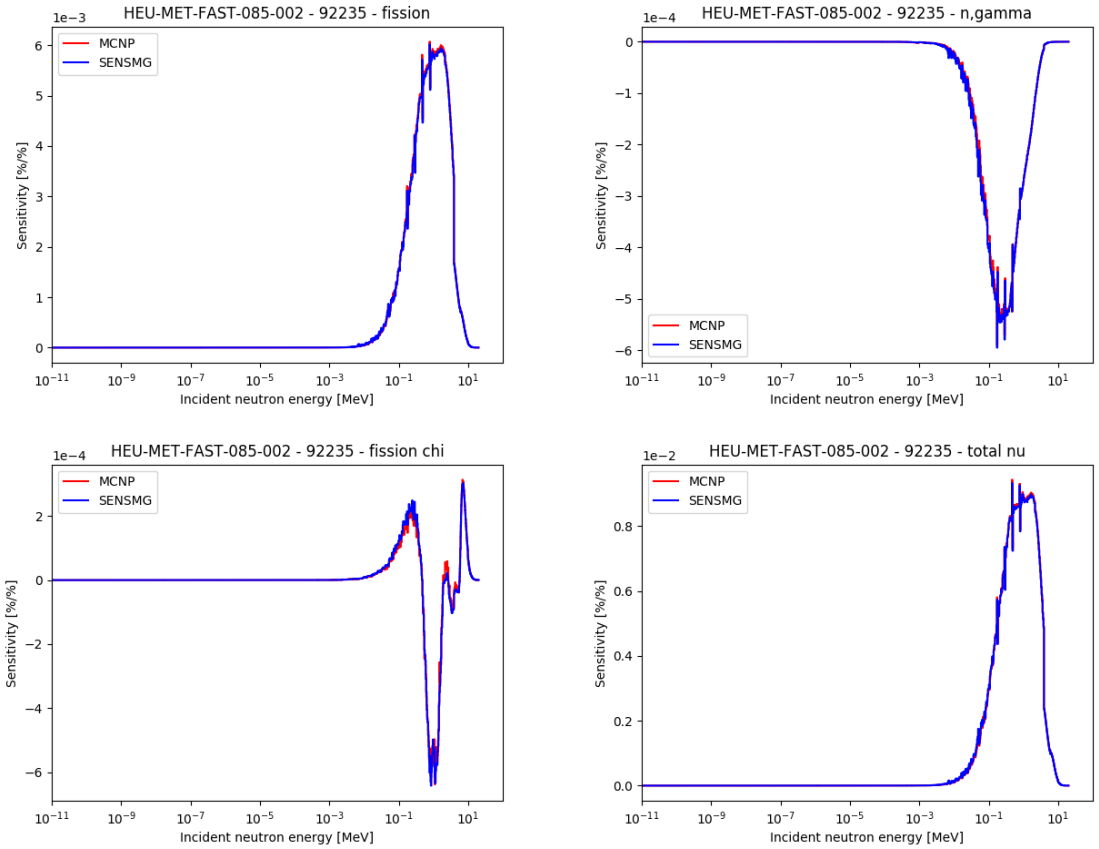

Figure 5.49: Sensitivity profiles for U235 in HEU-MET-FAST-085-002.

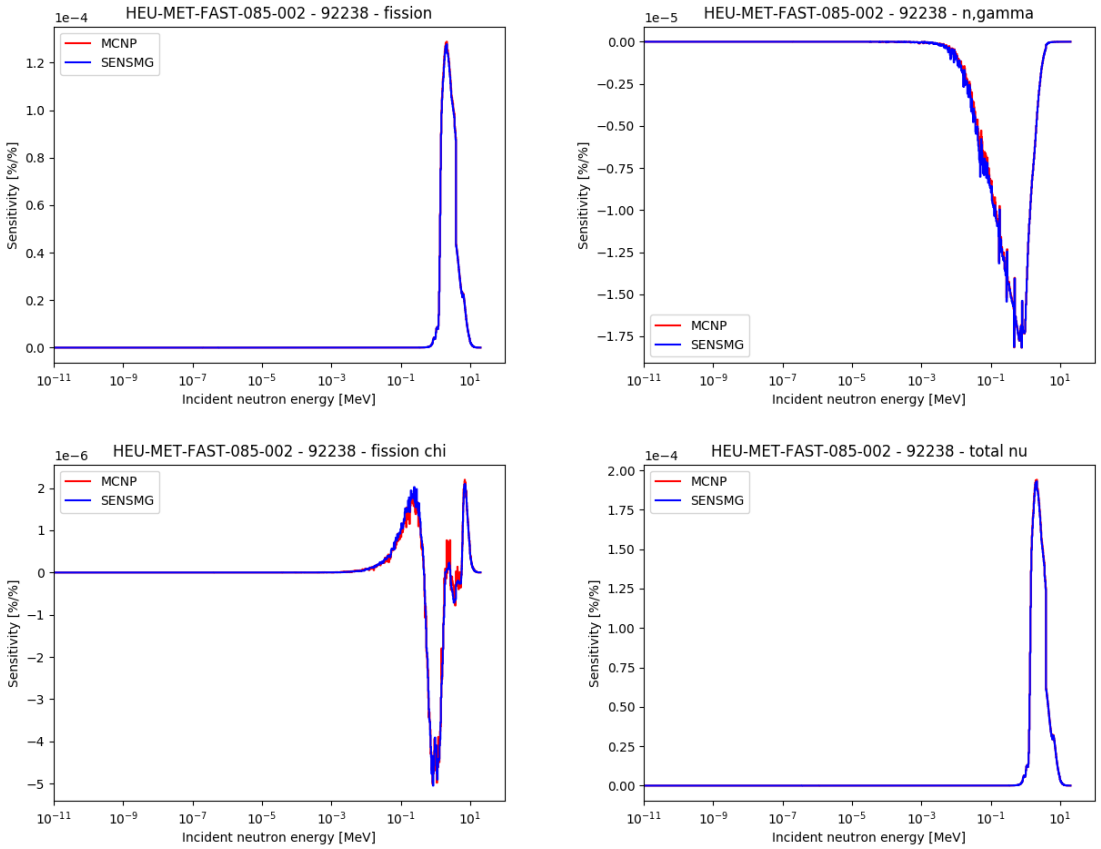

Figure 5.50: Sensitivity profiles for U238 in HEU-MET-FAST-085-002.

5.14 HEU-MET-FAST-085-003

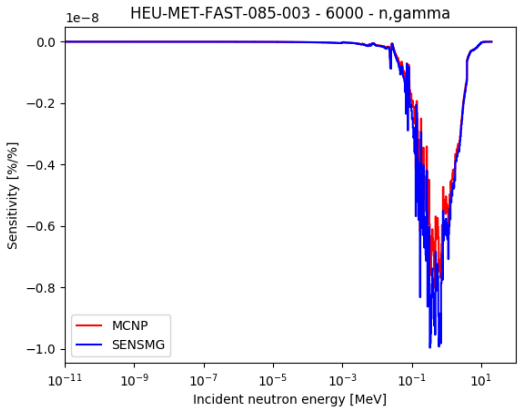

Figure 5.51: Sensitivity profiles for C in HEU-MET-FAST-085-003.

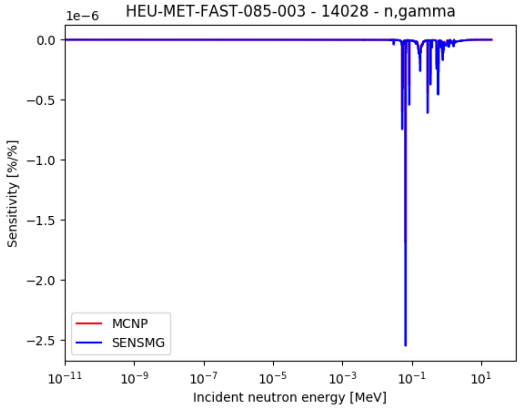

Figure 5.52: Sensitivity profiles for Si28 in HEU-MET-FAST-085-003.

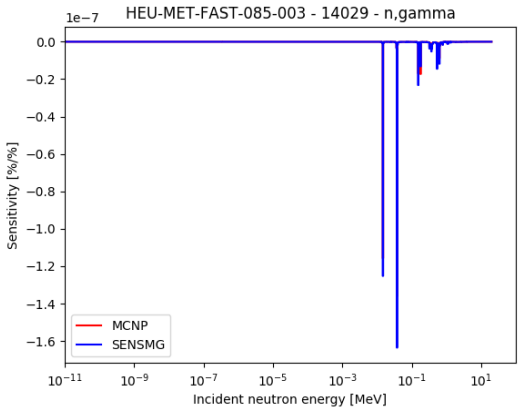

Figure 5.53: Sensitivity profiles for Si29 in HEU-MET-FAST-085-003.

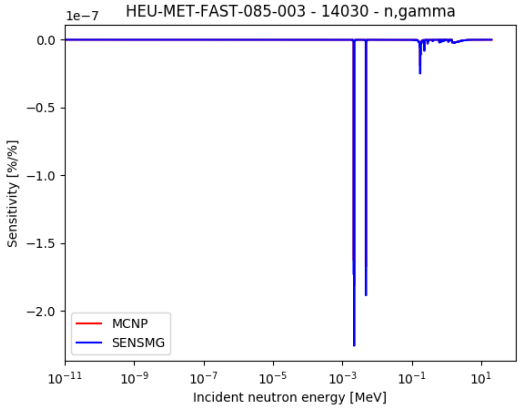

Figure 5.54: Sensitivity profiles for Si30 in HEU-MET-FAST-085-003.

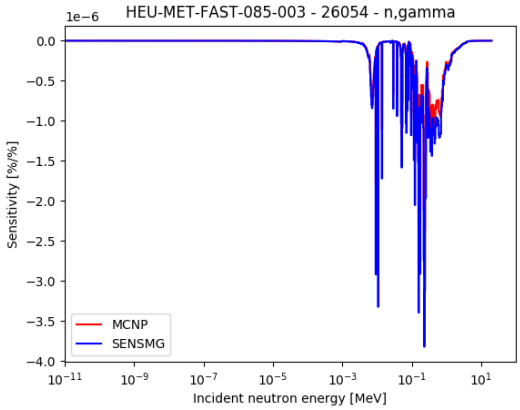

Figure 5.55: Sensitivity profiles for Fe54 in HEU-MET-FAST-085-003.

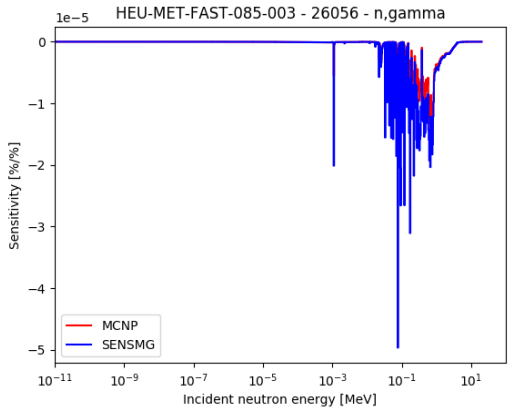

Figure 5.56: Sensitivity profiles for Fe56 in HEU-MET-FAST-085-003.

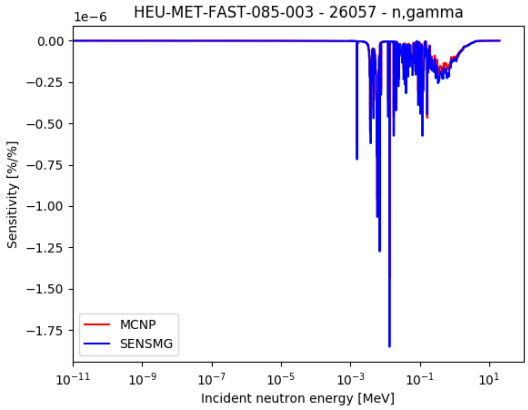

Figure 5.57: Sensitivity profiles for Fe57 in HEU-MET-FAST-085-003.

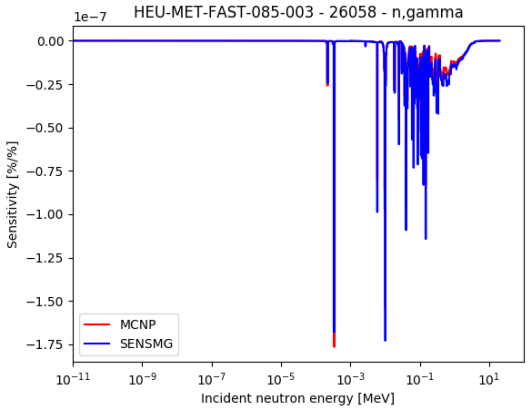

Figure 5.58: Sensitivity profiles for Fe58 in HEU-MET-FAST-085-003.

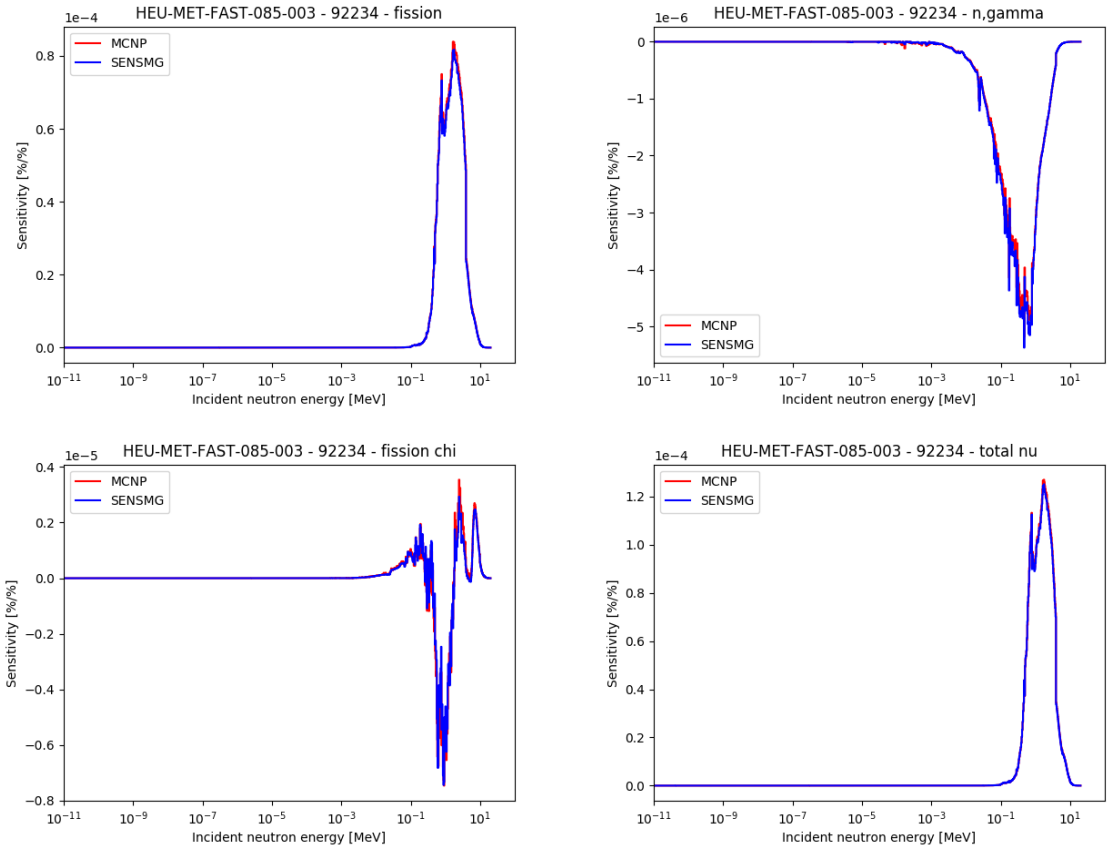

Figure 5.59: Sensitivity profiles for U234 in HEU-MET-FAST-085-003.

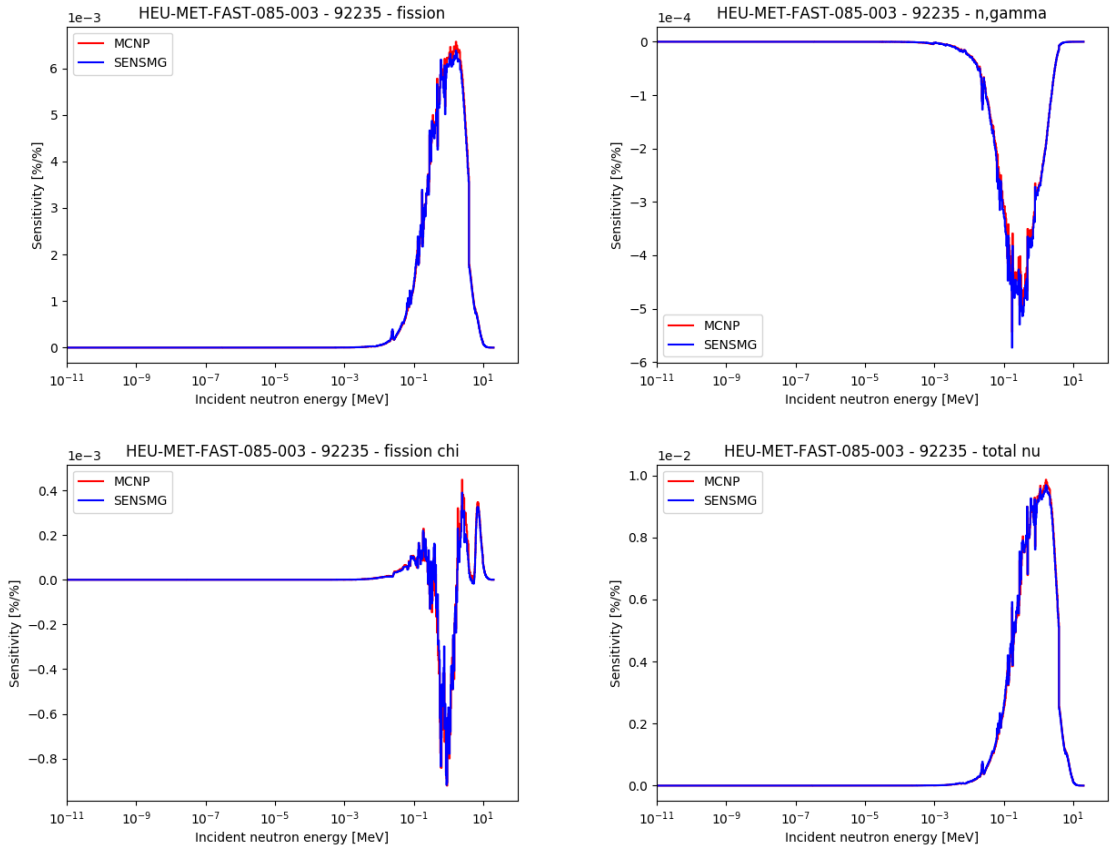

Figure 5.60: Sensitivity profiles for U235 in HEU-MET-FAST-085-003.

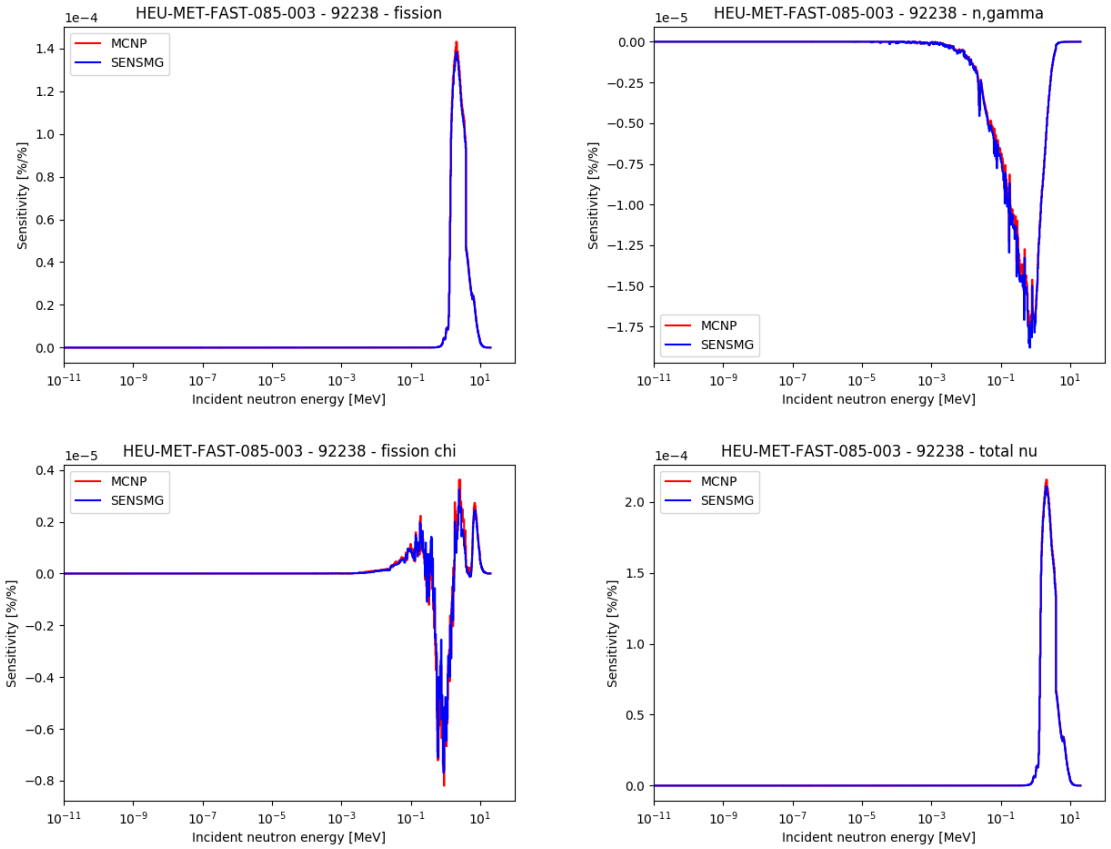

Figure 5.61: Sensitivity profiles for U238 in HEU-MET-FAST-085-003.

5.15 HEU-MET-FAST-085-004

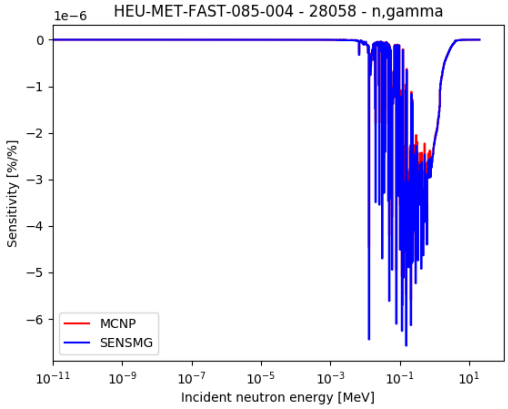

Figure 5.62: Sensitivity profiles for Ni58 in HEU-MET-FAST-085-004.

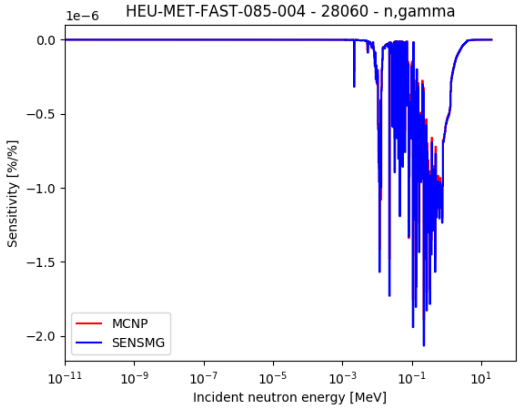

Figure 5.63: Sensitivity profiles for Ni60 in HEU-MET-FAST-085-004.

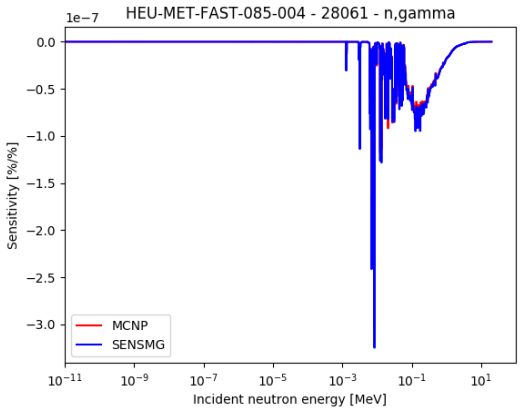

Figure 5.64: Sensitivity profiles for Ni61 in HEU-MET-FAST-085-004.

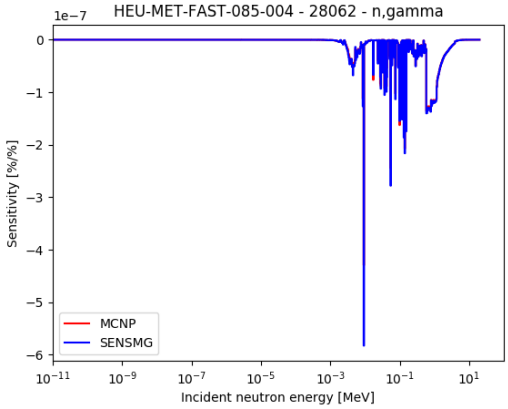

Figure 5.65: Sensitivity profiles for Ni62 in HEU-MET-FAST-085-004.

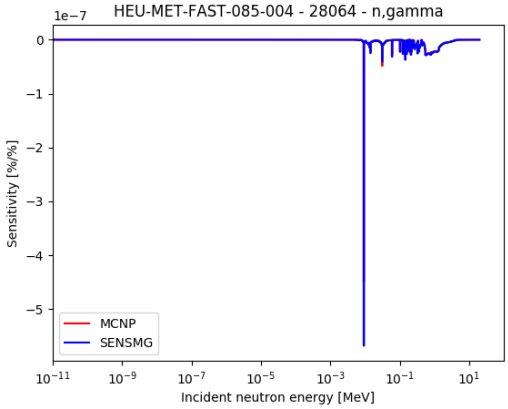

Figure 5.66: Sensitivity profiles for Ni64 in HEU-MET-FAST-085-004.

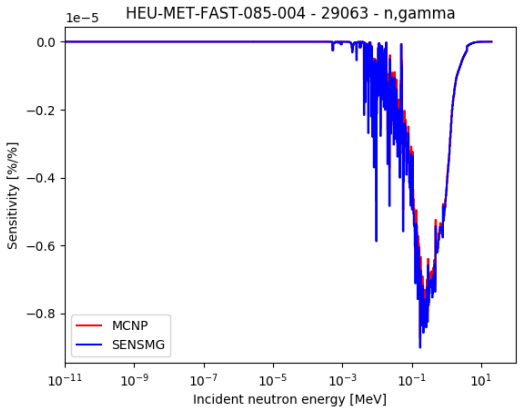

Figure 5.67: Sensitivity profiles for Cu63 in HEU-MET-FAST-085-004.

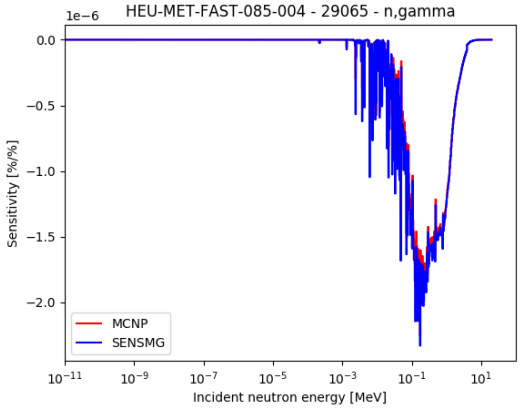

Figure 5.68: Sensitivity profiles for Cu65 in HEU-MET-FAST-085-004.

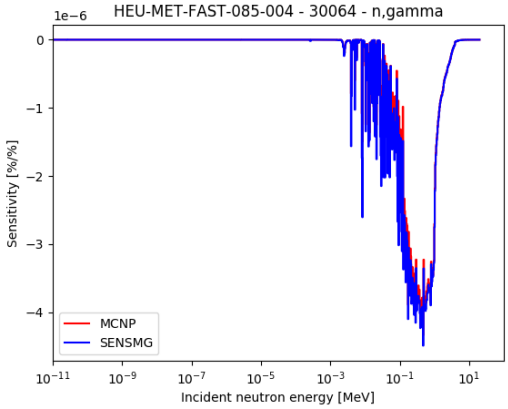

Figure 5.69: Sensitivity profiles for Zn64 in HEU-MET-FAST-085-004.

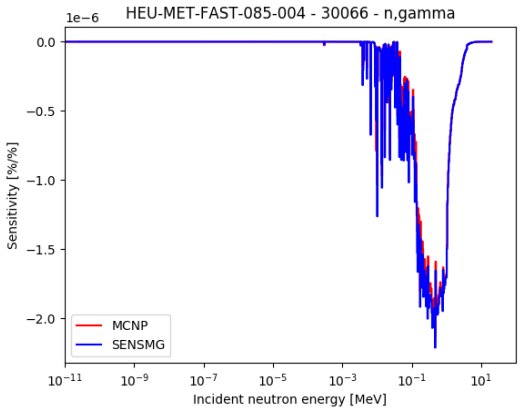

Figure 5.70: Sensitivity profiles for Zn66 in HEU-MET-FAST-085-004.

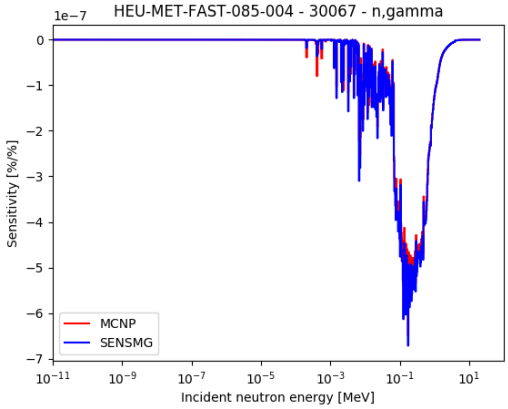

Figure 5.71: Sensitivity profiles for Zn67 in HEU-MET-FAST-085-004.

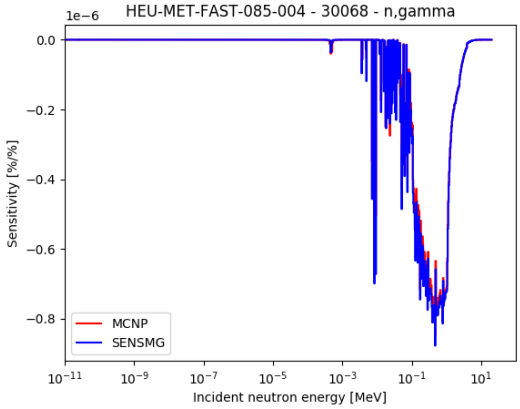

Figure 5.72: Sensitivity profiles for Zn68 in HEU-MET-FAST-085-004.

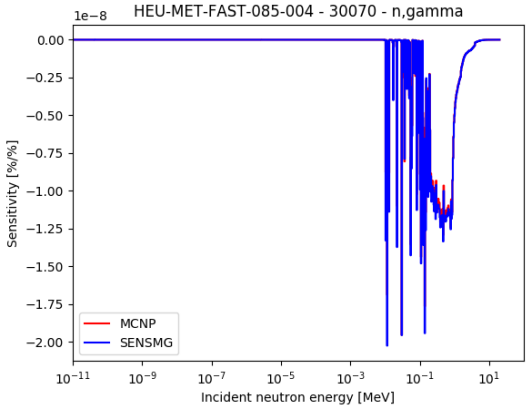

Figure 5.73: Sensitivity profiles for Zn70 in HEU-MET-FAST-085-004.

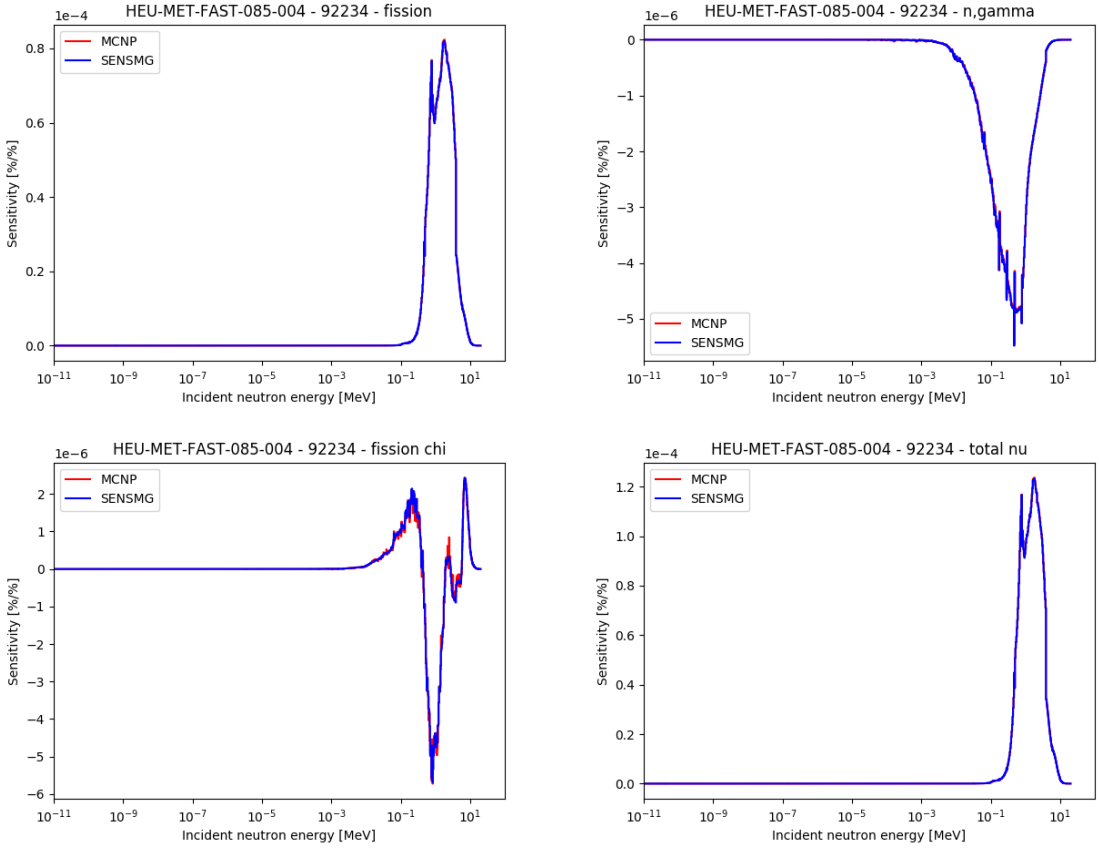

Figure 5.74: Sensitivity profiles for U234 in HEU-MET-FAST-085-004.

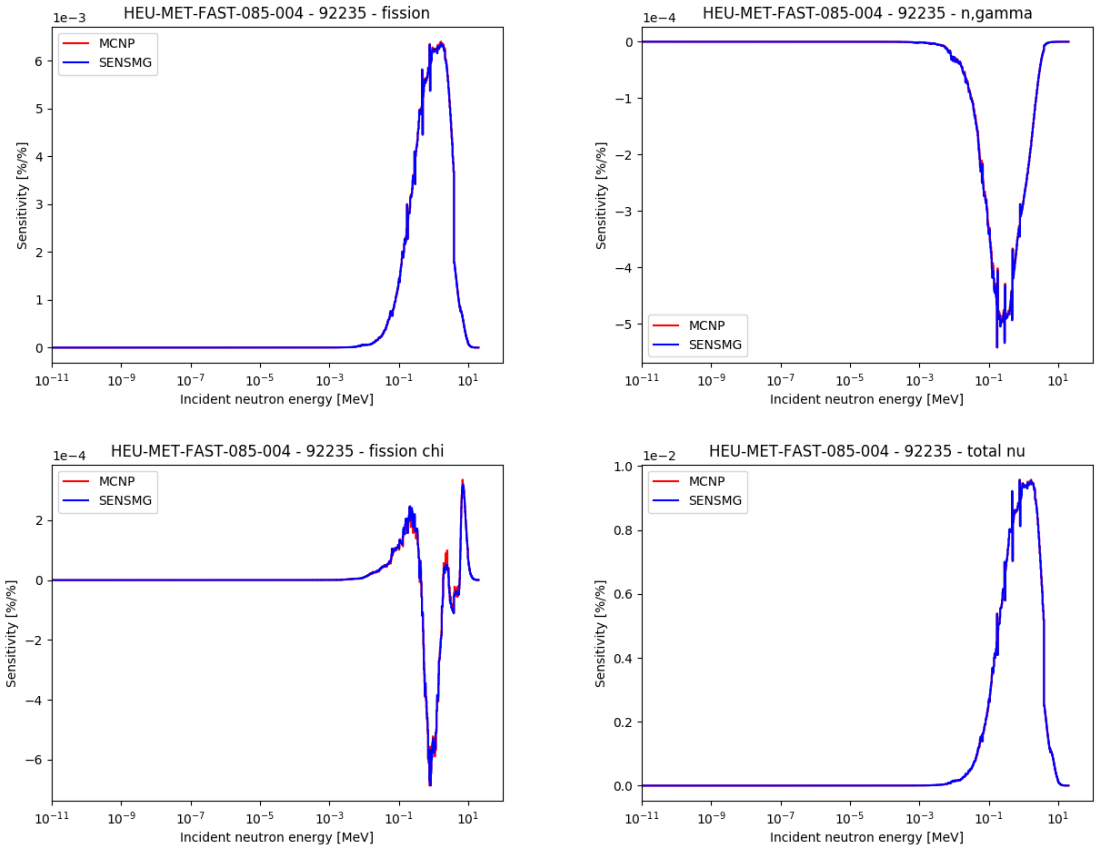

Figure 5.75: Sensitivity profiles for U235 in HEU-MET-FAST-085-004.

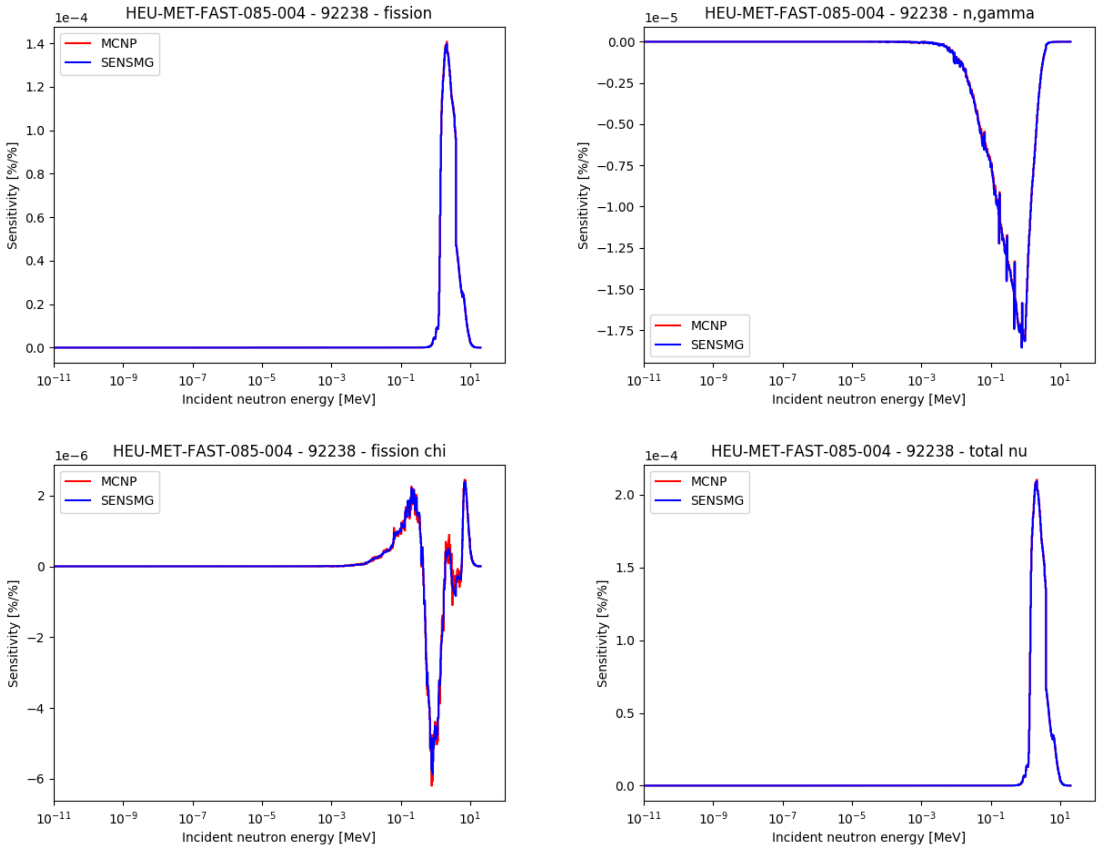

Figure 5.76: Sensitivity profiles for U238 in HEU-MET-FAST-085-004.

5.16 HEU-MET-FAST-085-005

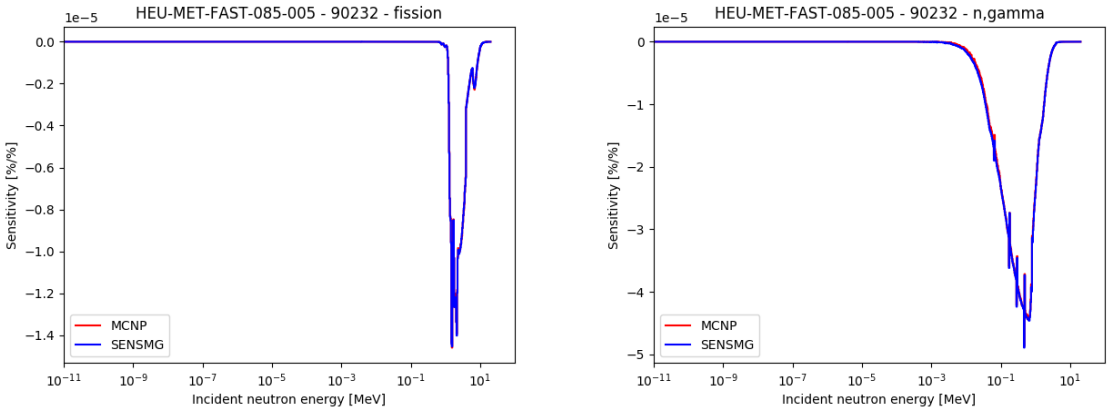

Figure 5.77: Sensitivity profiles for Th232 in HEU-MET-FAST-085-005.

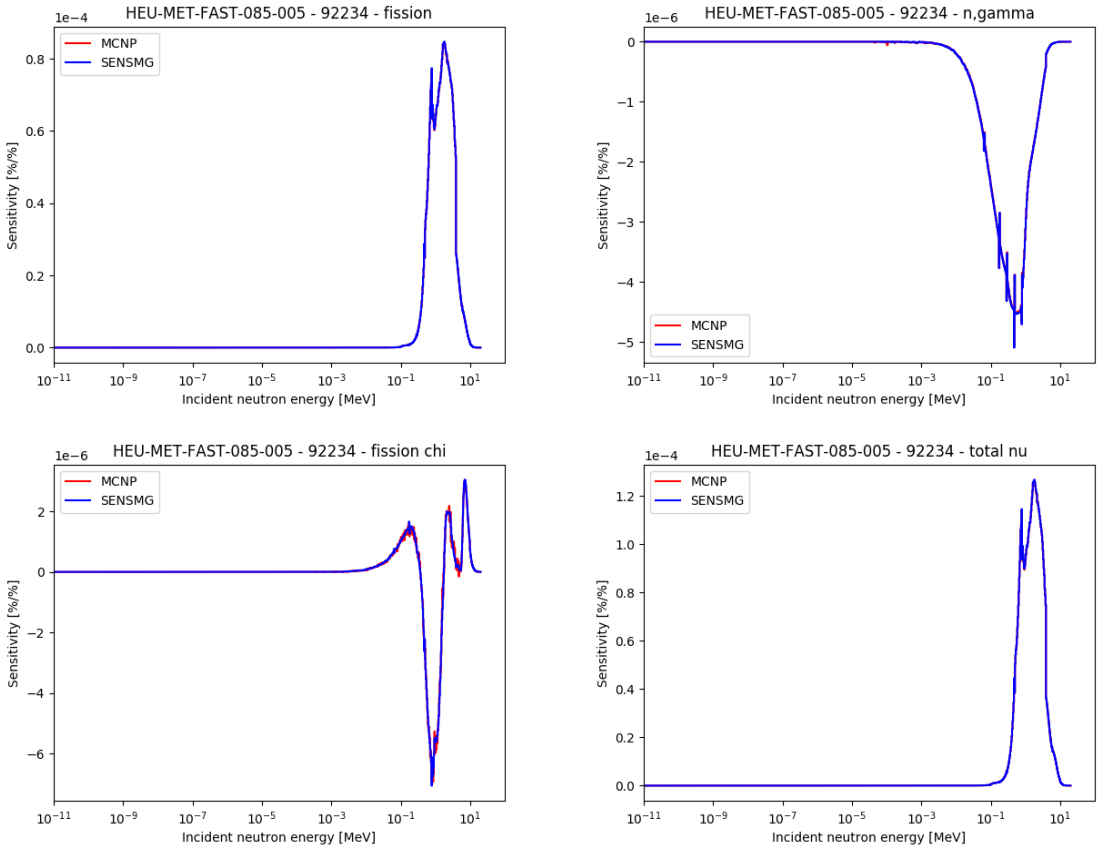

Figure 5.78: Sensitivity profiles for U234 in HEU-MET-FAST-085-005.

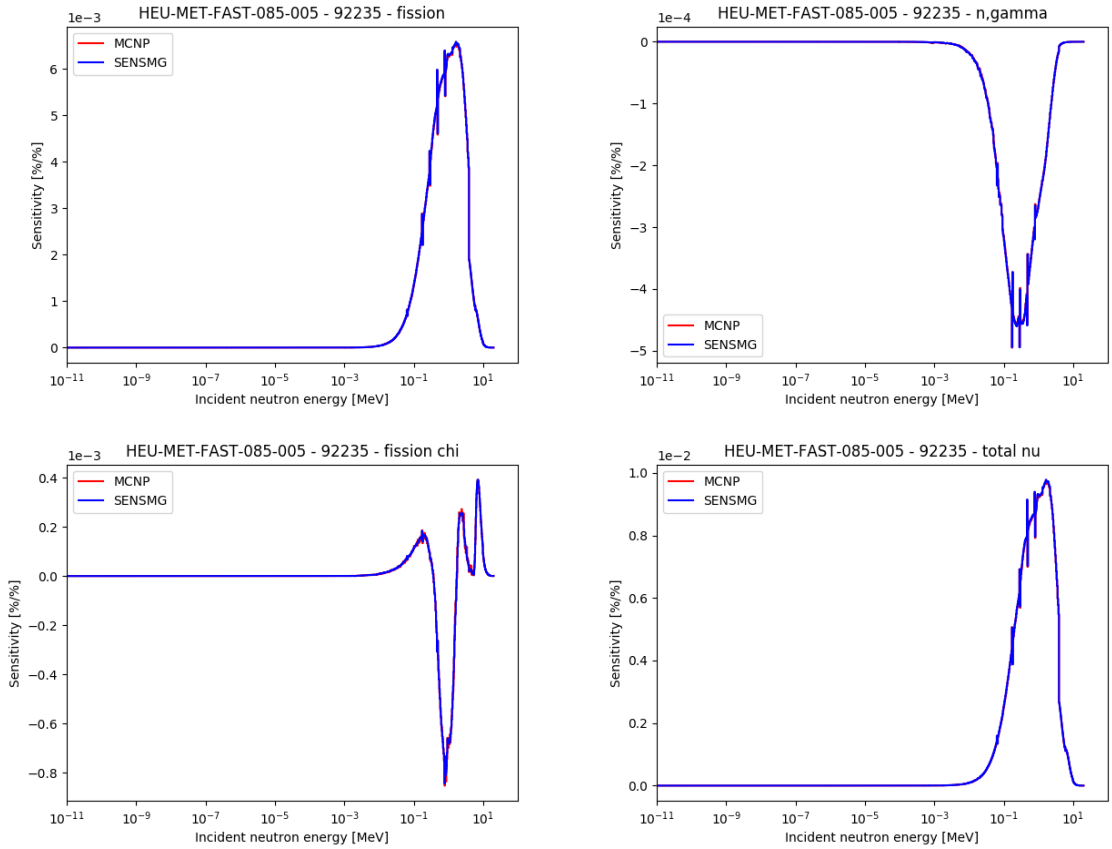

Figure 5.79: Sensitivity profiles for U235 in HEU-MET-FAST-085-005.

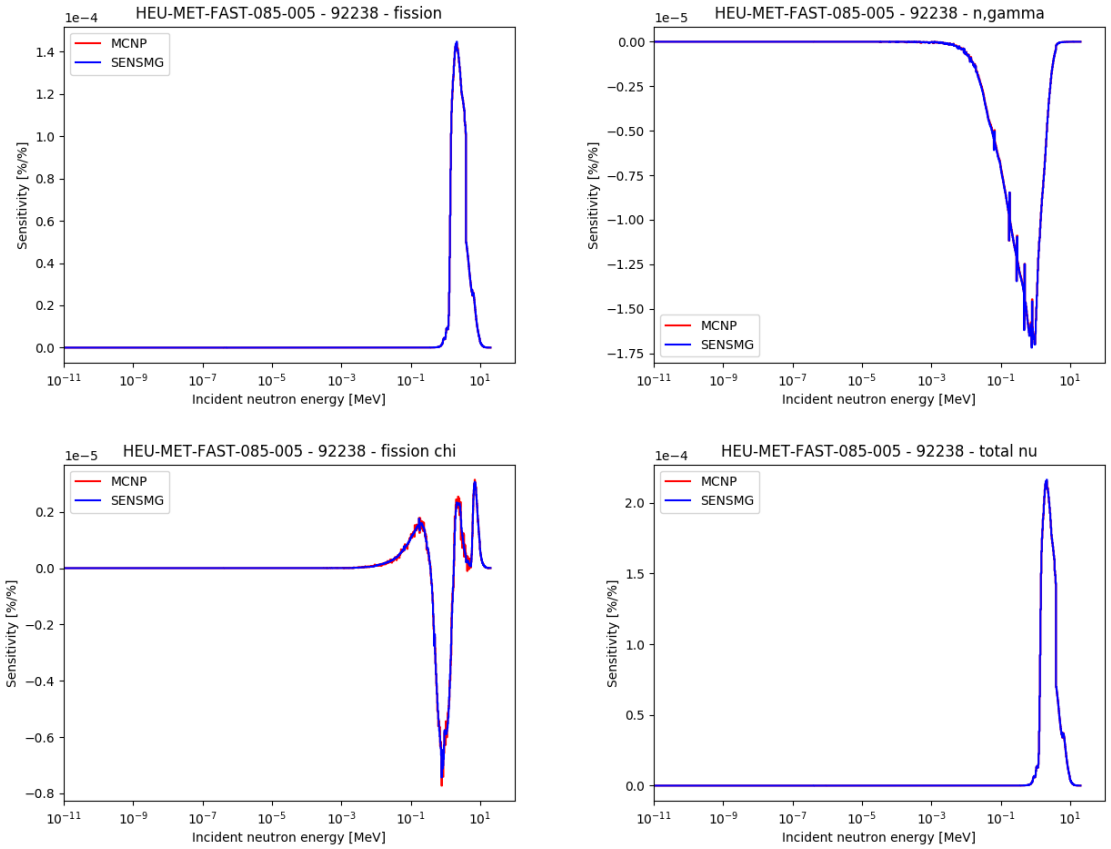

Figure 5.80: Sensitivity profiles for U238 in HEU-MET-FAST-085-005.

5.17 HEU-MET-FAST-085-006

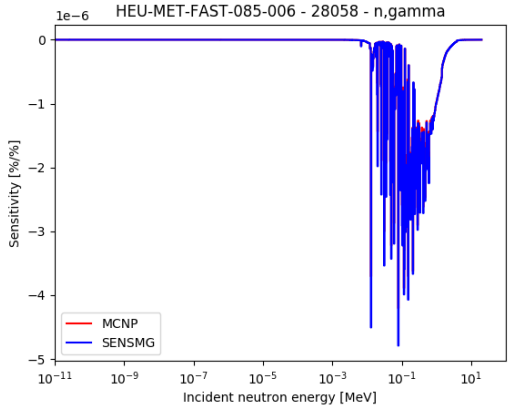

Figure 5.81: Sensitivity profiles for Ni58 in HEU-MET-FAST-085-006.

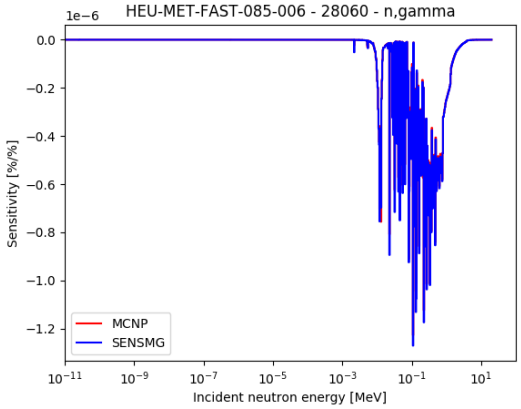

Figure 5.82: Sensitivity profiles for Ni60 in HEU-MET-FAST-085-006.

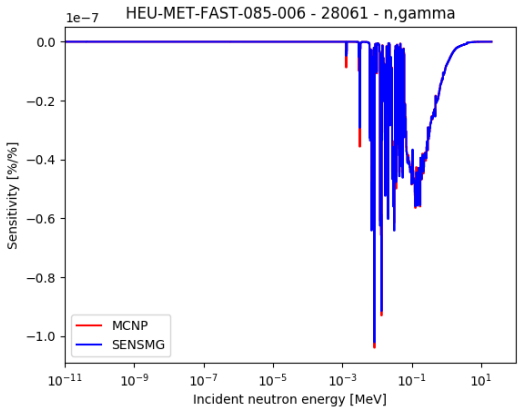

Figure 5.83: Sensitivity profiles for Ni61 in HEU-MET-FAST-085-006.

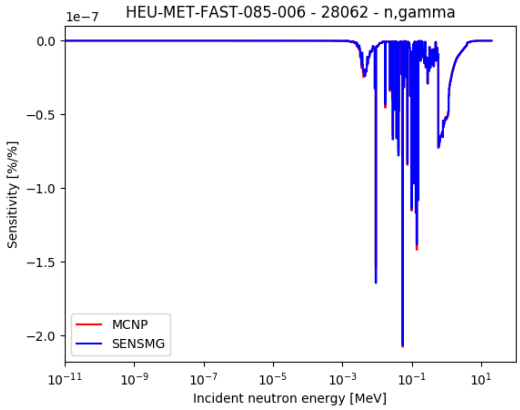

Figure 5.84: Sensitivity profiles for Ni62 in HEU-MET-FAST-085-006.

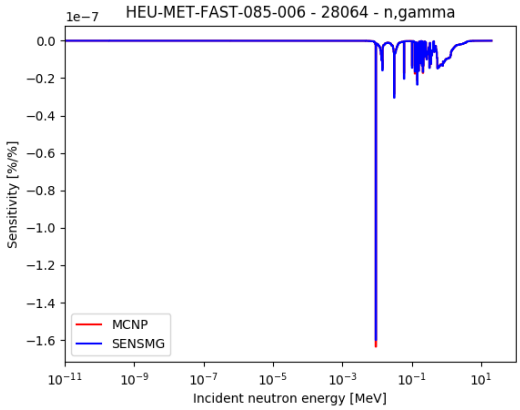

Figure 5.85: Sensitivity profiles for Ni64 in HEU-MET-FAST-085-006.

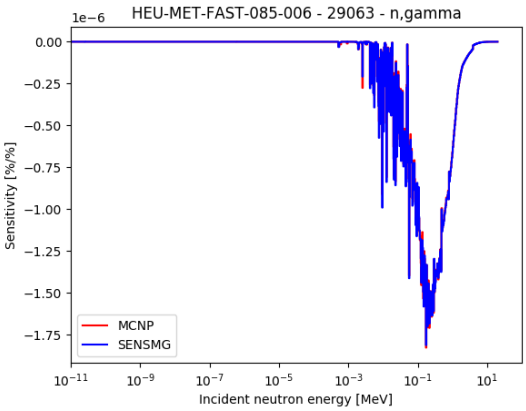

Figure 5.86: Sensitivity profiles for Cu63 in HEU-MET-FAST-085-006.

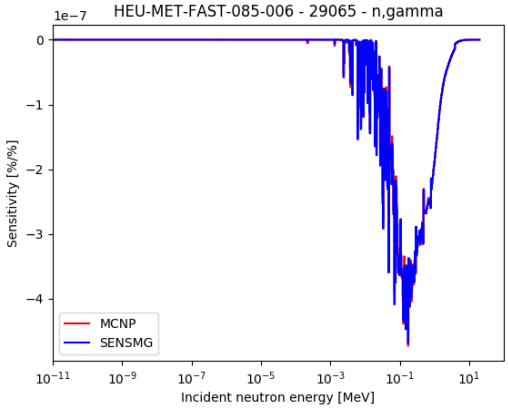

Figure 5.87: Sensitivity profiles for Cu65 in HEU-MET-FAST-085-006.

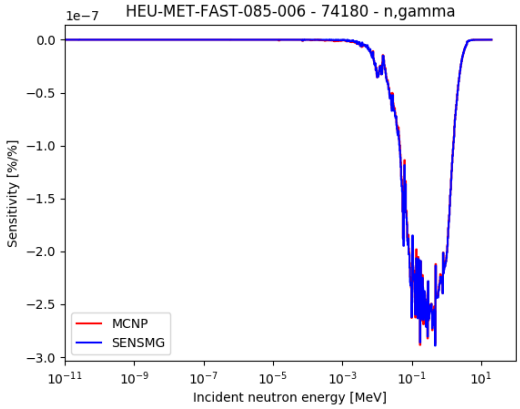

Figure 5.88: Sensitivity profiles for W180 in HEU-MET-FAST-085-006.

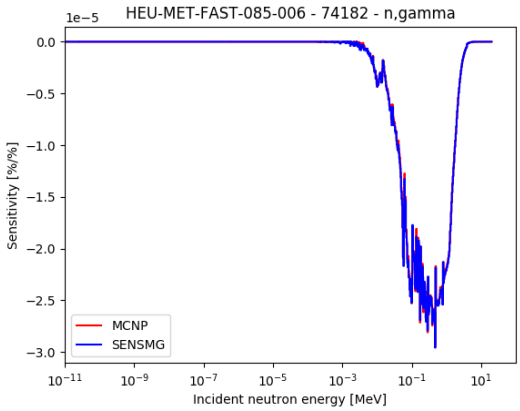

Figure 5.89: Sensitivity profiles for W182 in HEU-MET-FAST-085-006.

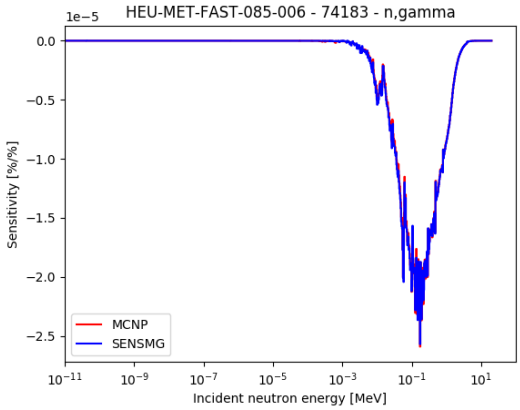

Figure 5.90: Sensitivity profiles for W183 in HEU-MET-FAST-085-006.

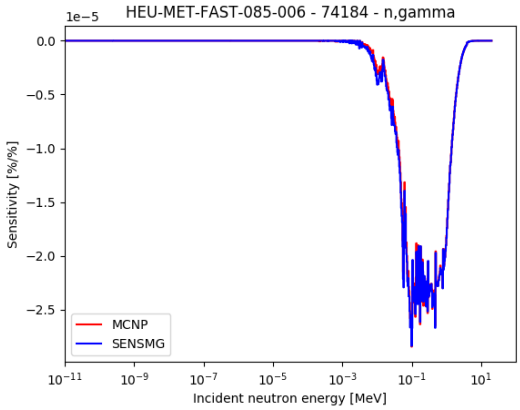

Figure 5.91: Sensitivity profiles for W184 in HEU-MET-FAST-085-006.

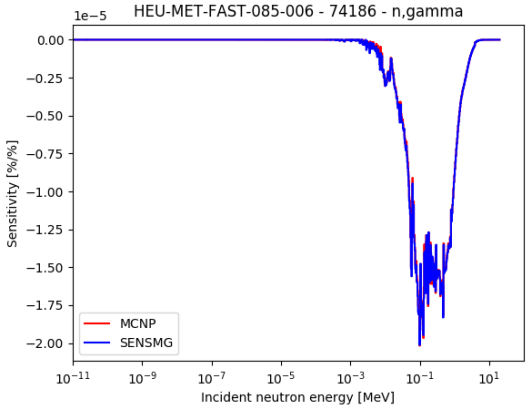

Figure 5.92: Sensitivity profiles for W186 in HEU-MET-FAST-085-006.

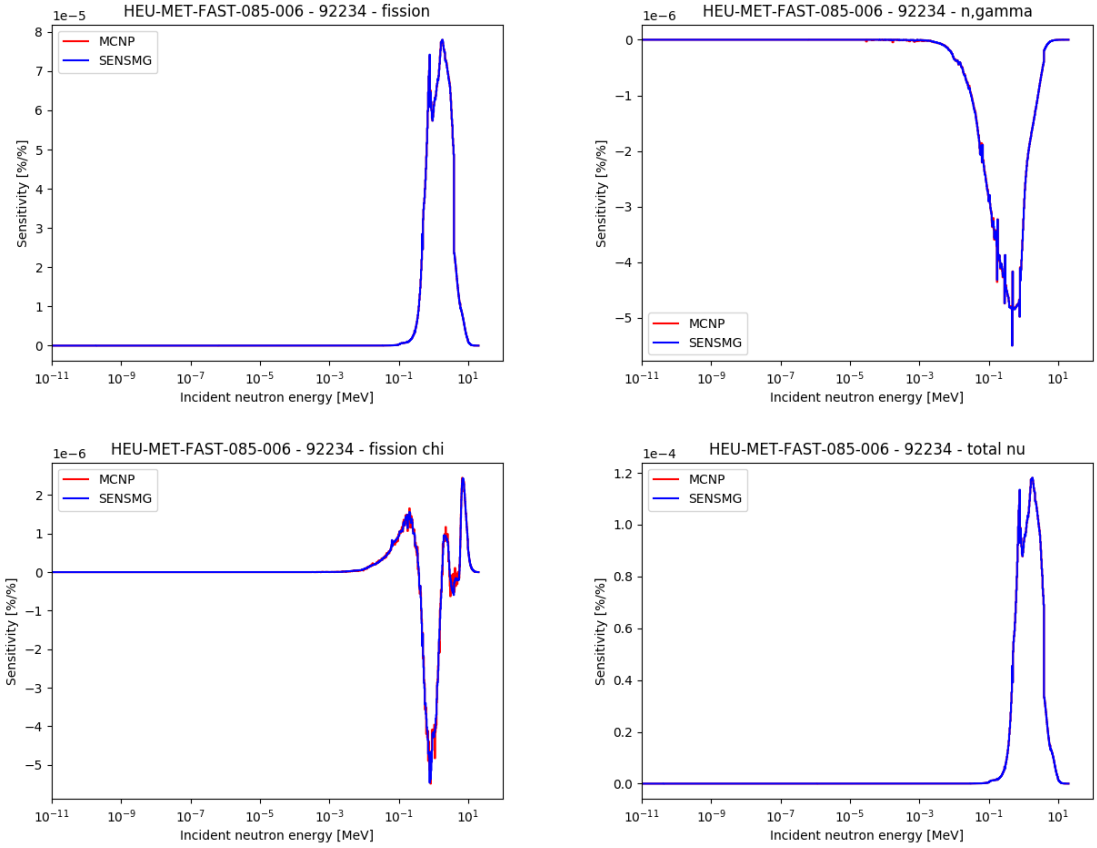

Figure 5.93: Sensitivity profiles for U234 in HEU-MET-FAST-085-006.

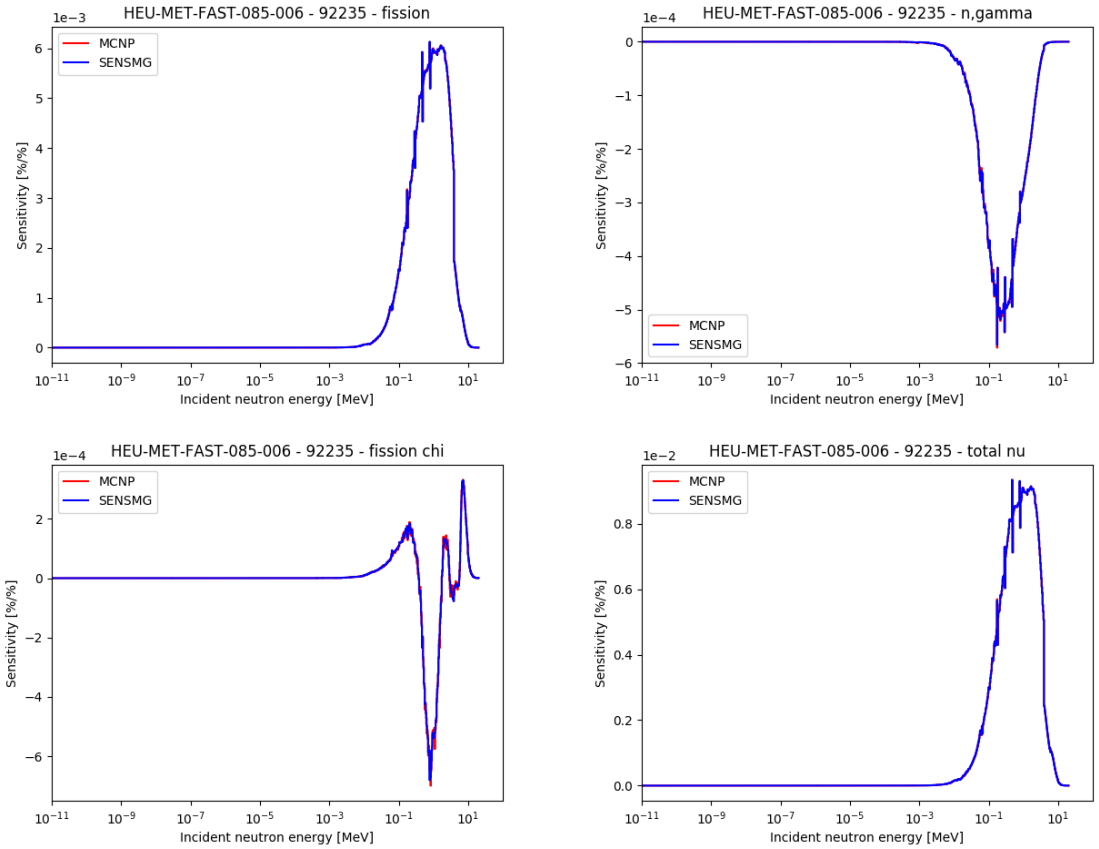

Figure 5.94: Sensitivity profiles for U235 in HEU-MET-FAST-085-006.

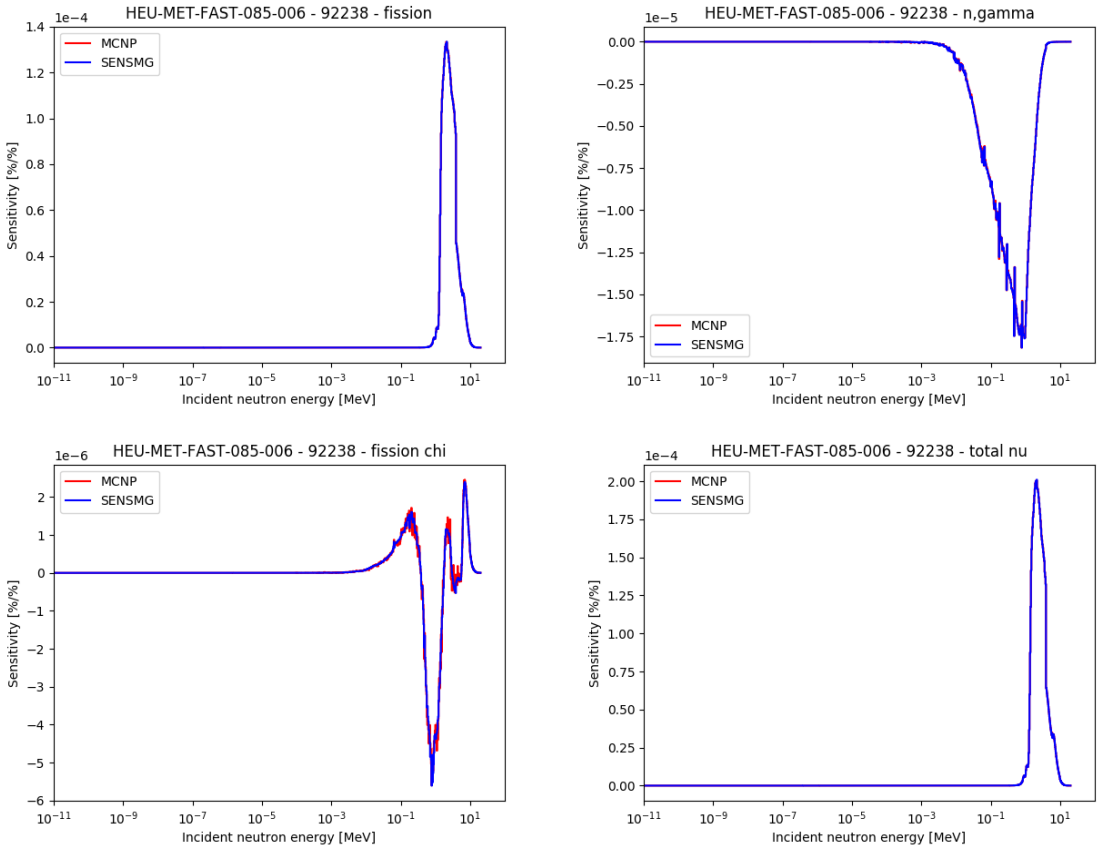

Figure 5.95: Sensitivity profiles for U238 in HEU-MET-FAST-085-006.

5.18 HEU-COMP-INTER-003-001

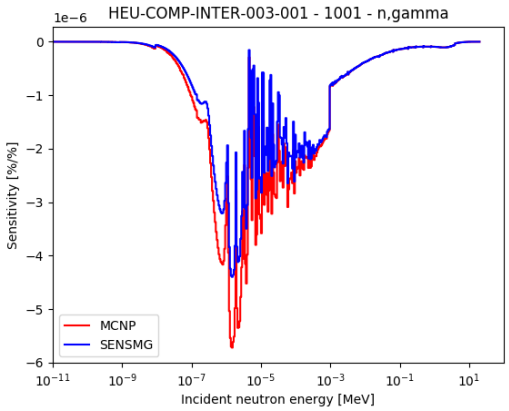

Figure 5.96: Sensitivity profiles for H1 in HEU-COMP-INTER-003-001.

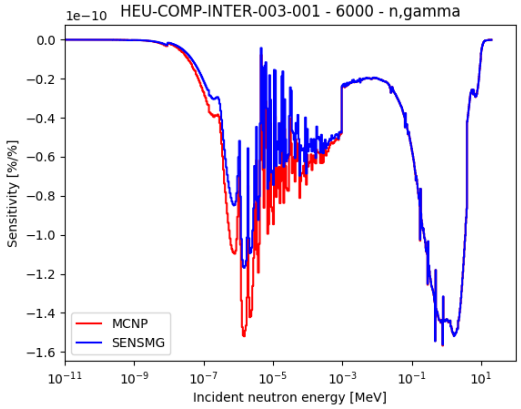

Figure 5.97: Sensitivity profiles for C in HEU-COMP-INTER-003-001.

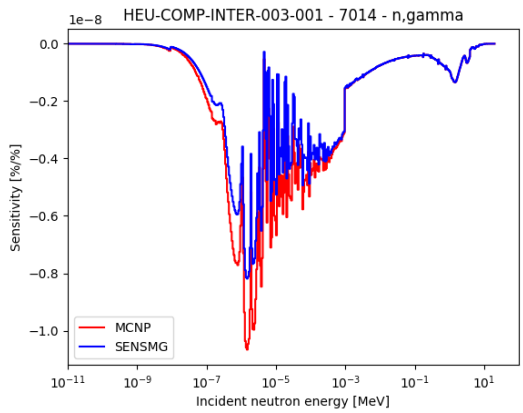

Figure 5.98: Sensitivity profiles for N14 in HEU-COMP-INTER-003-001.

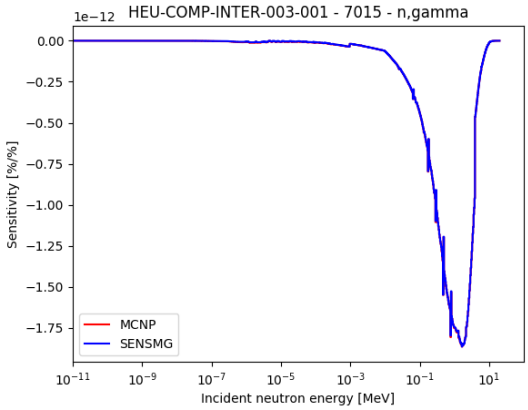

Figure 5.99: Sensitivity profiles for N15 in HEU-COMP-INTER-003-001.

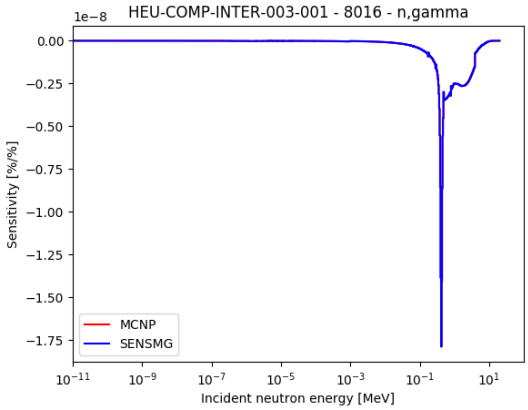

Figure 5.100: Sensitivity profiles for O16 in HEU-COMP-INTER-003-001.

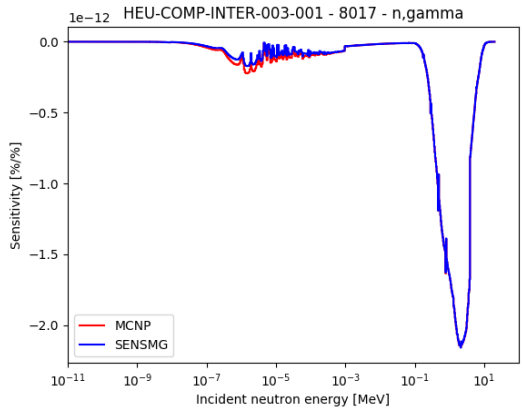

Figure 5.101: Sensitivity profiles for O17 in HEU-COMP-INTER-003-001.

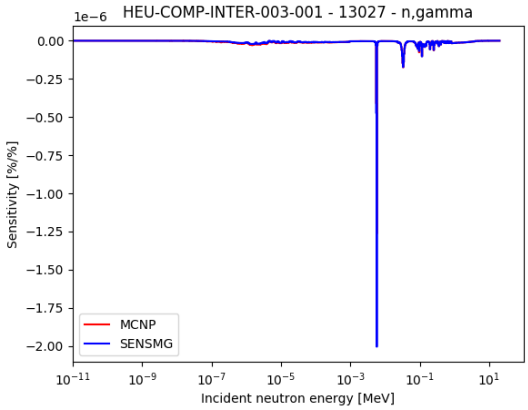

Figure 5.102: Sensitivity profiles for Al27 in HEU-COMP-INTER-003-001.

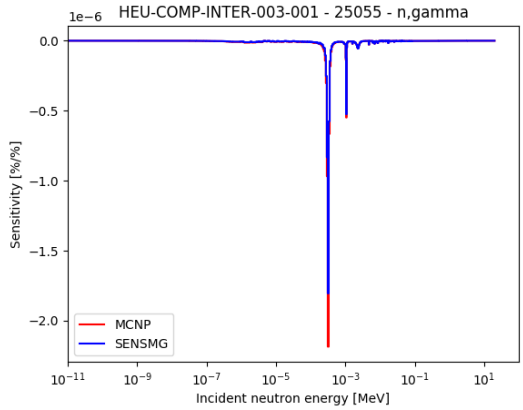

Figure 5.103: Sensitivity profiles for Mn55 in HEU-COMP-INTER-003-001.

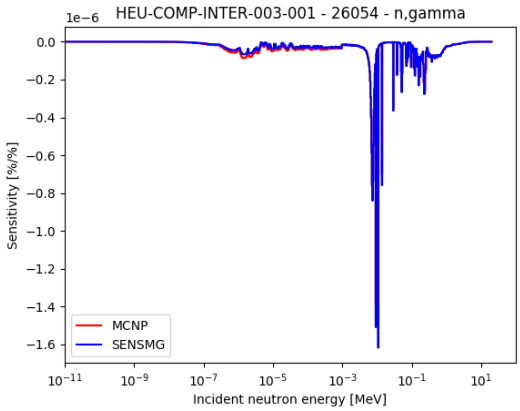

Figure 5.104: Sensitivity profiles for Fe54 in HEU-COMP-INTER-003-001.

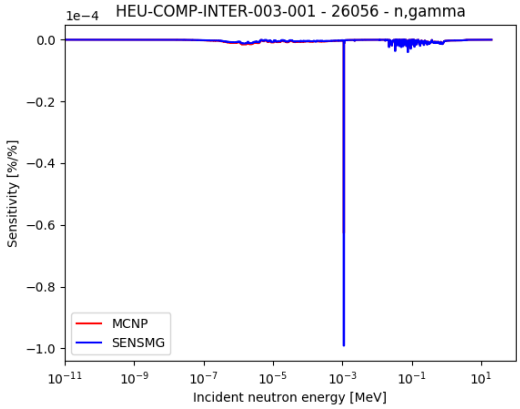

Figure 5.105: Sensitivity profiles for Fe55 in HEU-COMP-INTER-003-001.

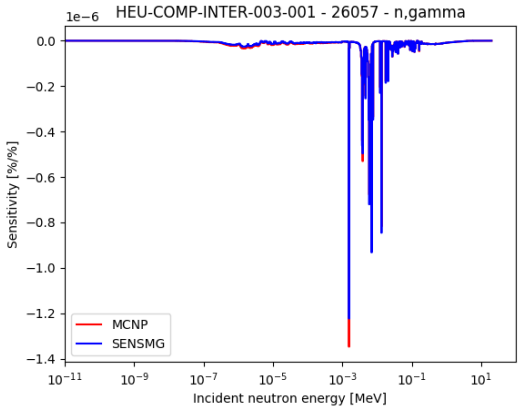

Figure 5.106: Sensitivity profiles for Fe57 in HEU-COMP-INTER-003-001.

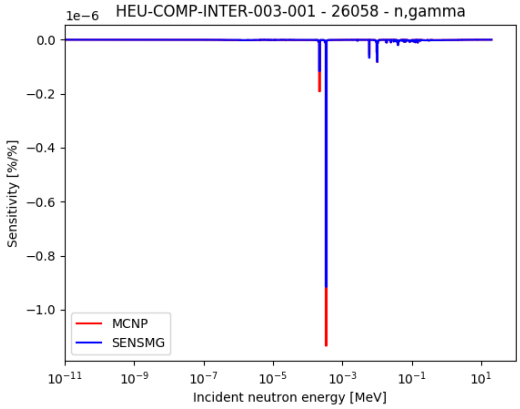

Figure 5.107: Sensitivity profiles for Fe58 in HEU-COMP-INTER-003-001.

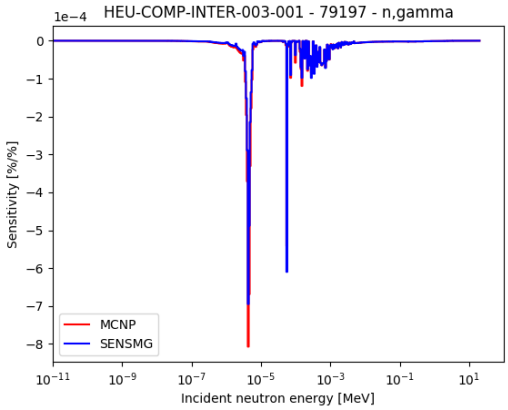

Figure 5.108: Sensitivity profiles for Au197 in HEU-COMP-INTER-003-001.

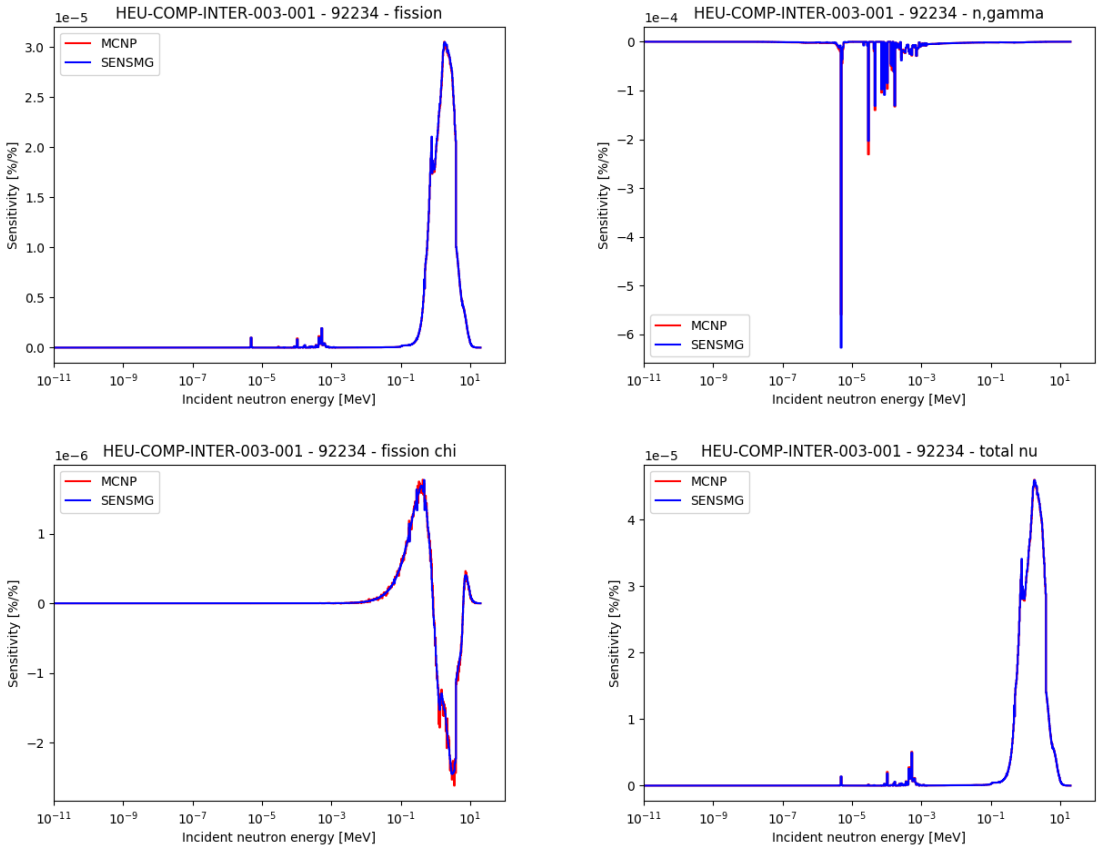

Figure 5.109: Sensitivity profiles for U234 in HEU-COMP-INTER-003-001.

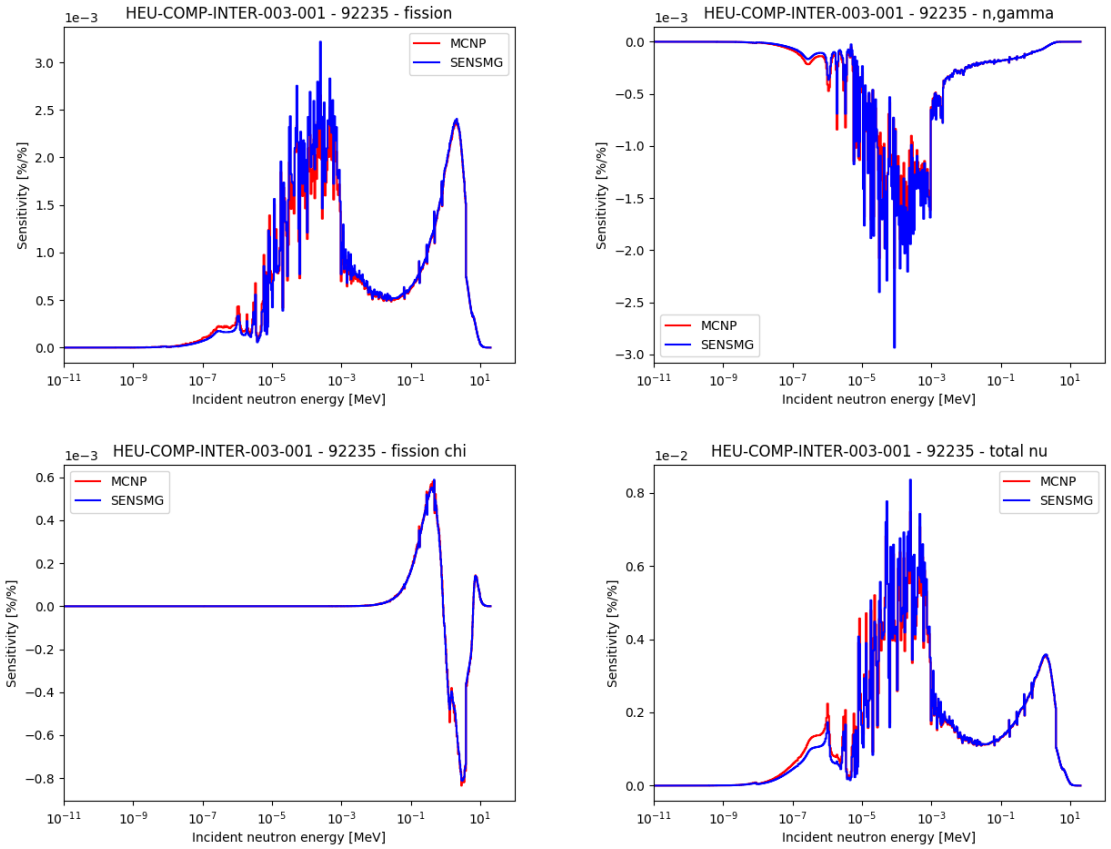

Figure 5.110: Sensitivity profiles for U235 in HEU-COMP-INTER-003-001.

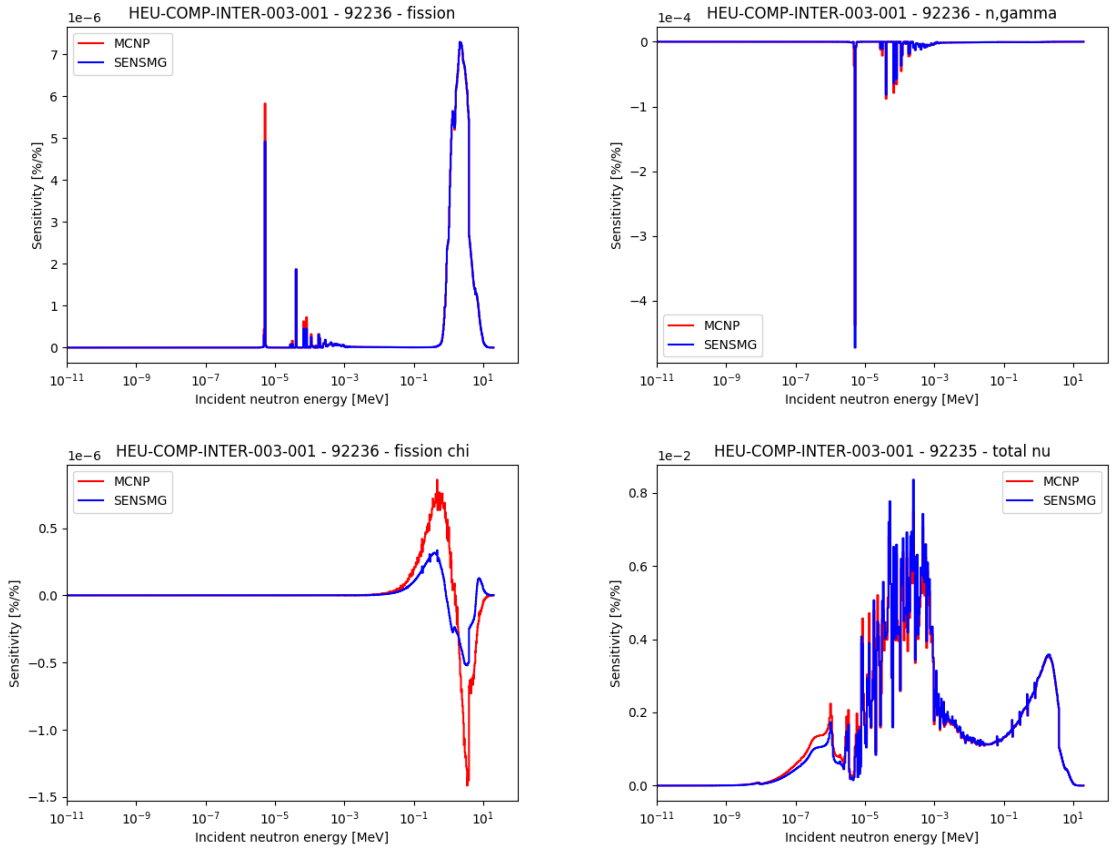

Figure 5.111: Sensitivity profiles for U236 in HEU-COMP-INTER-003-001.

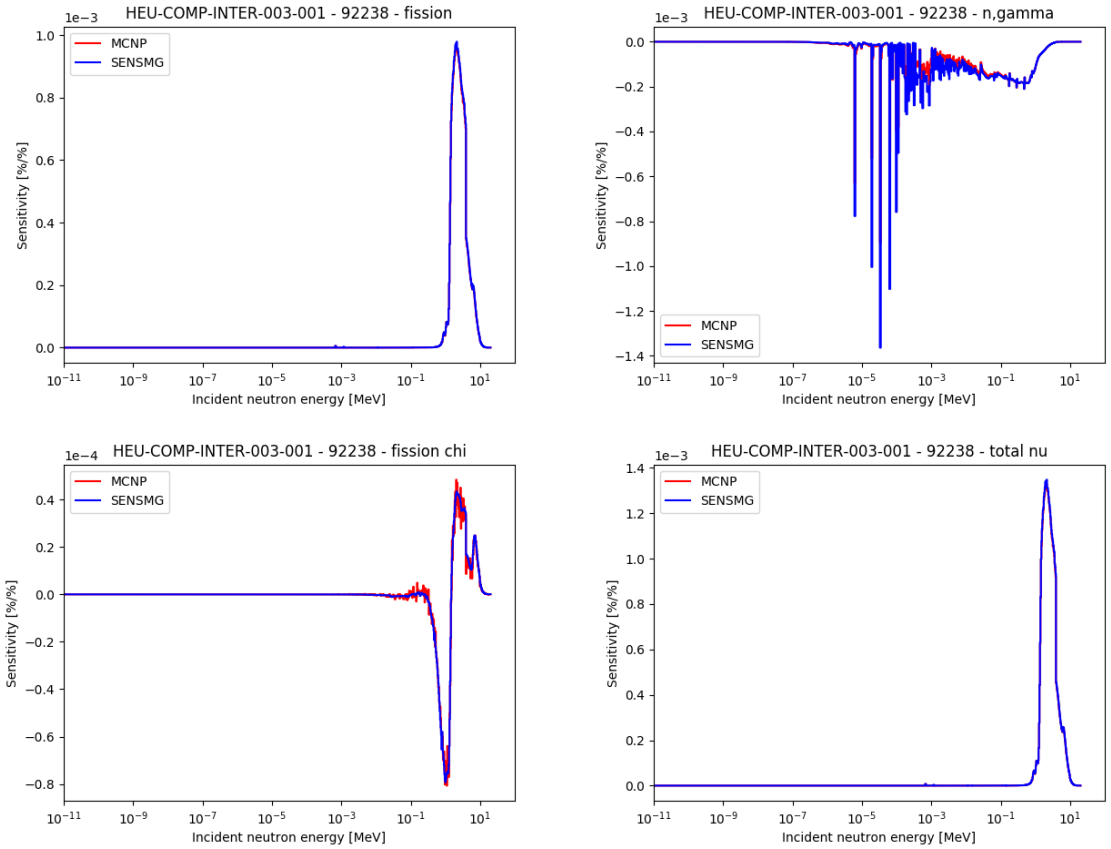

Figure 5.112: Sensitivity profiles for U238 in HEU-COMP-INTER-003-001.

5.19 HEU-COMP-INTER-003-002

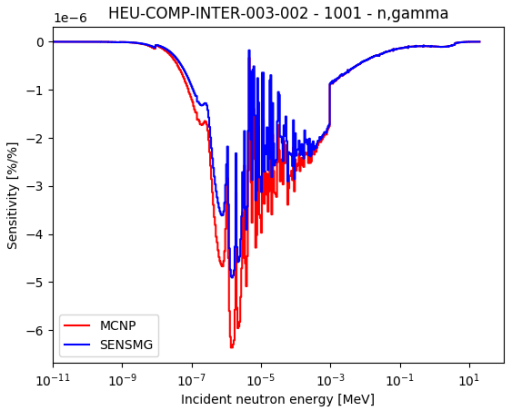

Figure 5.113: Sensitivity profiles for H1 in HEU-COMP-INTER-003-002.

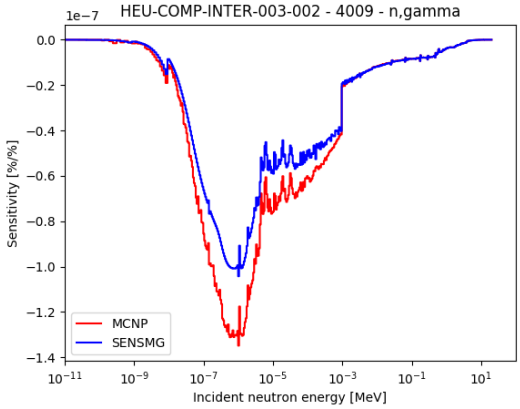

Figure 5.114: Sensitivity profiles for Be9 in HEU-COMP-INTER-003-002.

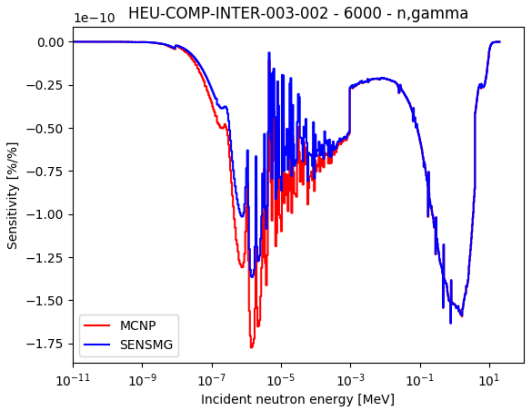

Figure 5.115: Sensitivity profiles for C in HEU-COMP-INTER-003-002.

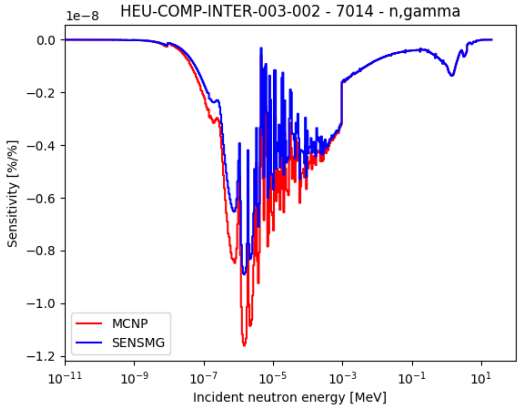

Figure 5.116: Sensitivity profiles for N14 in HEU-COMP-INTER-003-002.

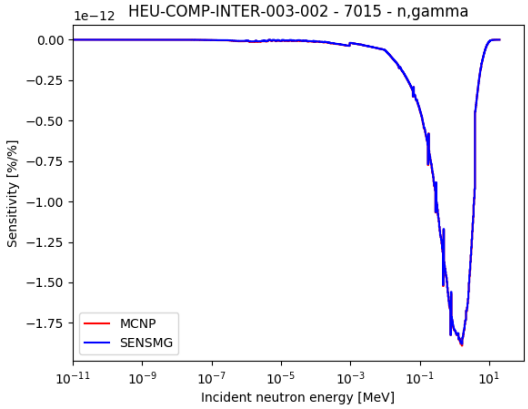

Figure 5.117: Sensitivity profiles for N15 in HEU-COMP-INTER-003-002.

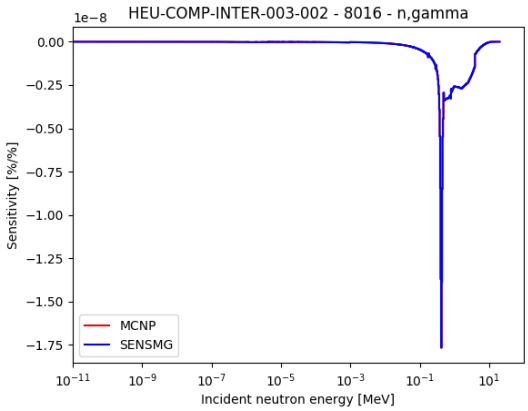

Figure 5.118: Sensitivity profiles for O16 in HEU-COMP-INTER-003-002.

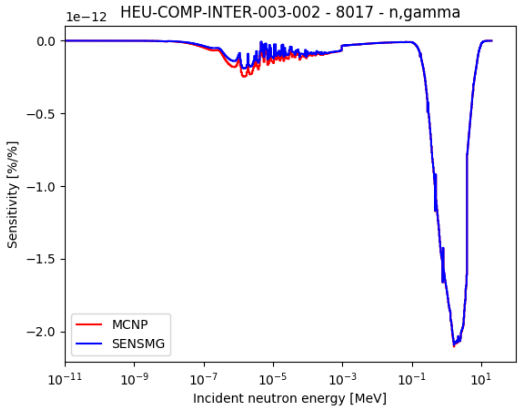

Figure 5.119: Sensitivity profiles for O17 in HEU-COMP-INTER-003-002.

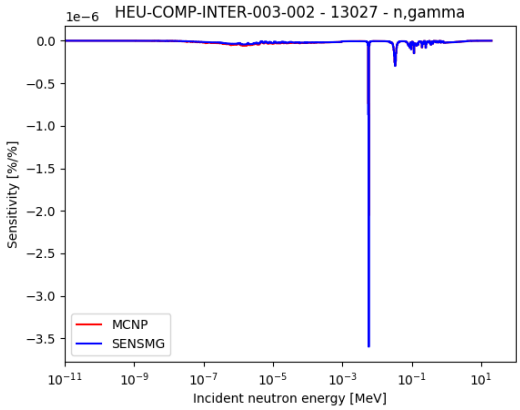

Figure 5.120: Sensitivity profiles for Al27 in HEU-COMP-INTER-003-002.

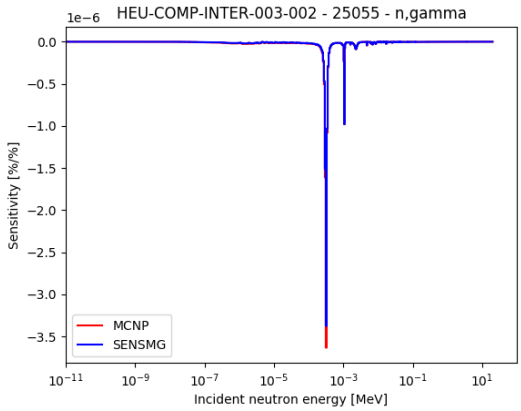

Figure 5.121: Sensitivity profiles for Mn55 in HEU-COMP-INTER-003-002.

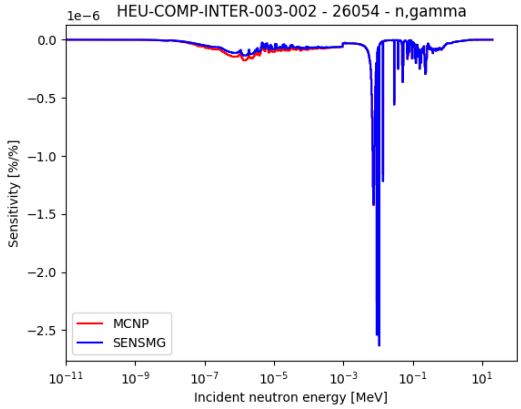

Figure 5.122: Sensitivity profiles for Fe54 in HEU-COMP-INTER-003-002.

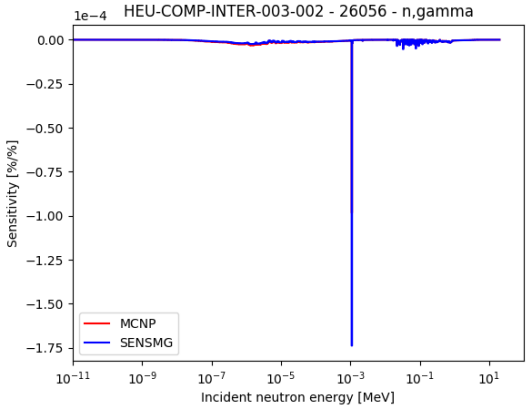

Figure 5.123: Sensitivity profiles for Fe55 in HEU-COMP-INTER-003-002.

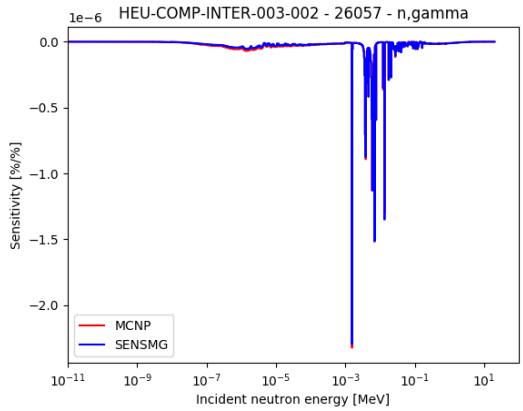

Figure 5.124: Sensitivity profiles for Fe57 in HEU-COMP-INTER-003-002.

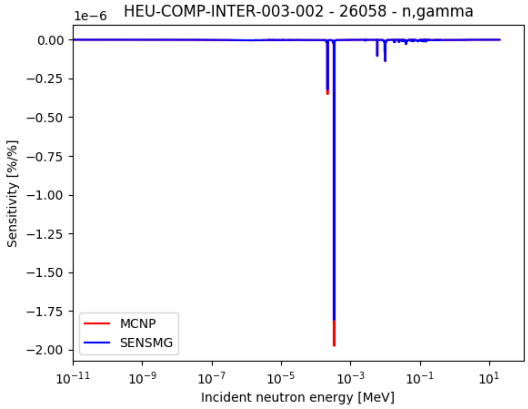

Figure 5.125: Sensitivity profiles for Fe58 in HEU-COMP-INTER-003-002.

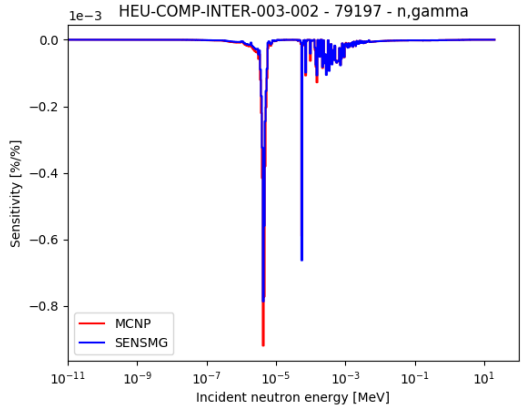

Figure 5.126: Sensitivity profiles for Au197 in HEU-COMP-INTER-003-002.

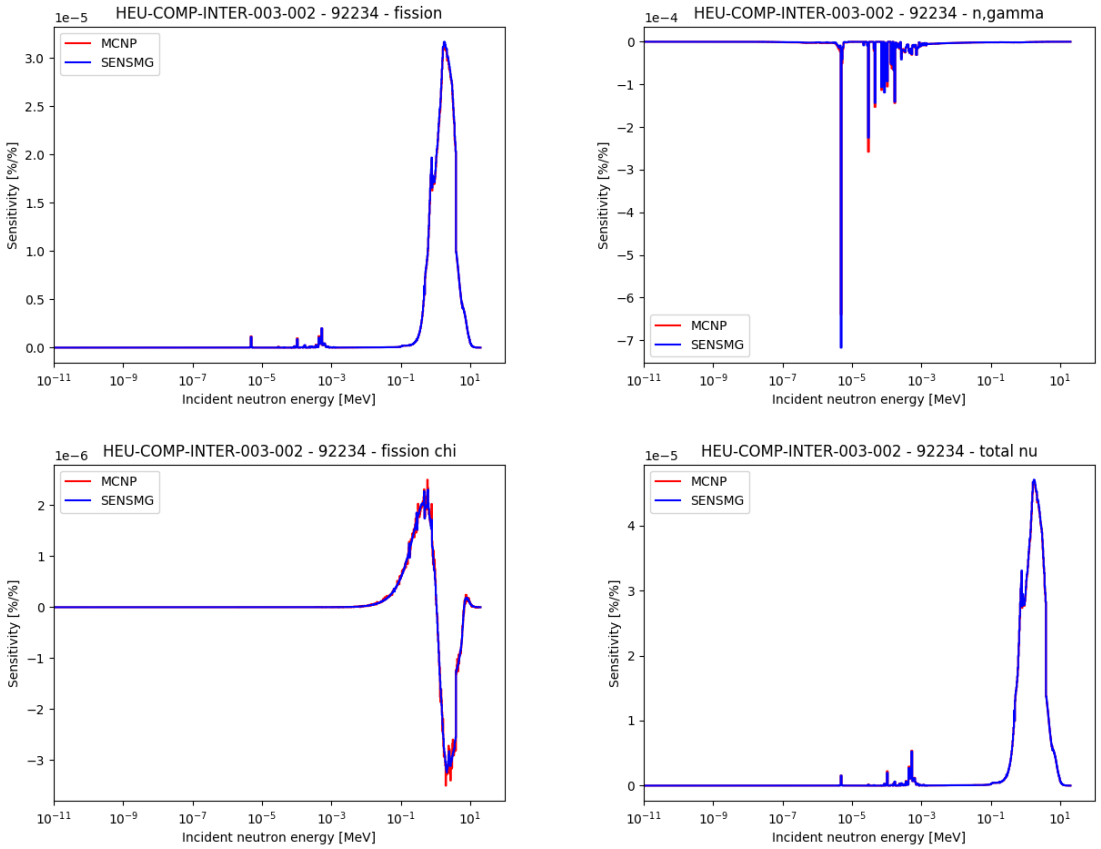

Figure 5.127: Sensitivity profiles for U234 in HEU-COMP-INTER-003-002.

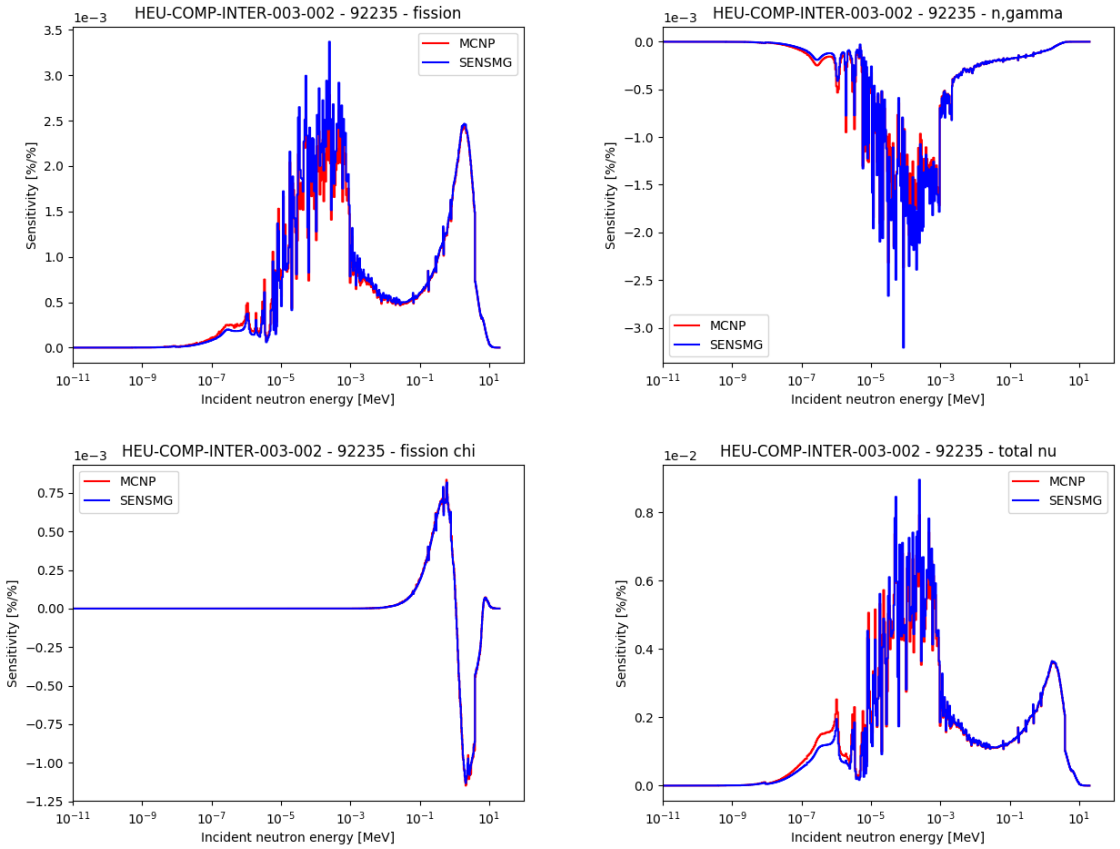

Figure 5.128: Sensitivity profiles for U235 in HEU-COMP-INTER-003-002.

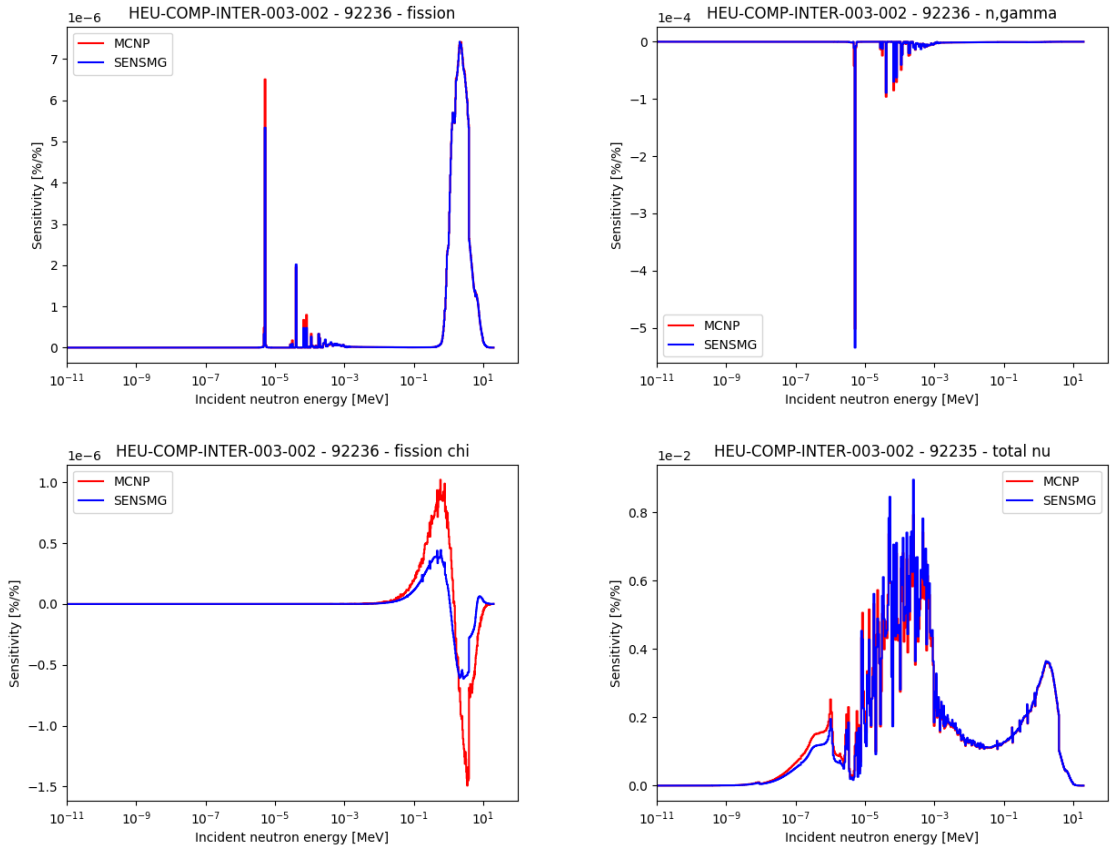

Figure 5.129: Sensitivity profiles for U236 in HEU-COMP-INTER-003-002.

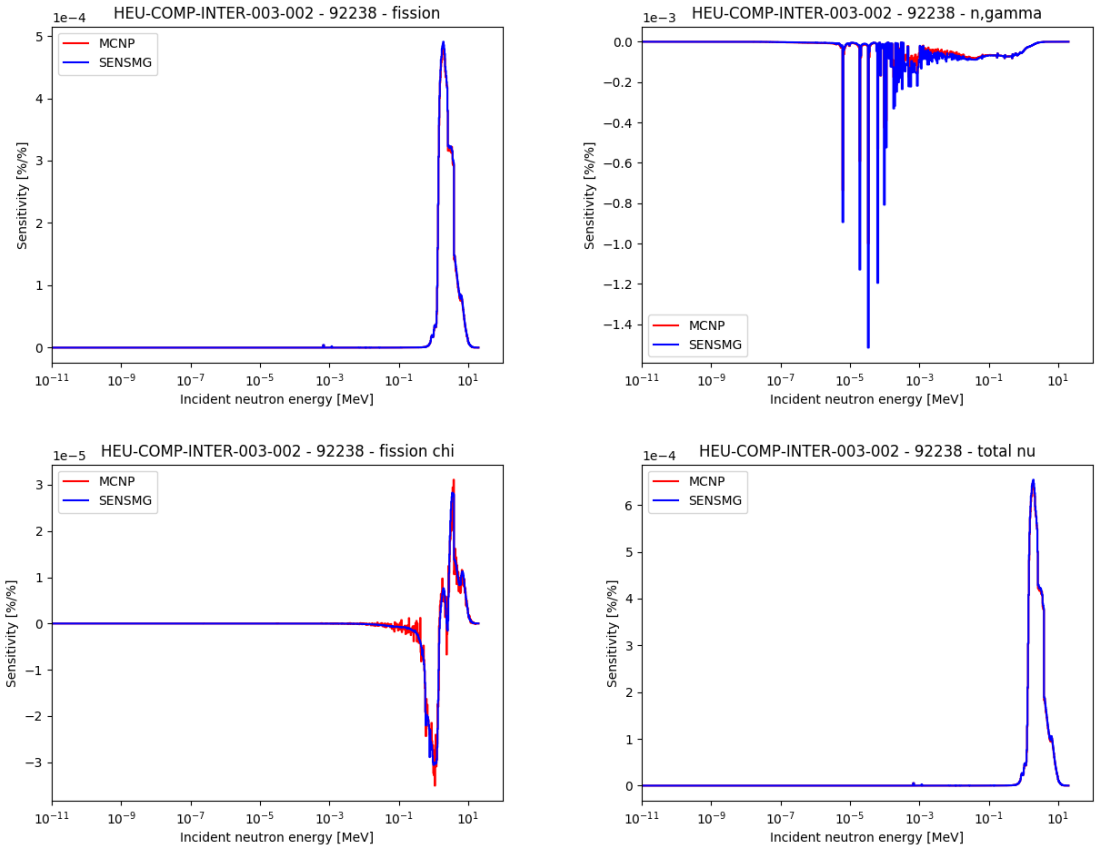

Figure 5.130: Sensitivity profiles for U238 in HEU-COMP-INTER-003-002.

5.20 HEU-COMP-INTER-003-003

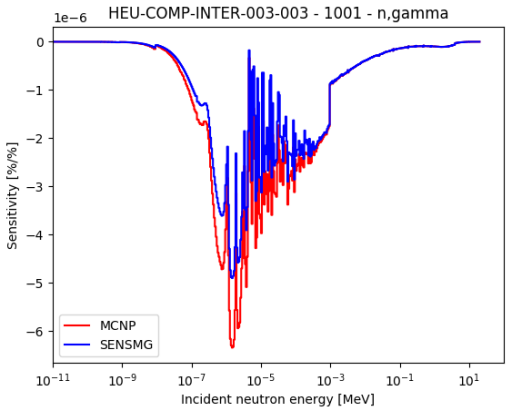

Figure 5.131: Sensitivity profiles for H1 in HEU-COMP-INTER-003-003.

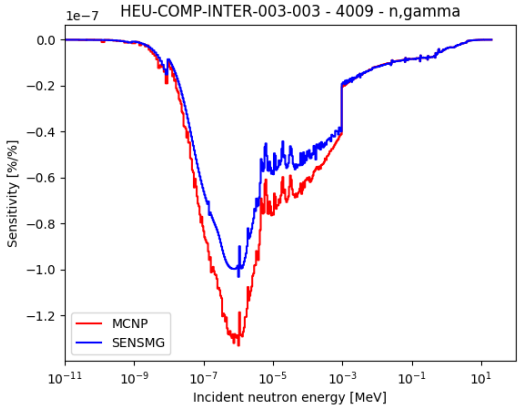

Figure 5.132: Sensitivity profiles for Be9 in HEU-COMP-INTER-003-003.

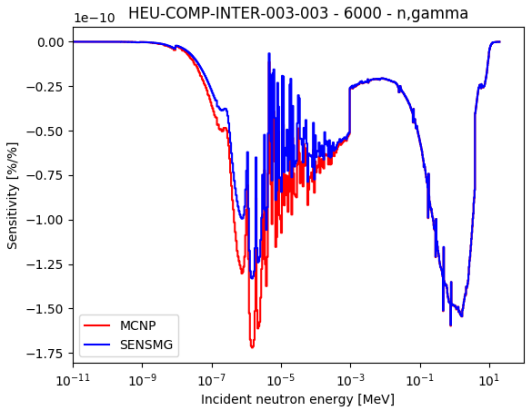

Figure 5.133: Sensitivity profiles for C in HEU-COMP-INTER-003-003.

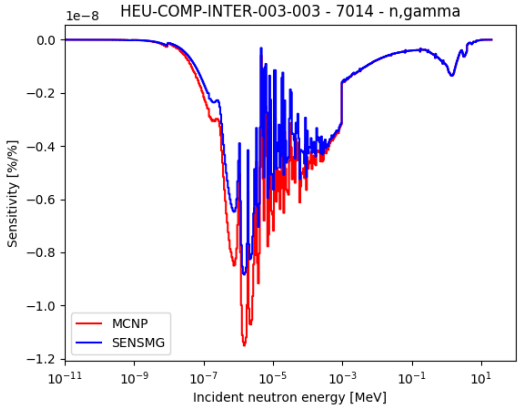

Figure 5.134: Sensitivity profiles for N14 in HEU-COMP-INTER-003-003.

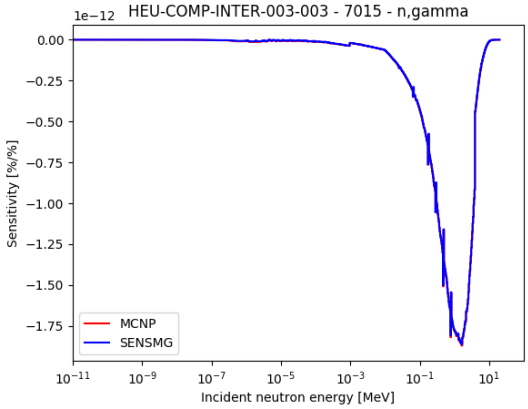

Figure 5.135: Sensitivity profiles for N15 in HEU-COMP-INTER-003-003.

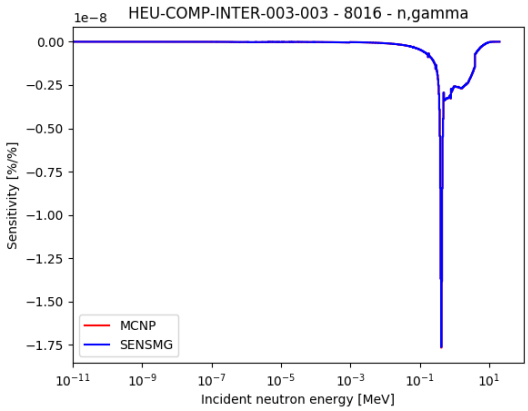

Figure 5.136: Sensitivity profiles for O16 in HEU-COMP-INTER-003-003.

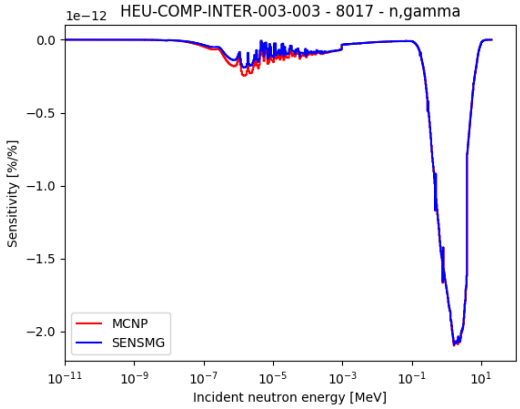

Figure 5.137: Sensitivity profiles for O17 in HEU-COMP-INTER-003-003.

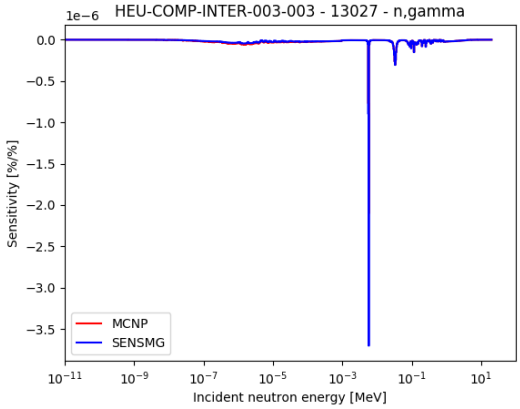

Figure 5.138: Sensitivity profiles for Al27 in HEU-COMP-INTER-003-003.

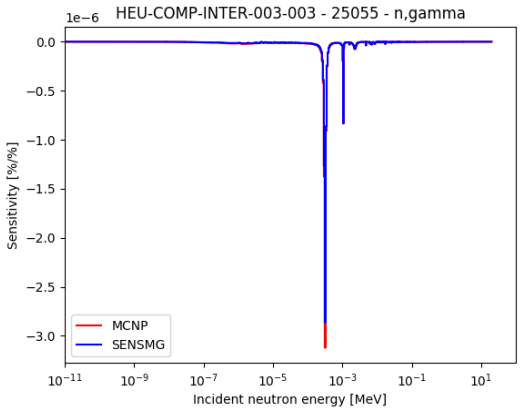

Figure 5.139: Sensitivity profiles for Mn55 in HEU-COMP-INTER-003-003.

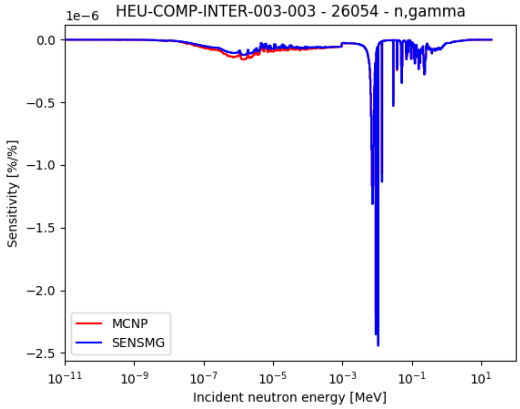

Figure 5.140: Sensitivity profiles for Fe54 in HEU-COMP-INTER-003-003.

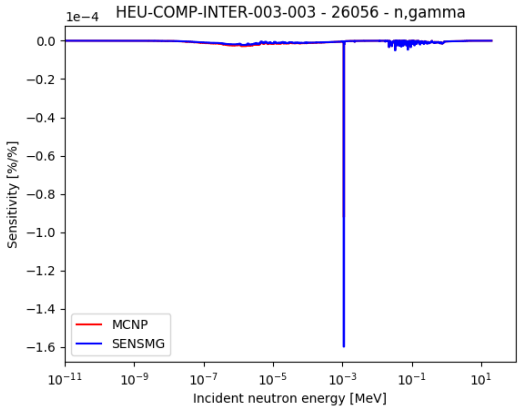

Figure 5.141: Sensitivity profiles for Fe55 in HEU-COMP-INTER-003-003.

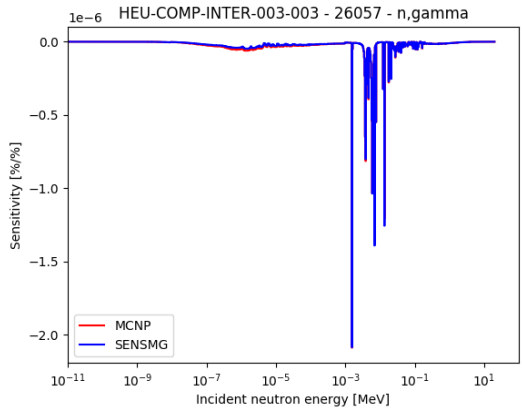

Figure 5.142: Sensitivity profiles for Fe57 in HEU-COMP-INTER-003-003.

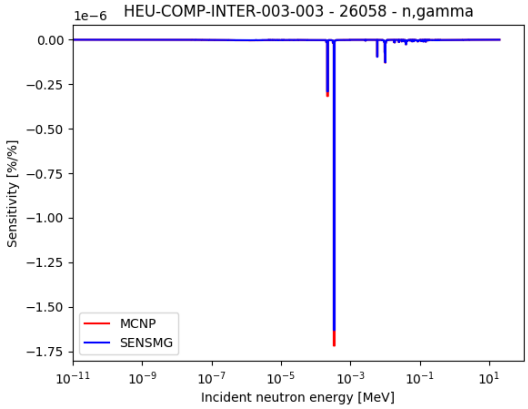

Figure 5.143: Sensitivity profiles for Fe58 in HEU-COMP-INTER-003-003.

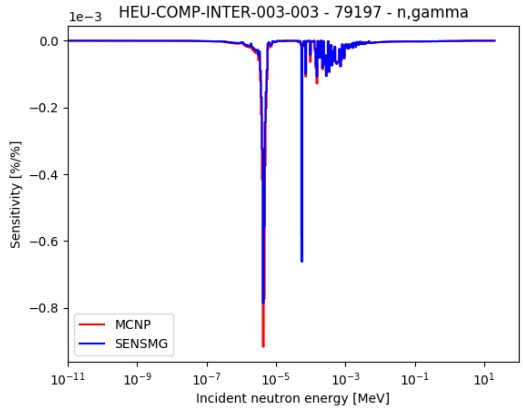

Figure 5.144: Sensitivity profiles for Au197 in HEU-COMP-INTER-003-003.

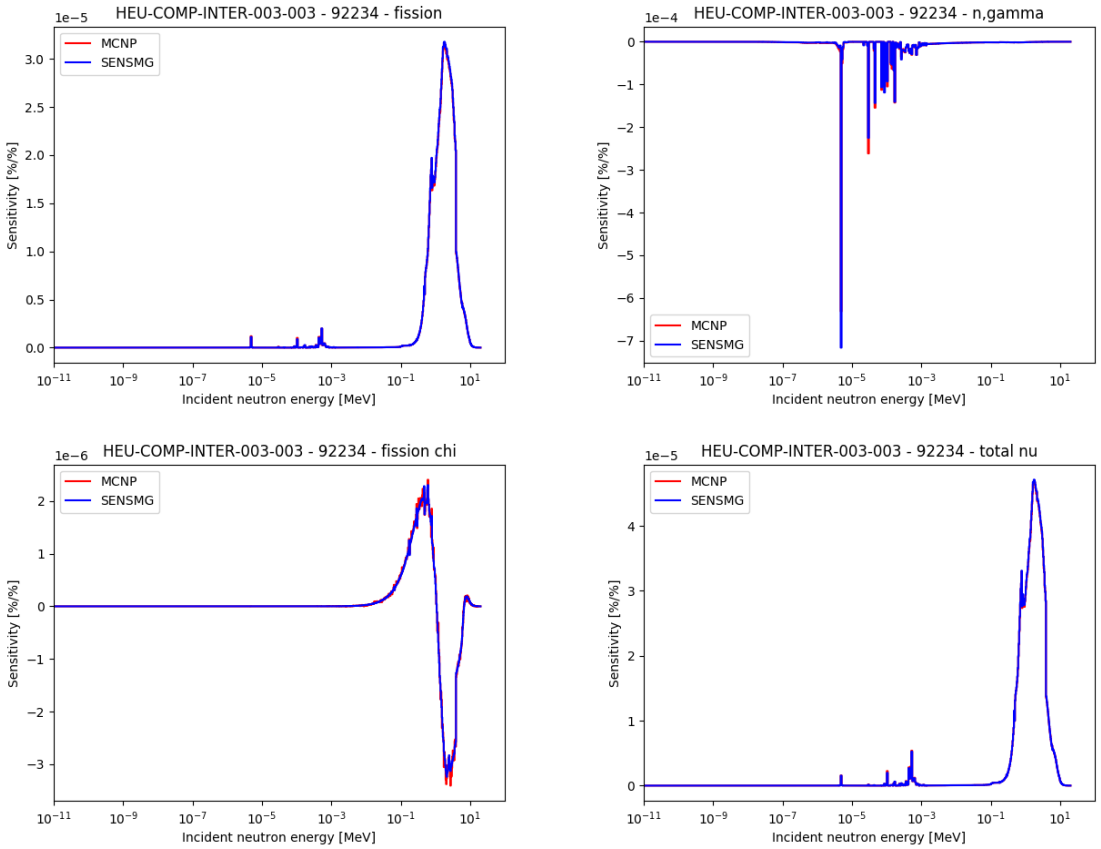

Figure 5.145: Sensitivity profiles for U234 in HEU-COMP-INTER-003-003.

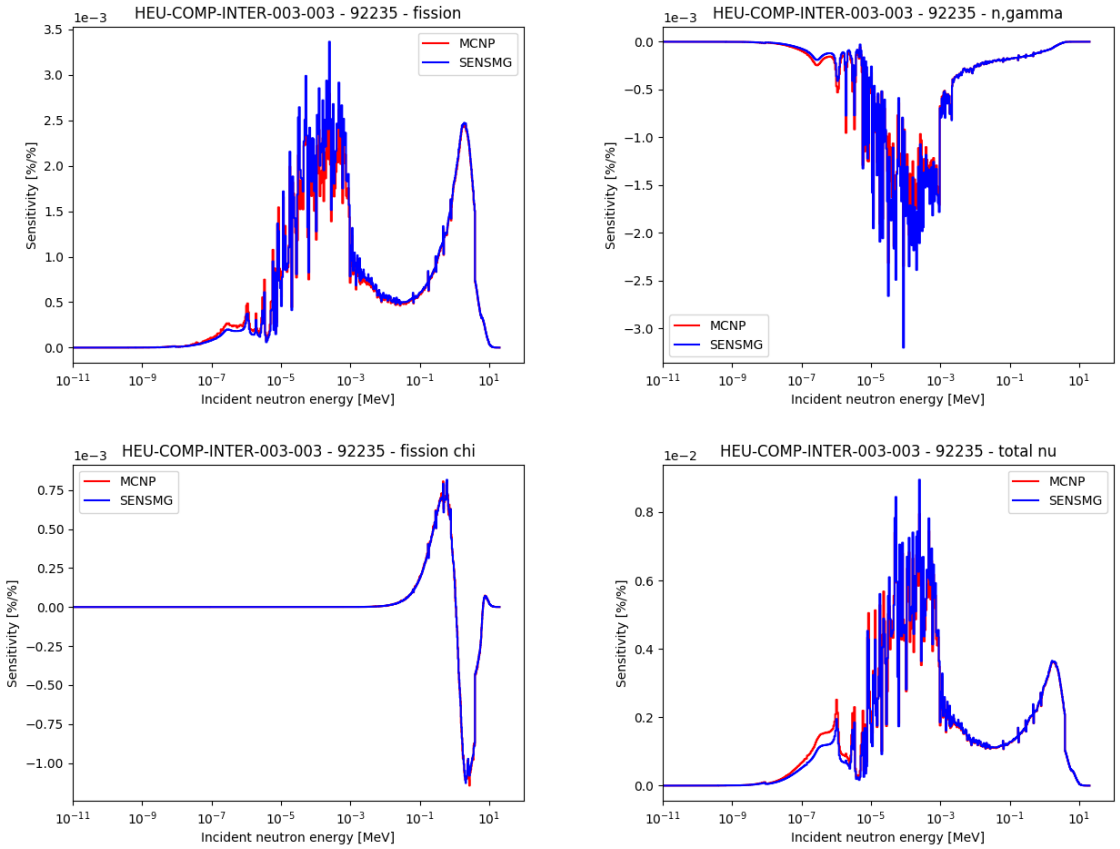

Figure 5.146: Sensitivity profiles for U235 in HEU-COMP-INTER-003-003.

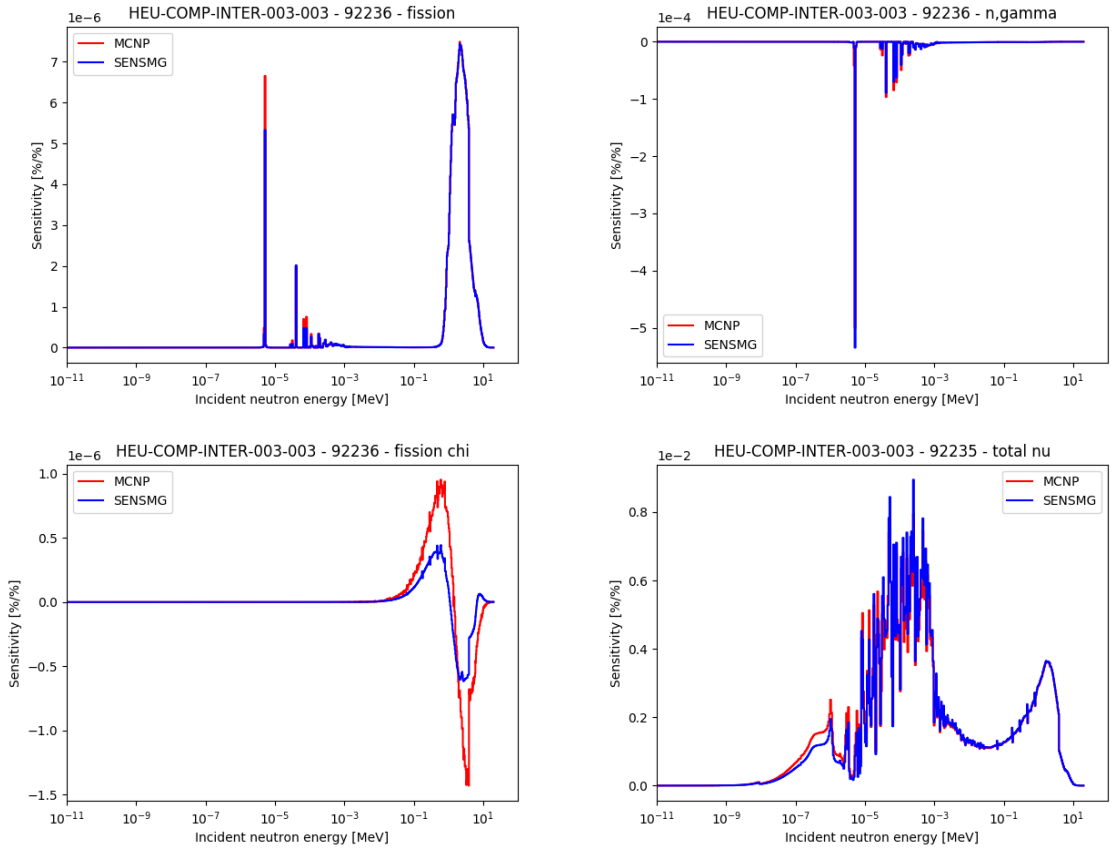

Figure 5.147: Sensitivity profiles for U236 in HEU-COMP-INTER-003-003.

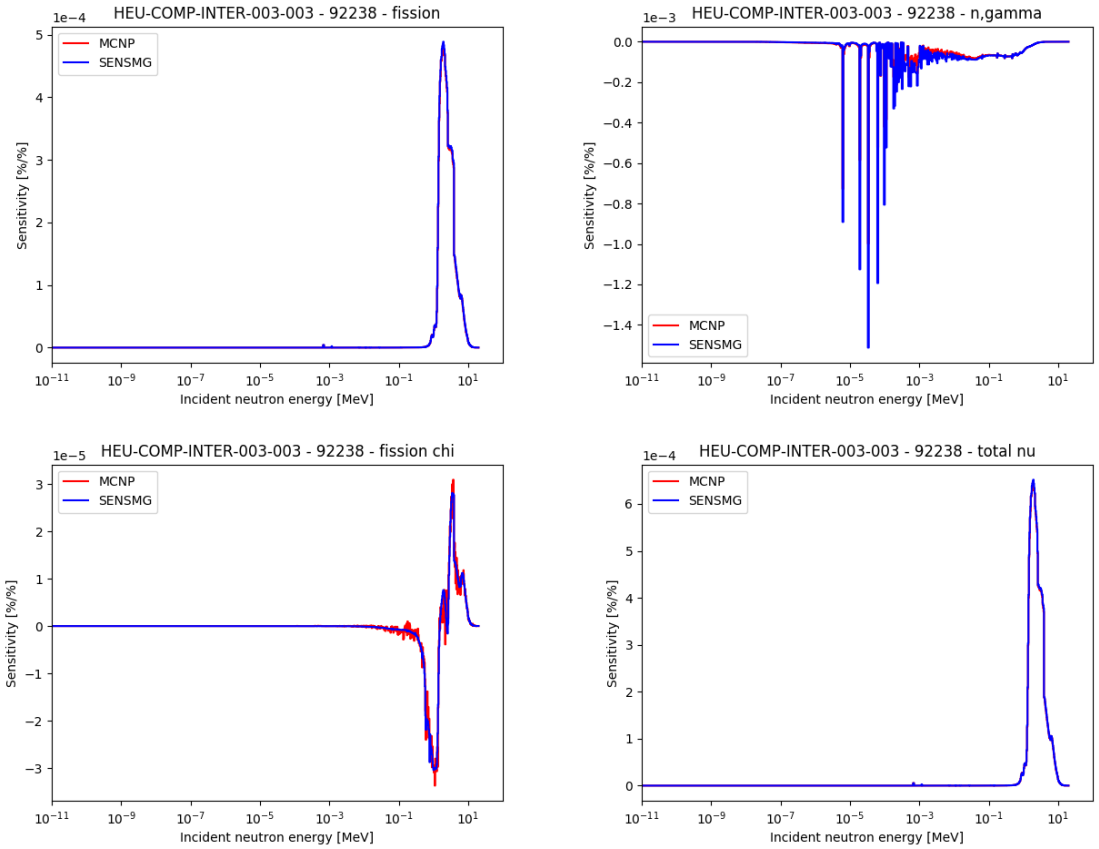

Figure 5.148: Sensitivity profiles for U238 in HEU-COMP-INTER-003-003.

5.21 HEU-COMP-INTER-003-004

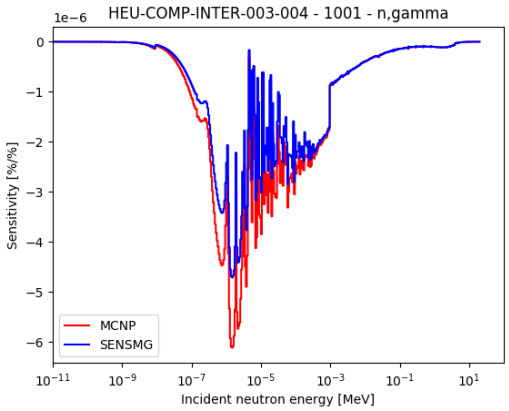

Figure 5.149: Sensitivity profiles for H1 in HEU-COMP-INTER-003-004.

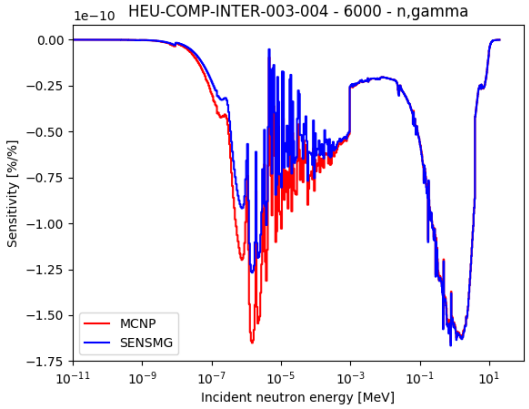

Figure 5.150: Sensitivity profiles for C in HEU-COMP-INTER-003-004.

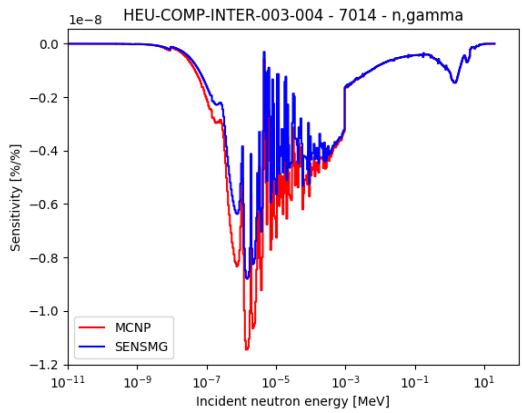

Figure 5.151: Sensitivity profiles for N14 in HEU-COMP-INTER-003-004.

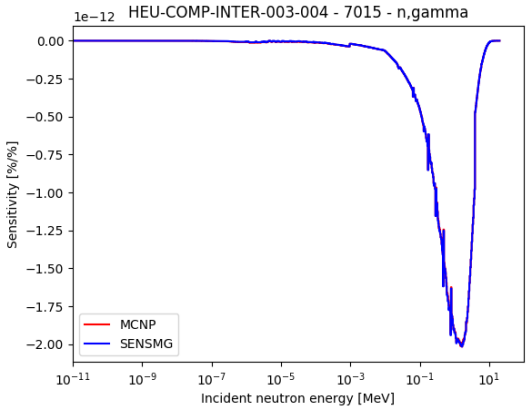

Figure 5.152: Sensitivity profiles for N15 in HEU-COMP-INTER-003-004.

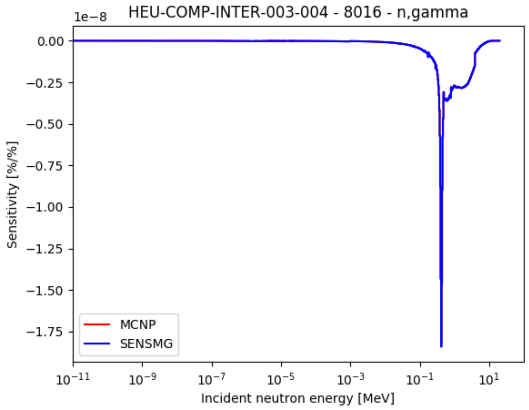

Figure 5.153: Sensitivity profiles for O16 in HEU-COMP-INTER-003-004.

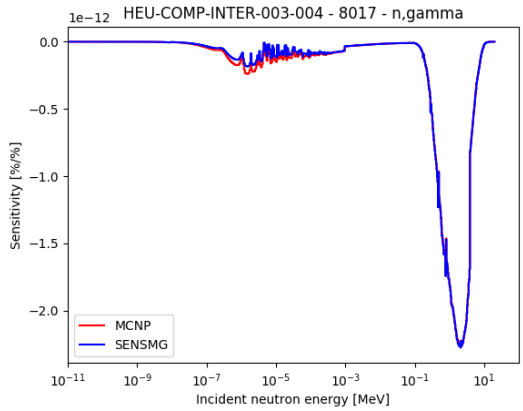

Figure 5.154: Sensitivity profiles for O17 in HEU-COMP-INTER-003-004.

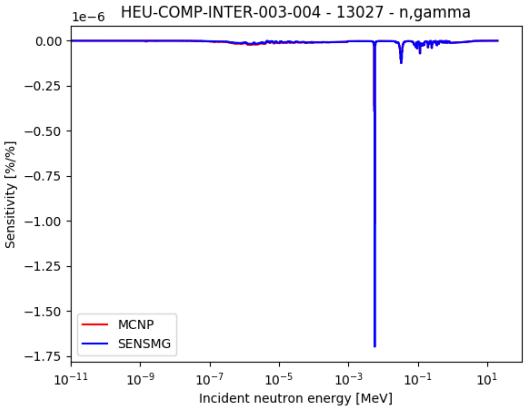

Figure 5.155: Sensitivity profiles for Al27 in HEU-COMP-INTER-003-004.

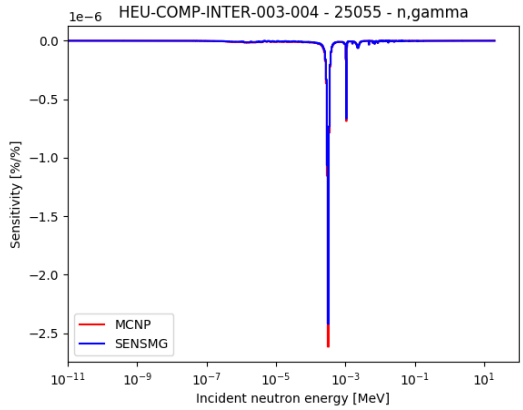

Figure 5.156: Sensitivity profiles for Mn55 in HEU-COMP-INTER-003-004.

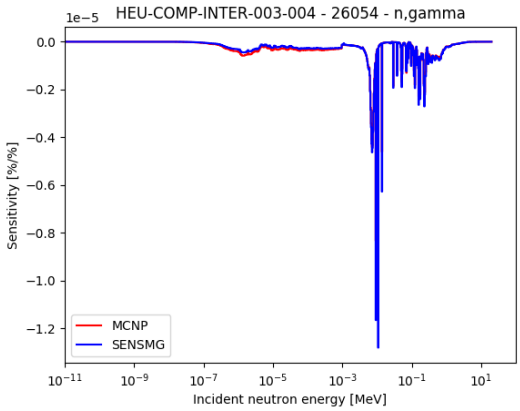

Figure 5.157: Sensitivity profiles for Fe54 in HEU-COMP-INTER-003-004.

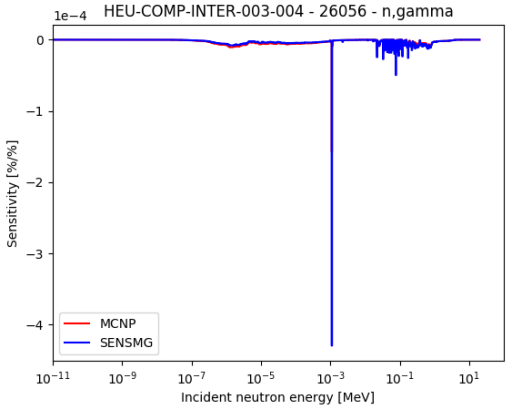

Figure 5.158: Sensitivity profiles for Fe55 in HEU-COMP-INTER-003-004.

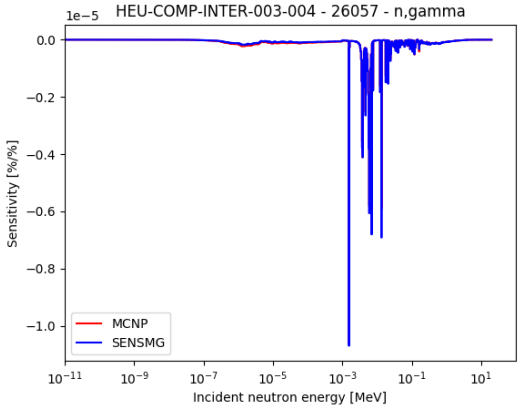

Figure 5.159: Sensitivity profiles for Fe57 in HEU-COMP-INTER-003-004.

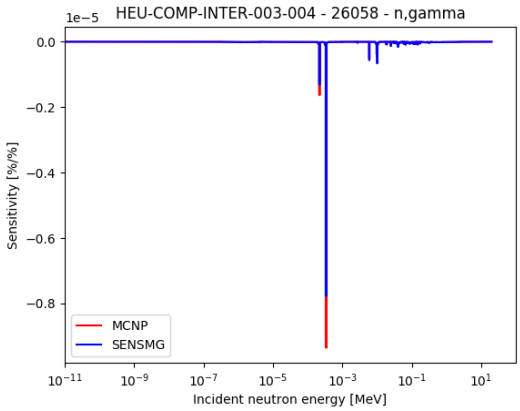

Figure 5.160: Sensitivity profiles for Fe58 in HEU-COMP-INTER-003-004.

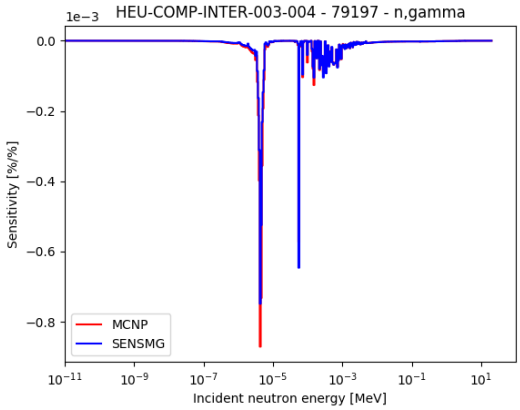

Figure 5.161: Sensitivity profiles for Au197 in HEU-COMP-INTER-003-004.

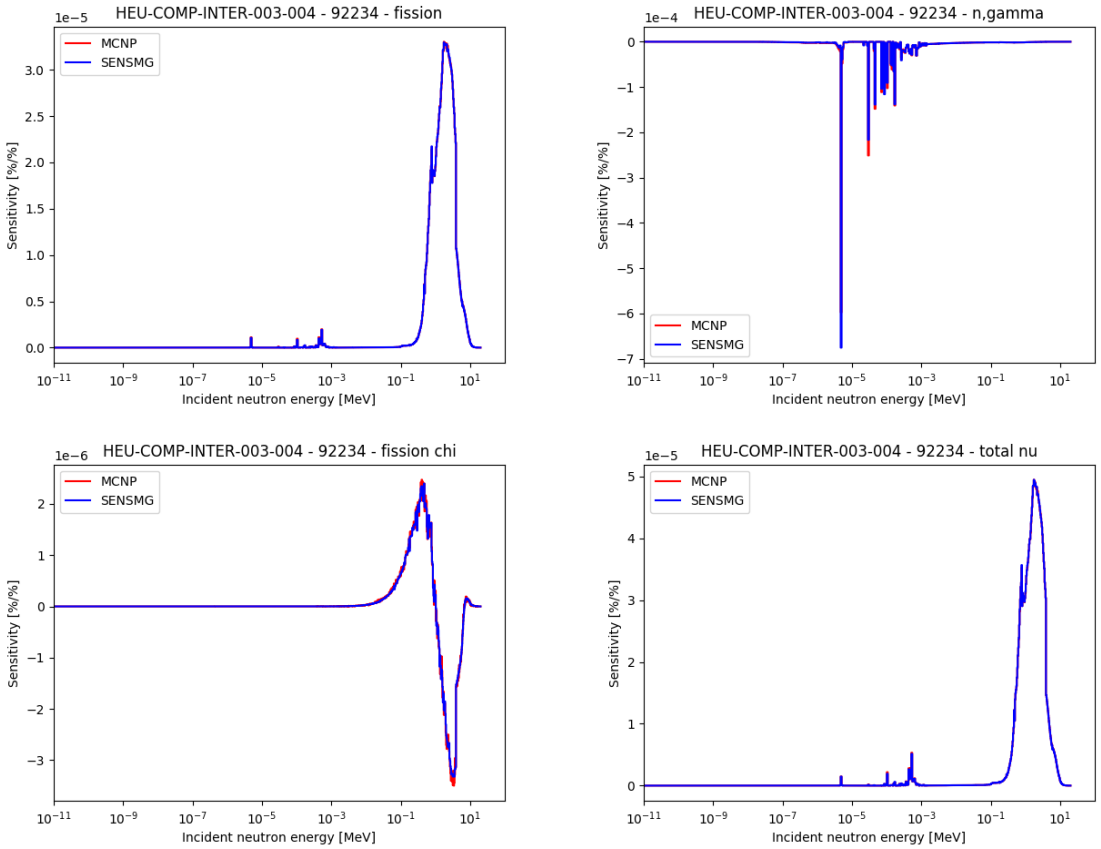

Figure 5.162: Sensitivity profiles for U234 in HEU-COMP-INTER-003-004.

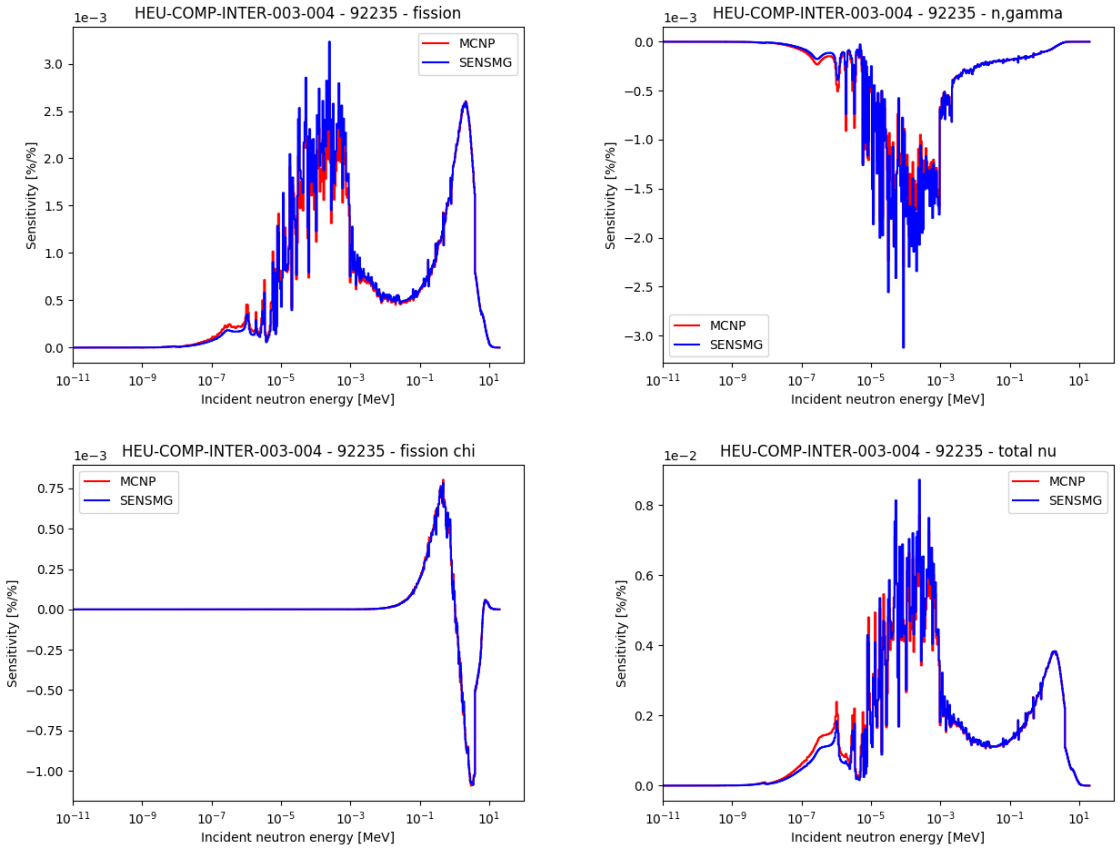

Figure 5.163: Sensitivity profiles for U235 in HEU-COMP-INTER-003-004.

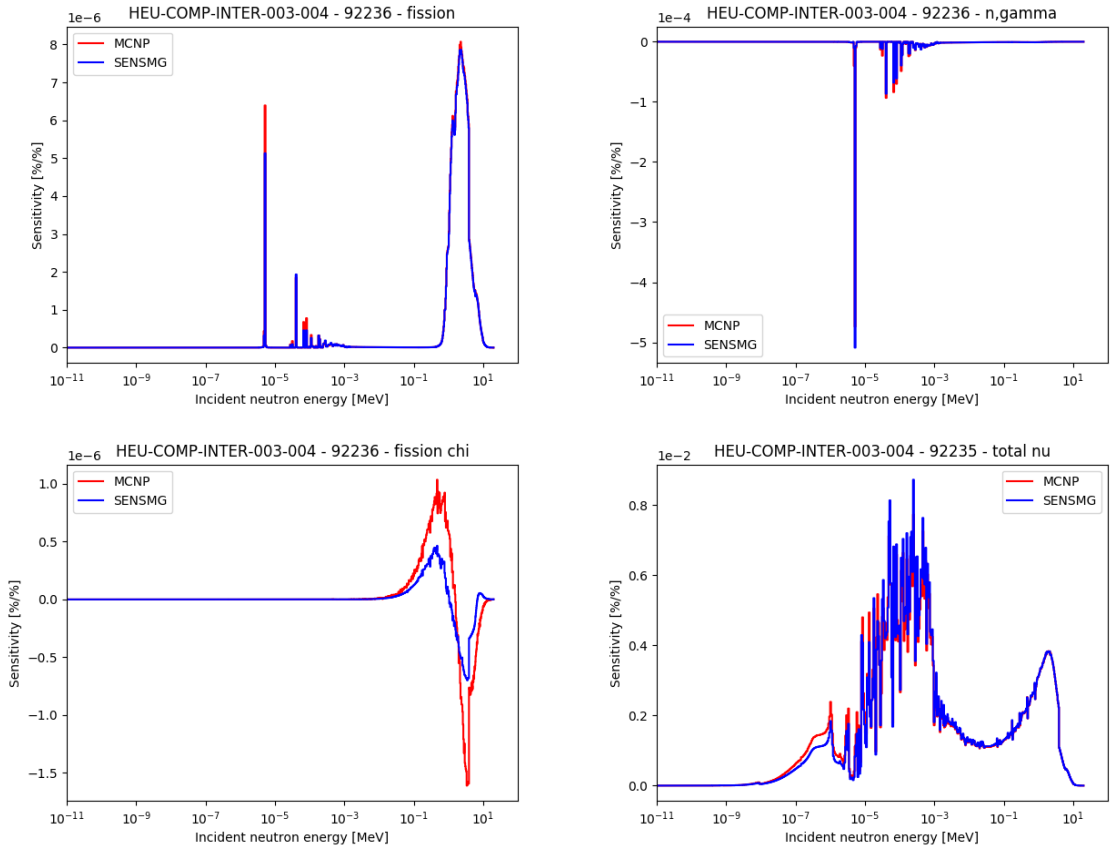

Figure 5.164: Sensitivity profiles for U236 in HEU-COMP-INTER-003-004.

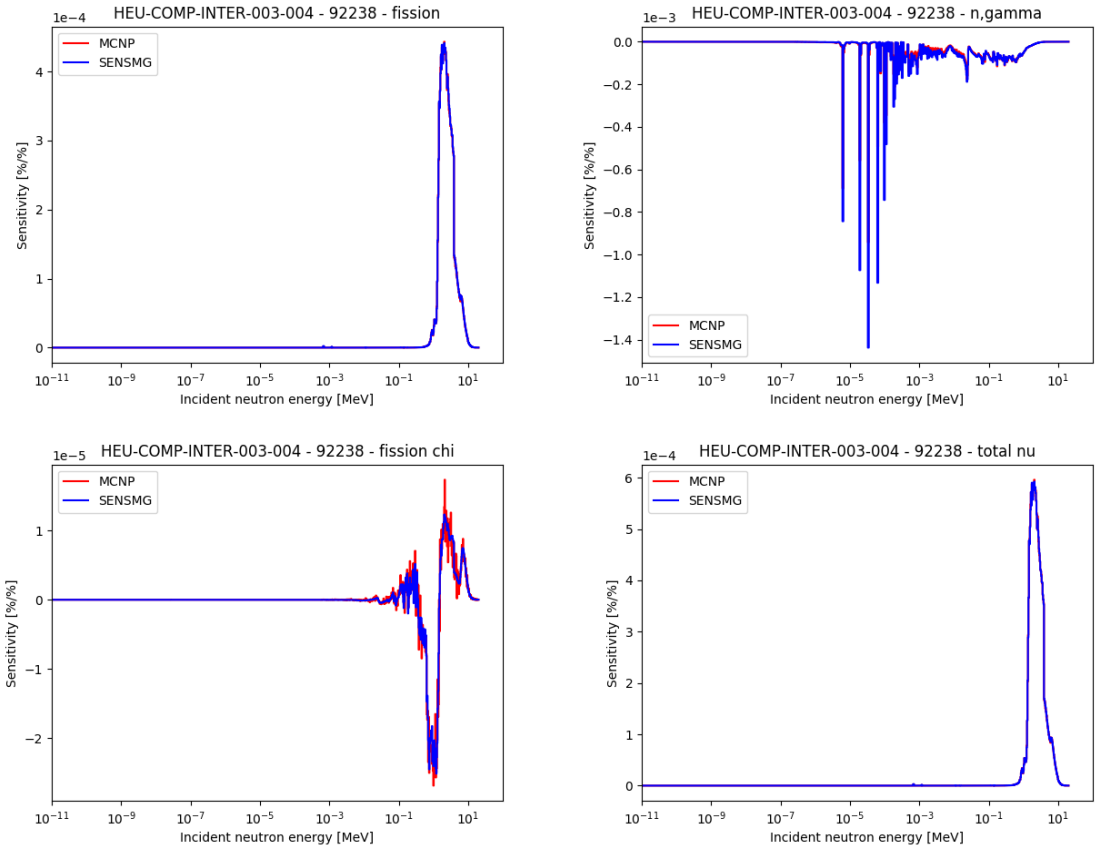

Figure 5.165: Sensitivity profiles for U238 in HEU-COMP-INTER-003-004.

5.22 HEU-COMP-INTER-003-005

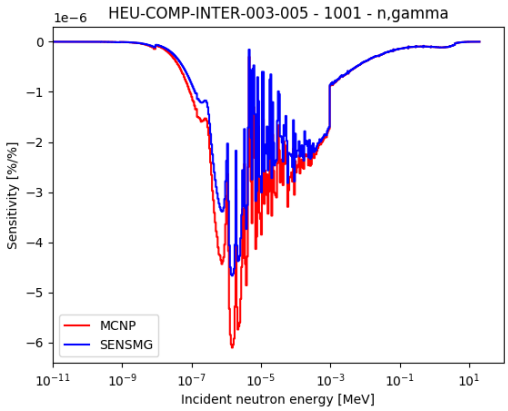

Figure 5.166: Sensitivity profiles for H1 in HEU-COMP-INTER-003-005.

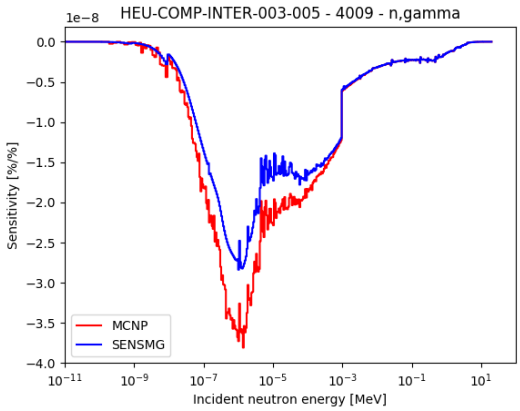

Figure 5.167: Sensitivity profiles for Be9 in HEU-COMP-INTER-003-005.

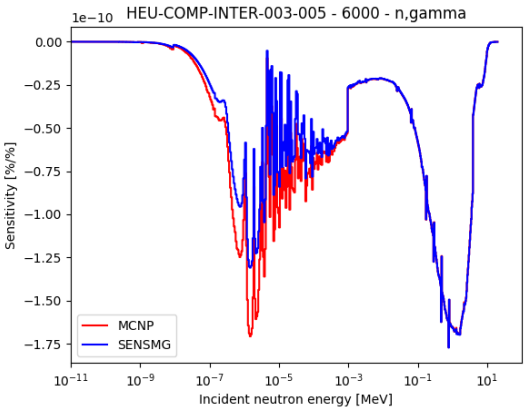

Figure 5.168: Sensitivity profiles for C in HEU-COMP-INTER-003-005.

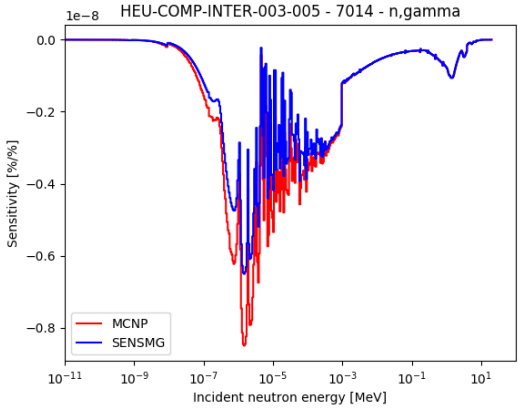

Figure 5.169: Sensitivity profiles for N14 in HEU-COMP-INTER-003-005.

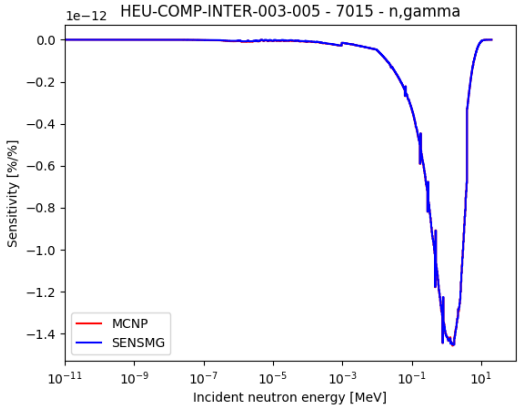

Figure 5.170: Sensitivity profiles for N15 in HEU-COMP-INTER-003-005.

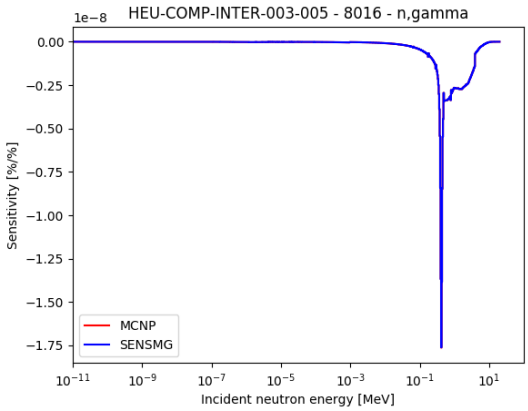

Figure 5.171: Sensitivity profiles for O16 in HEU-COMP-INTER-003-005.

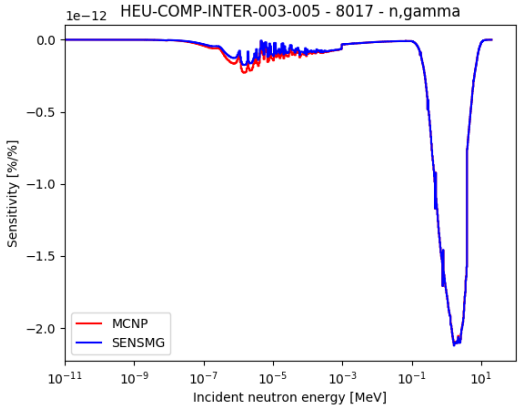

Figure 5.172: Sensitivity profiles for O17 in HEU-COMP-INTER-003-005.

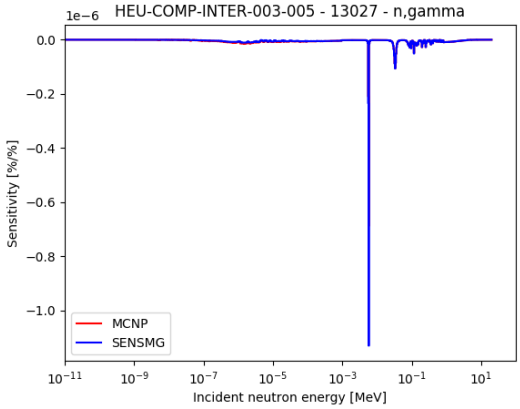

Figure 5.173: Sensitivity profiles for Al27 in HEU-COMP-INTER-003-005.

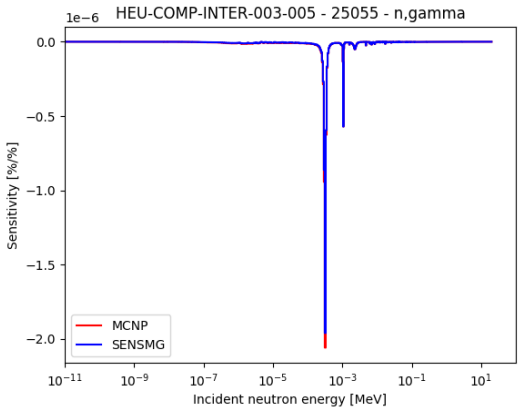

Figure 5.174: Sensitivity profiles for Mn55 in HEU-COMP-INTER-003-005.

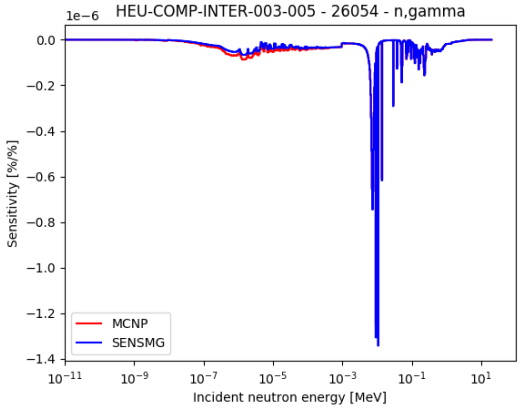

Figure 5.175: Sensitivity profiles for Fe54 in HEU-COMP-INTER-003-005.

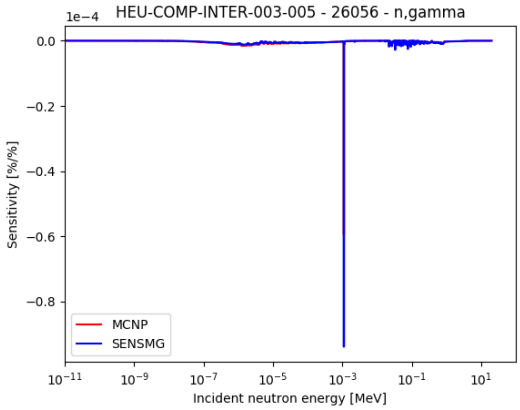

Figure 5.176: Sensitivity profiles for Fe55 in HEU-COMP-INTER-003-005.

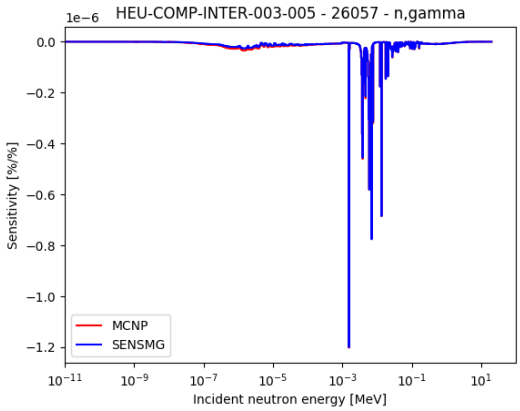

Figure 5.177: Sensitivity profiles for Fe57 in HEU-COMP-INTER-003-005.

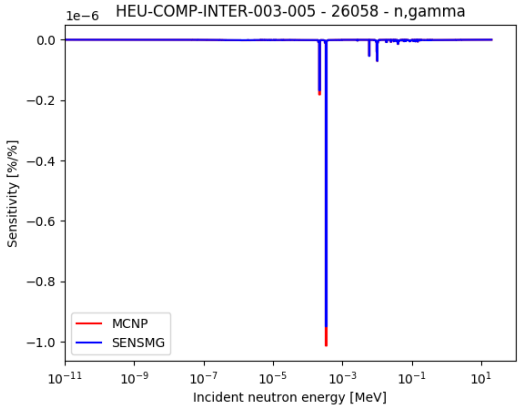

Figure 5.178: Sensitivity profiles for Fe58 in HEU-COMP-INTER-003-005.

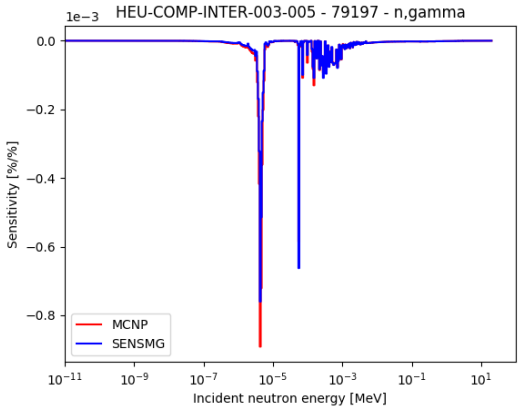

Figure 5.179: Sensitivity profiles for Au197 in HEU-COMP-INTER-003-005.

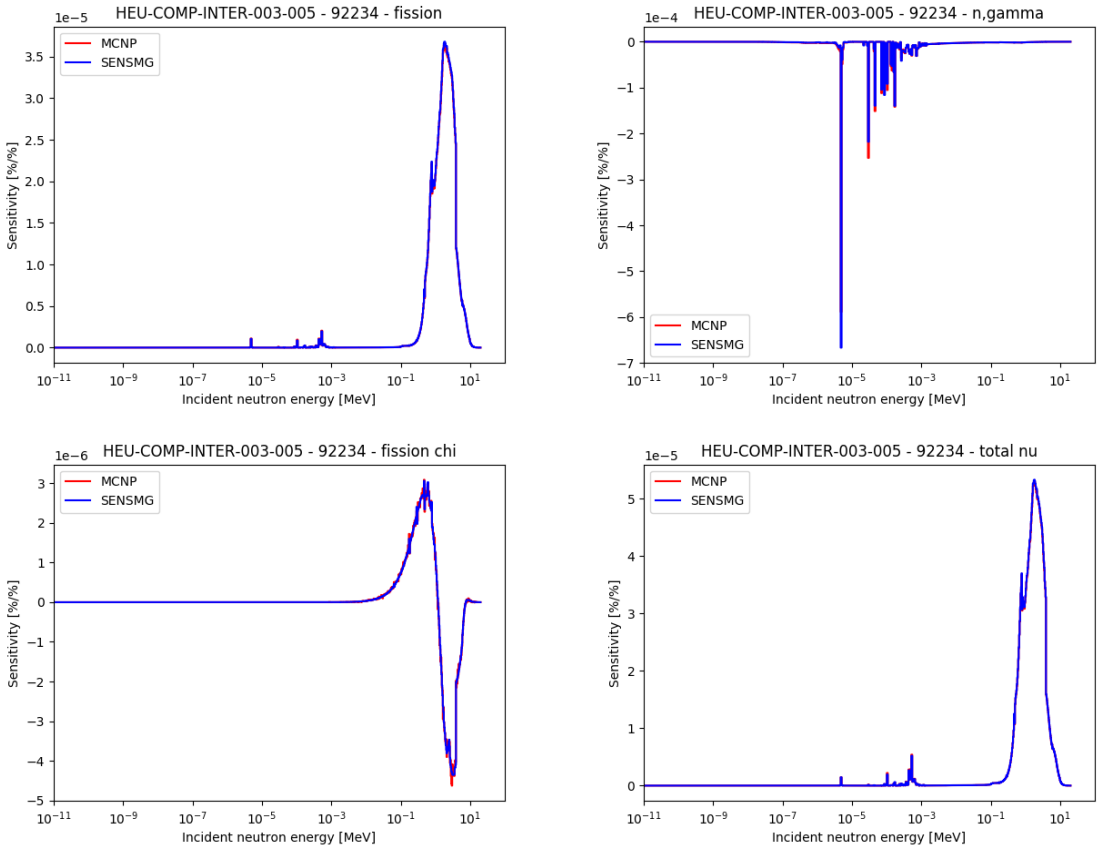

Figure 5.180: Sensitivity profiles for U234 in HEU-COMP-INTER-003-005.

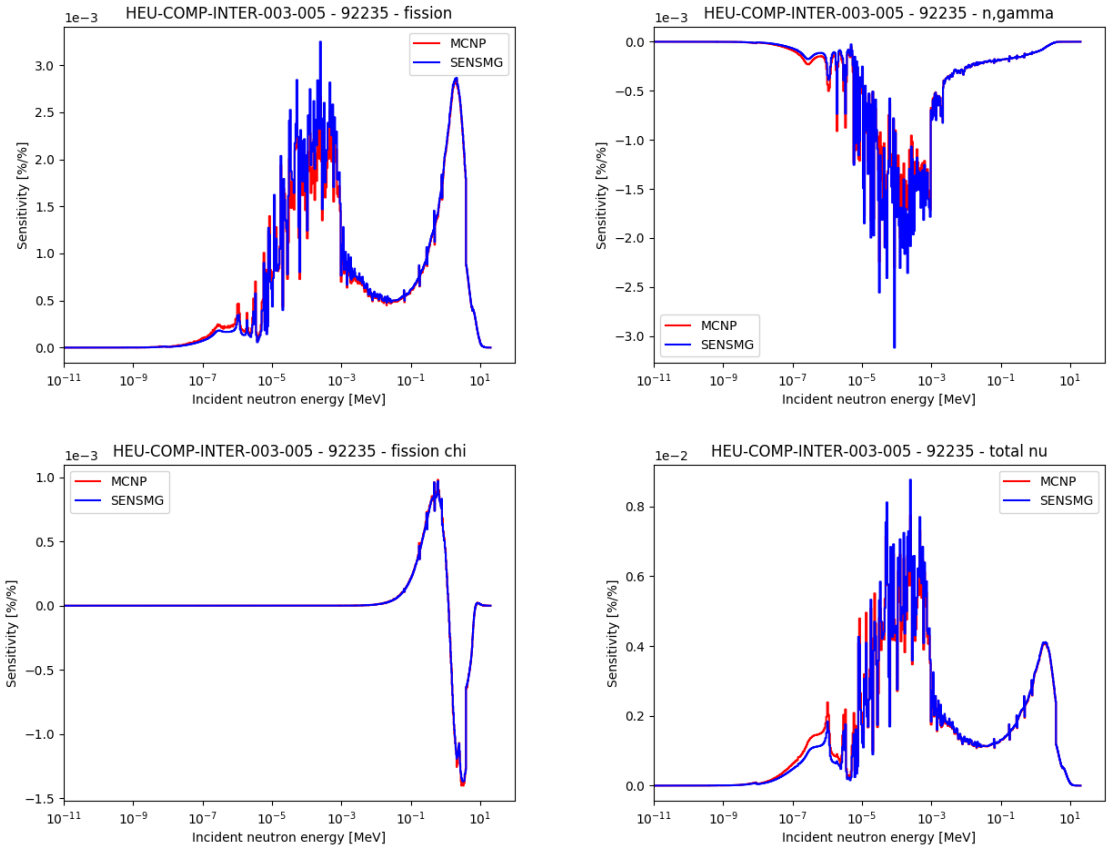

Figure 5.181: Sensitivity profiles for U235 in HEU-COMP-INTER-003-005.

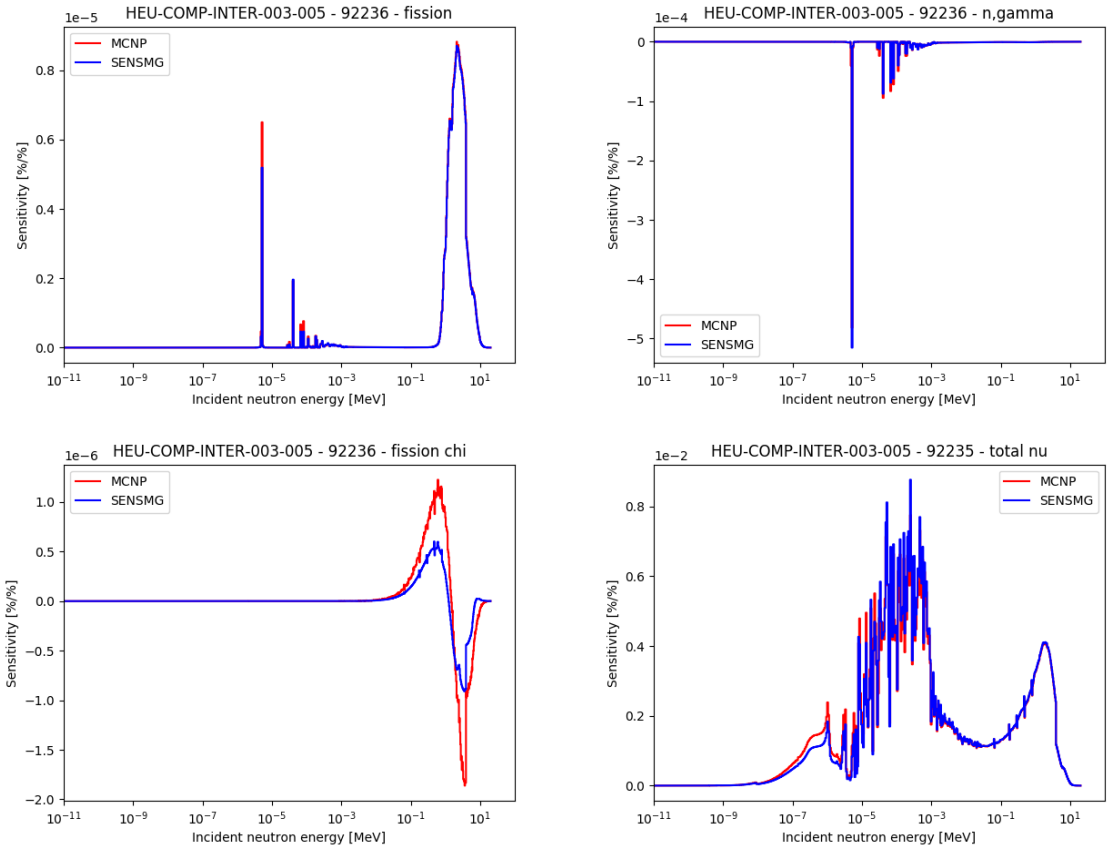

Figure 5.182: Sensitivity profiles for U236 in HEU-COMP-INTER-003-005.

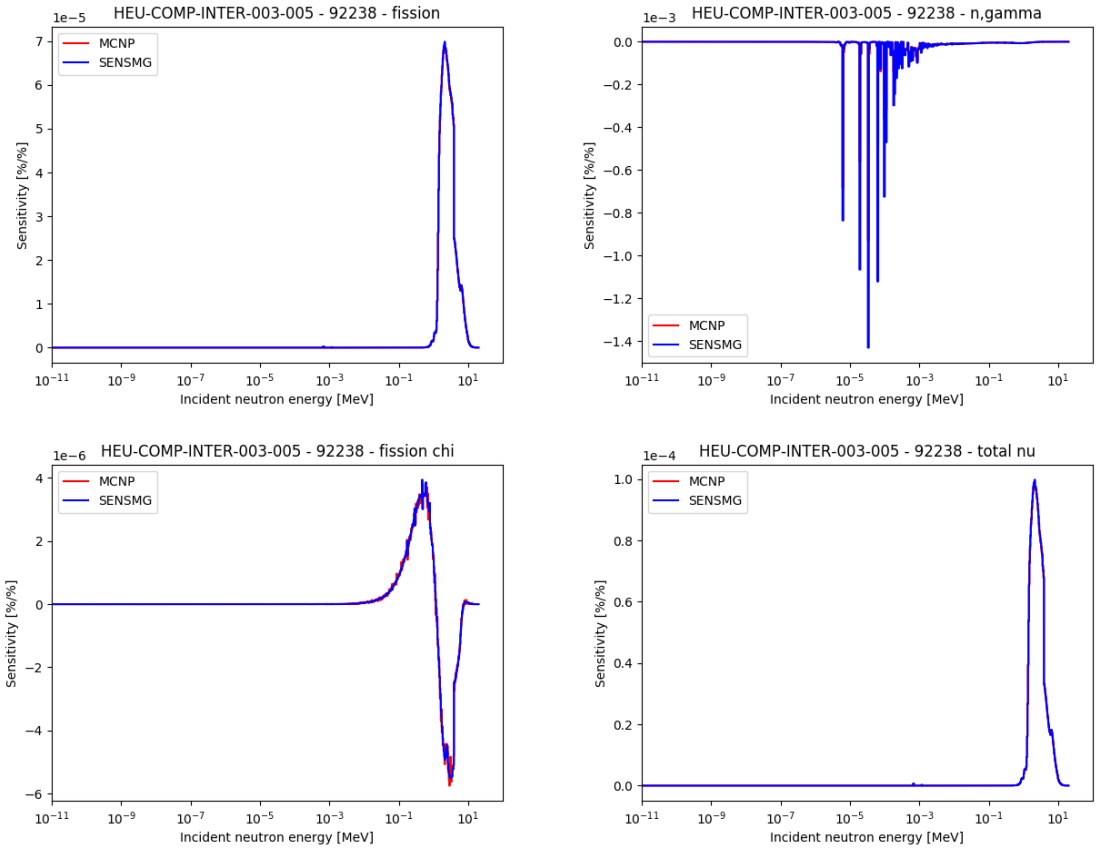

Figure 5.183: Sensitivity profiles for U238 in HEU-COMP-INTER-003-005.

5.23 HEU-COMP-INTER-003-006

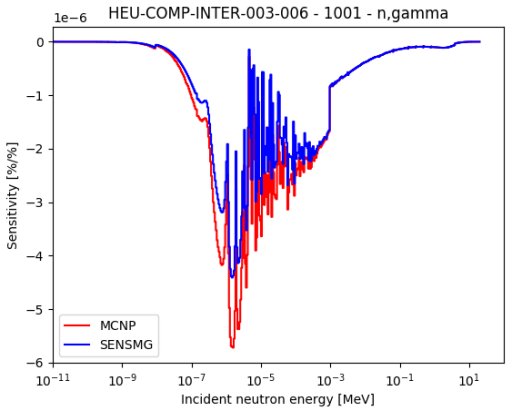

Figure 5.184: Sensitivity profiles for H1 in HEU-COMP-INTER-003-006.

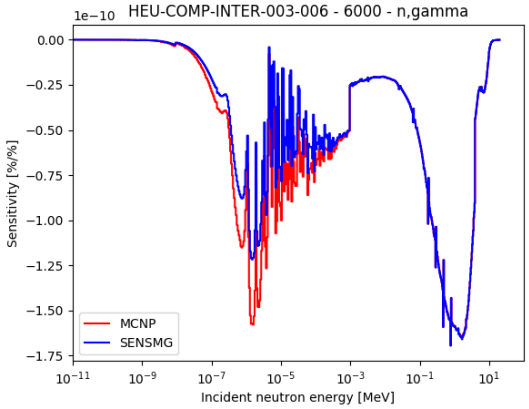

Figure 5.185: Sensitivity profiles for C in HEU-COMP-INTER-003-006.

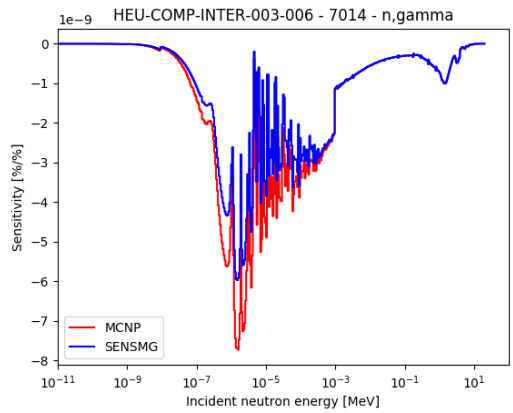

Figure 5.186: Sensitivity profiles for N14 in HEU-COMP-INTER-003-006.

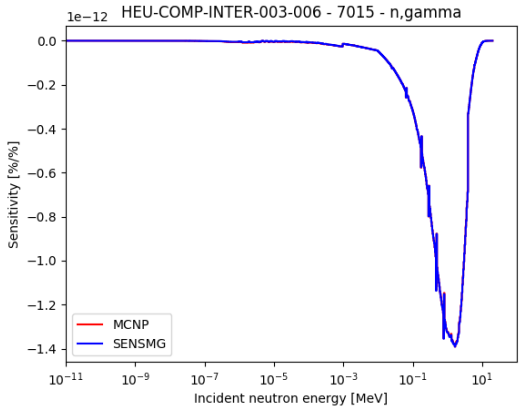

Figure 5.187: Sensitivity profiles for N15 in HEU-COMP-INTER-003-006.

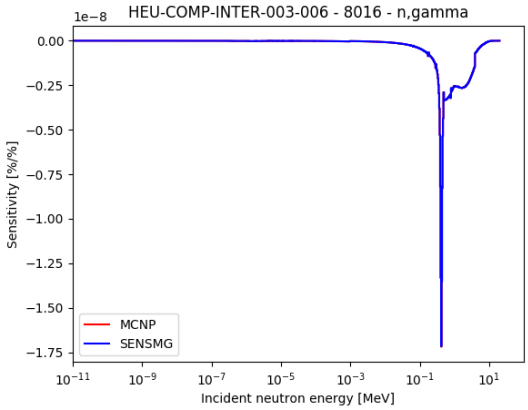

Figure 5.188: Sensitivity profiles for O16 in HEU-COMP-INTER-003-006.

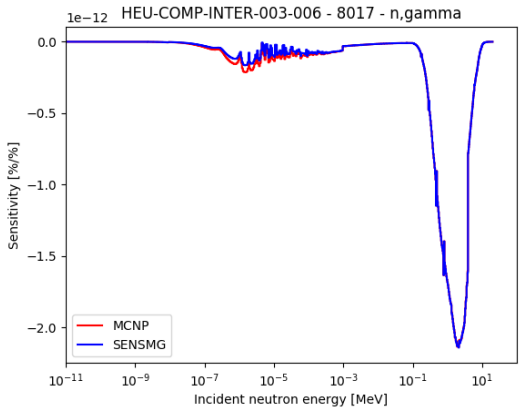

Figure 5.189: Sensitivity profiles for O17 in HEU-COMP-INTER-003-006.

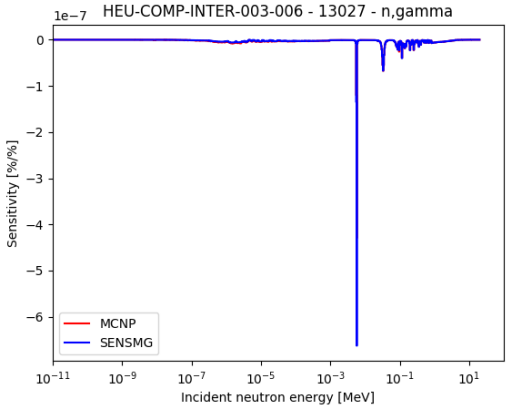

Figure 5.190: Sensitivity profiles for Al27 in HEU-COMP-INTER-003-006.

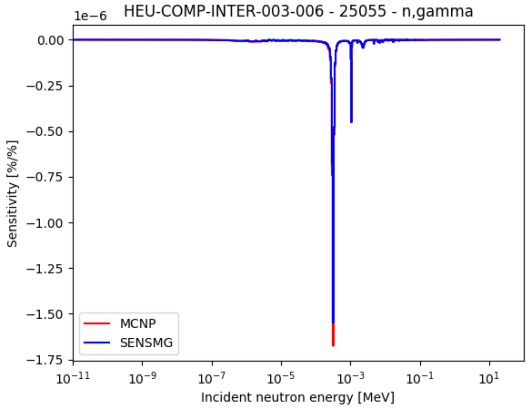

Figure 5.191: Sensitivity profiles for Mn55 in HEU-COMP-INTER-003-006.

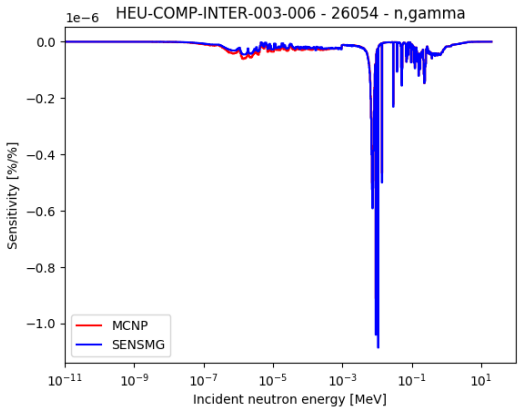

Figure 5.192: Sensitivity profiles for Fe54 in HEU-COMP-INTER-003-006.

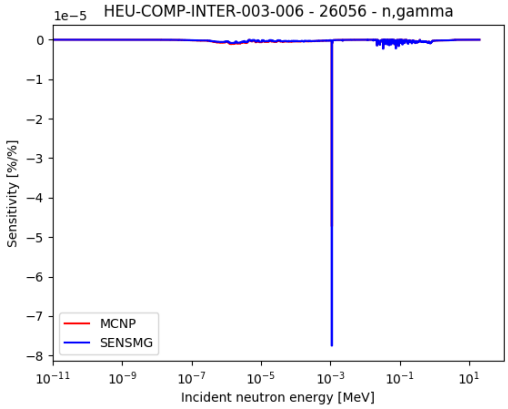

Figure 5.193: Sensitivity profiles for Fe55 in HEU-COMP-INTER-003-006.

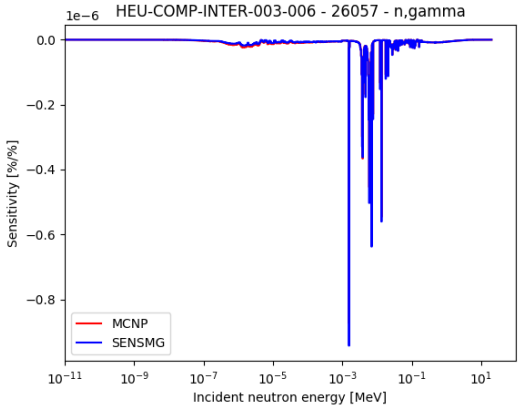

Figure 5.194: Sensitivity profiles for Fe57 in HEU-COMP-INTER-003-006.

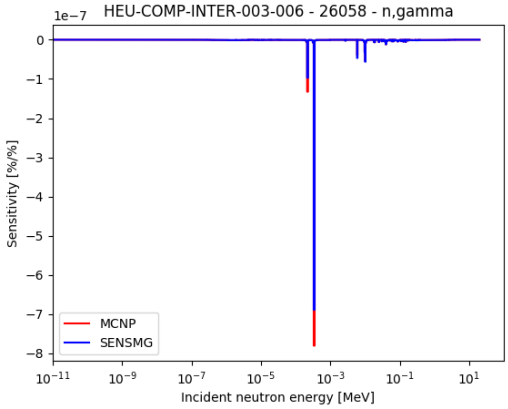

Figure 5.195: Sensitivity profiles for Fe58 in HEU-COMP-INTER-003-006.

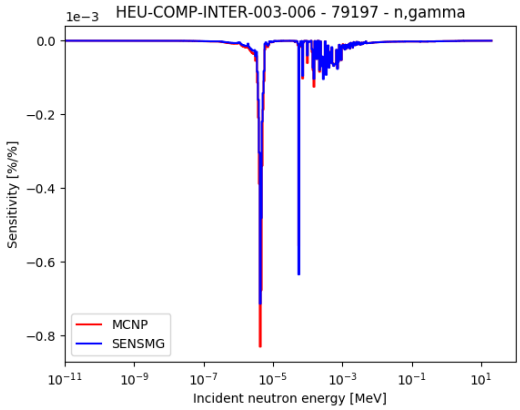

Figure 5.196: Sensitivity profiles for Au197 in HEU-COMP-INTER-003-006.

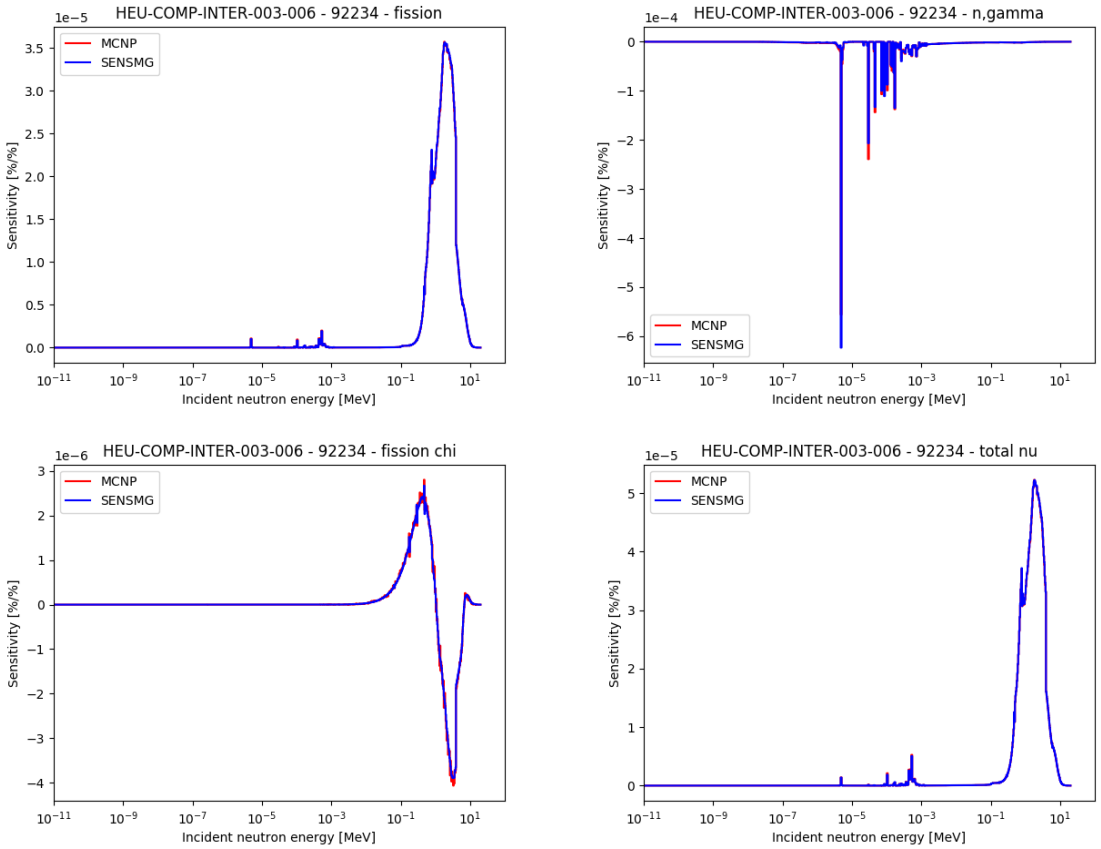

Figure 5.197: Sensitivity profiles for U234 in HEU-COMP-INTER-003-006.

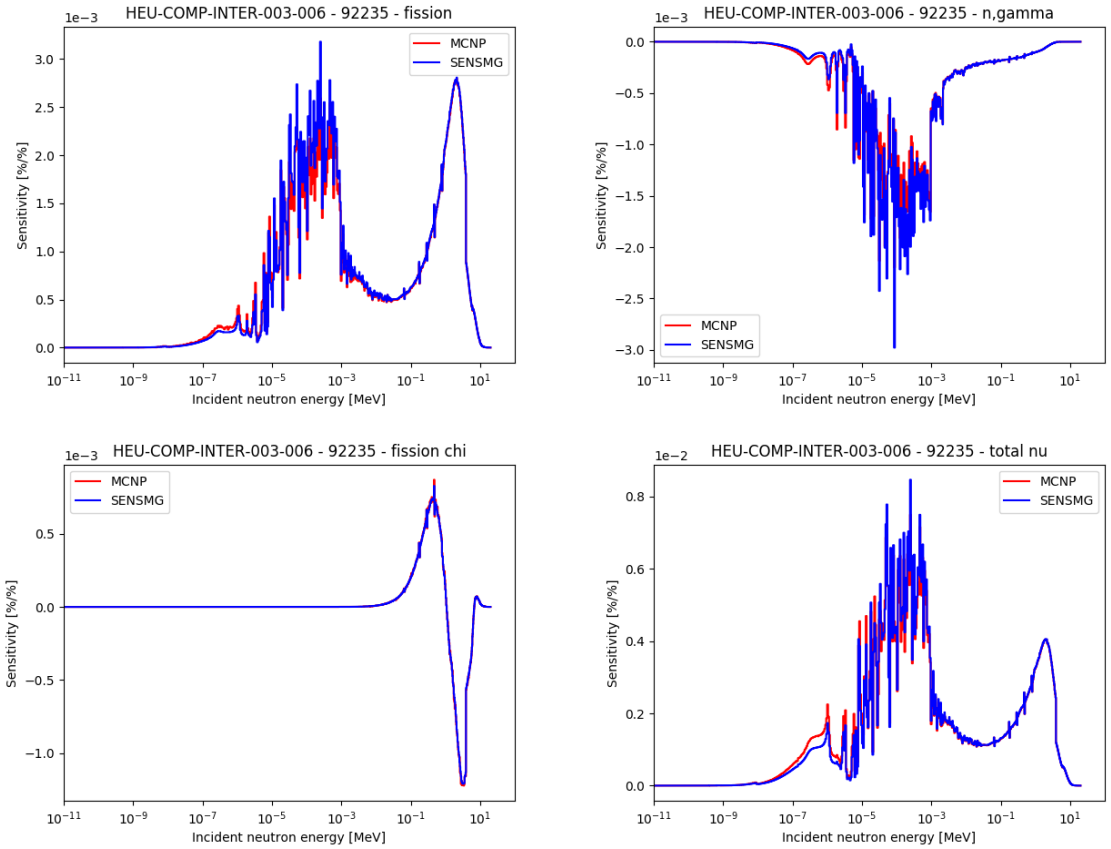

Figure 5.198: Sensitivity profiles for U235 in HEU-COMP-INTER-003-006.

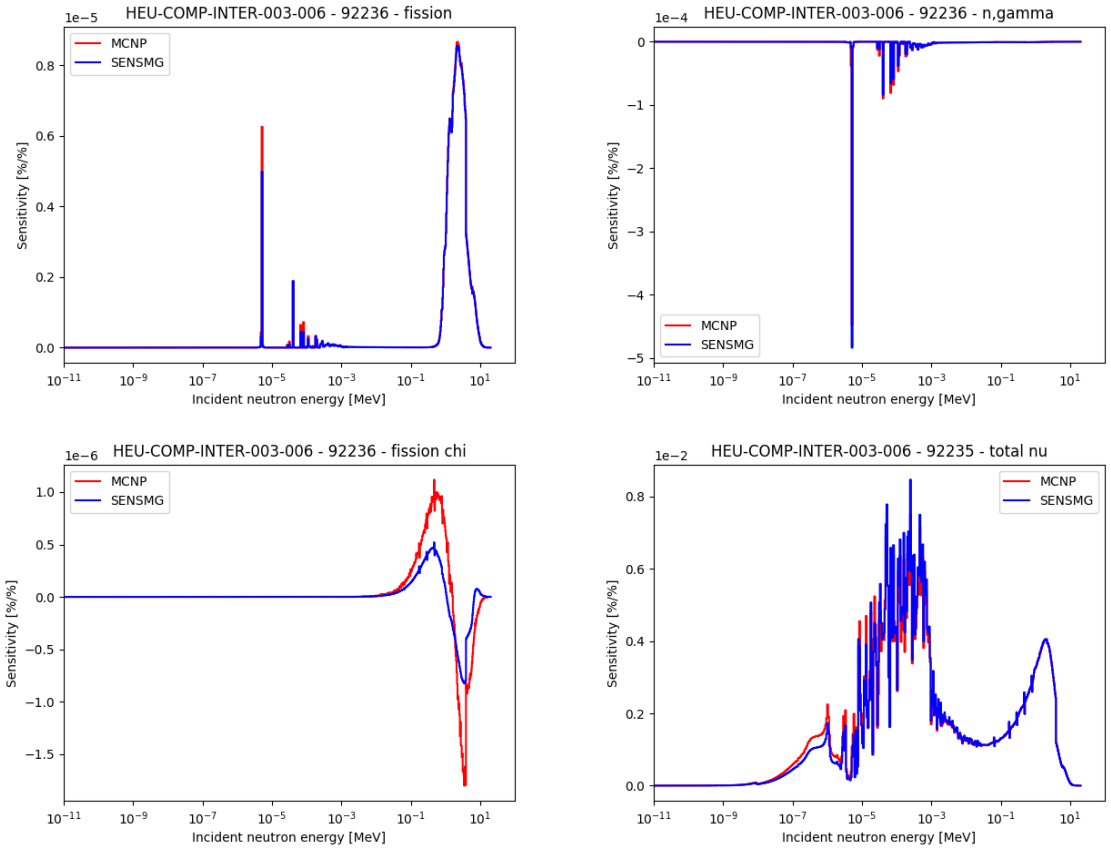

Figure 5.199: Sensitivity profiles for U236 in HEU-COMP-INTER-003-006.

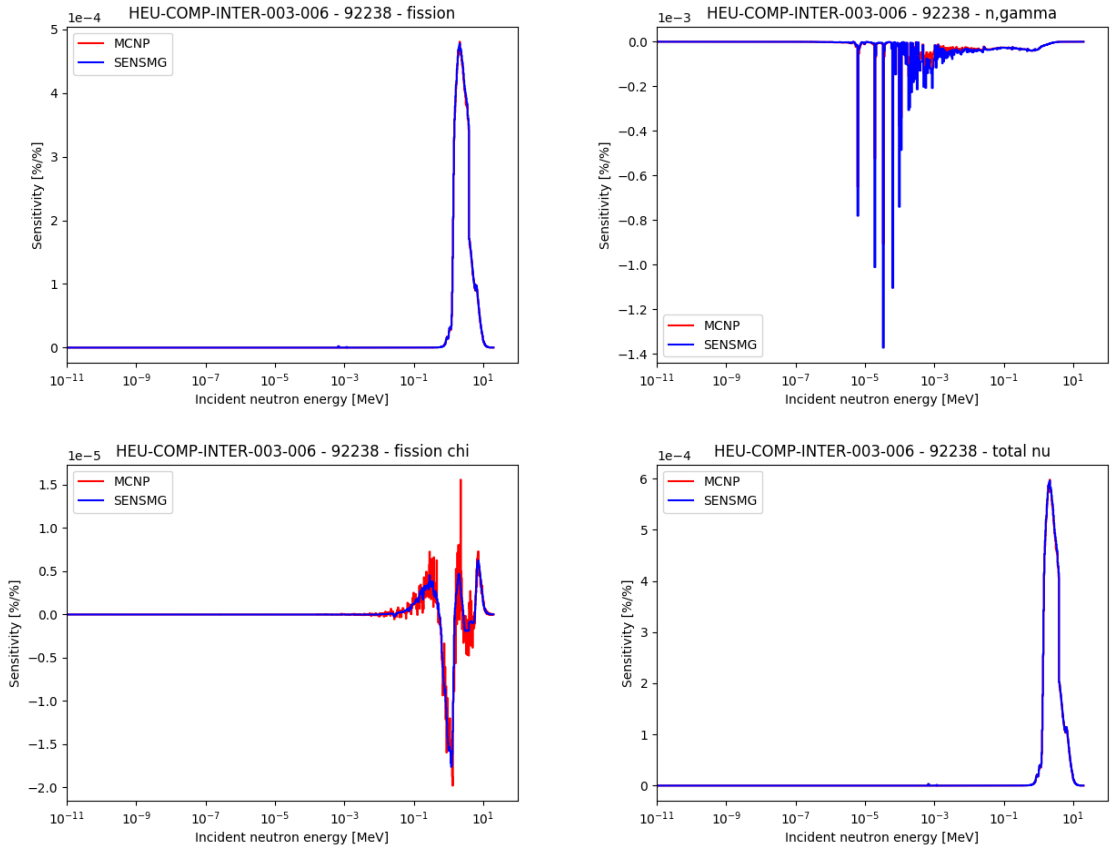

Figure 5.200: Sensitivity profiles for U238 in HEU-COMP-INTER-003-006.

5.24 HEU-COMP-INTER-003-007

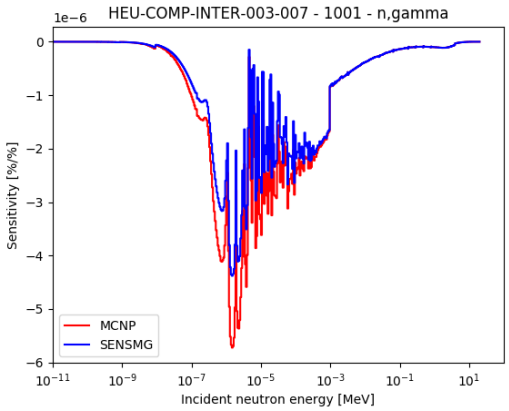

Figure 5.201: Sensitivity profiles for H1 in HEU-COMP-INTER-003-007.

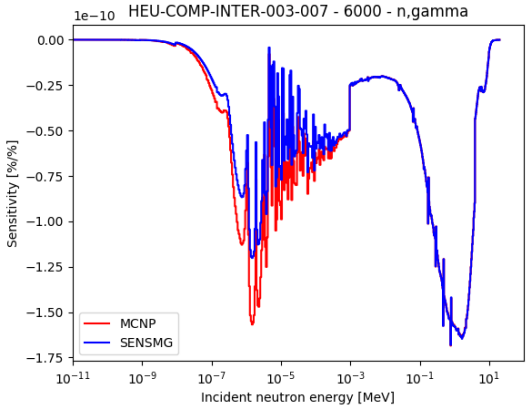

Figure 5.202: Sensitivity profiles for C in HEU-COMP-INTER-003-007.

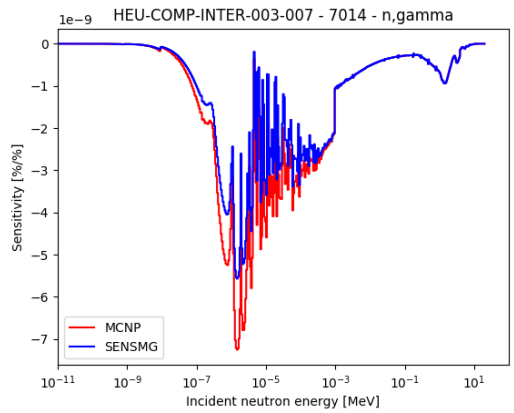

Figure 5.203: Sensitivity profiles for N14 in HEU-COMP-INTER-003-007.

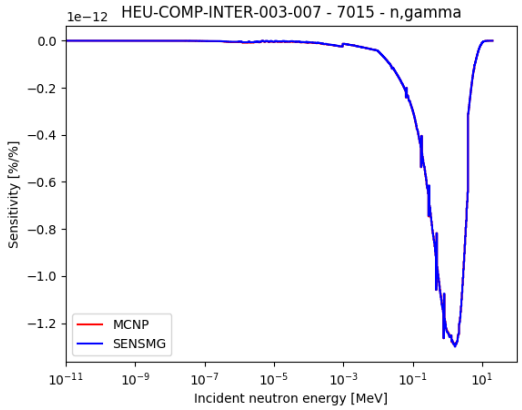

Figure 5.204: Sensitivity profiles for N15 in HEU-COMP-INTER-003-007.

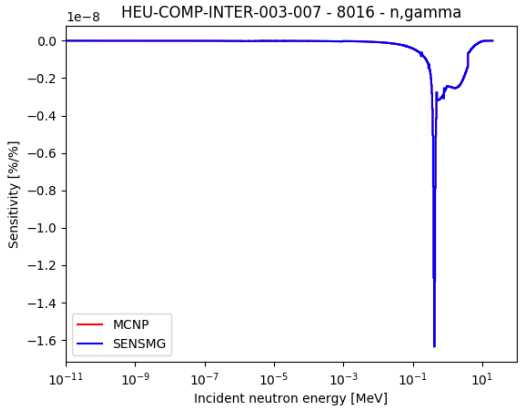

Figure 5.205: Sensitivity profiles for O16 in HEU-COMP-INTER-003-007.

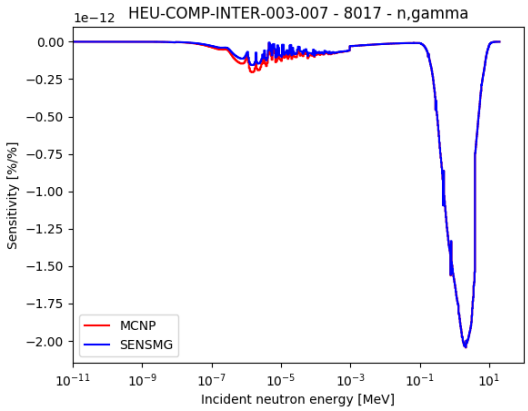

Figure 5.206: Sensitivity profiles for O17 in HEU-COMP-INTER-003-007.

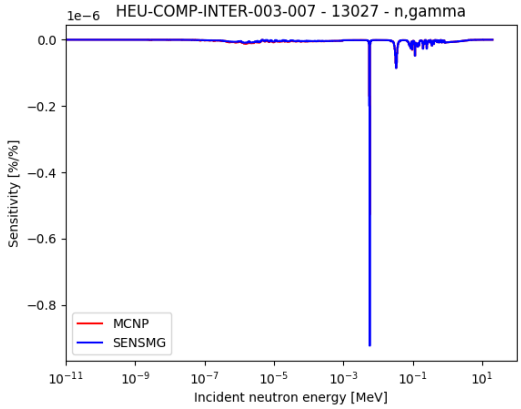

Figure 5.207: Sensitivity profiles for Al27 in HEU-COMP-INTER-003-007.

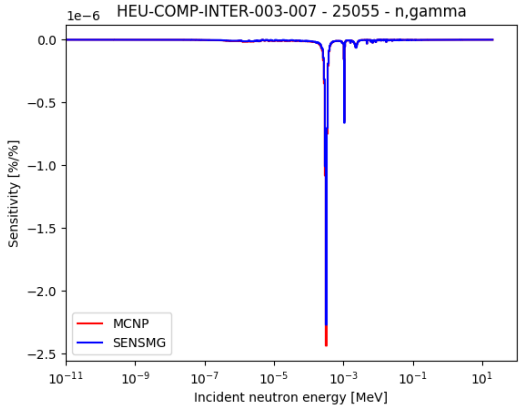

Figure 5.208: Sensitivity profiles for Mn55 in HEU-COMP-INTER-003-007.

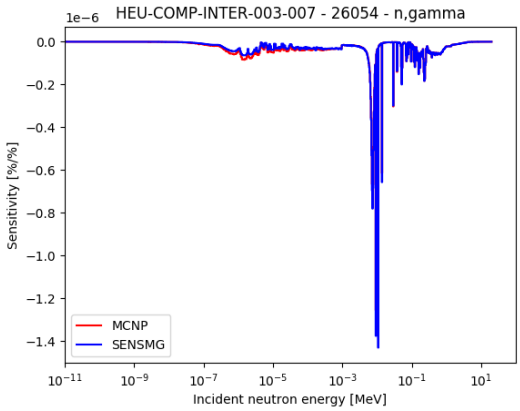

Figure 5.209: Sensitivity profiles for Fe54 in HEU-COMP-INTER-003-007.

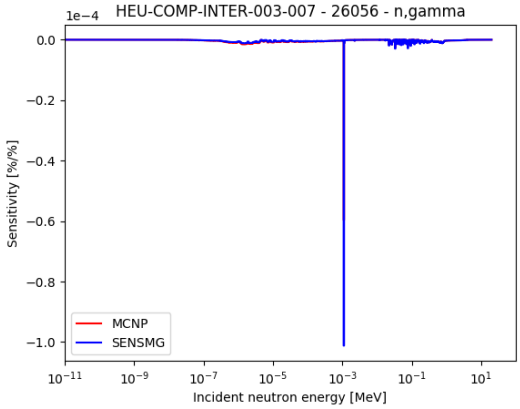

Figure 5.210: Sensitivity profiles for Fe55 in HEU-COMP-INTER-003-007.

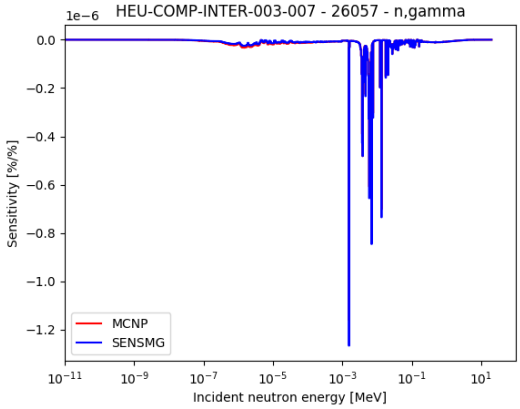

Figure 5.211: Sensitivity profiles for Fe57 in HEU-COMP-INTER-003-007.

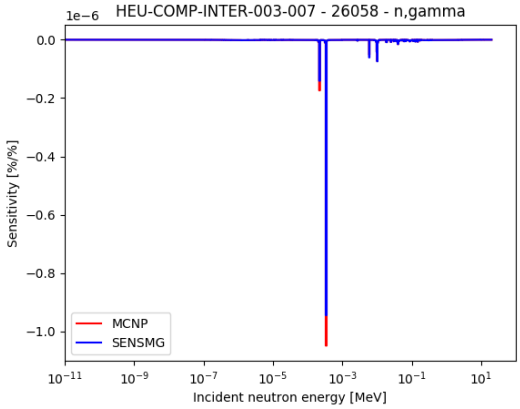

Figure 5.212: Sensitivity profiles for Fe58 in HEU-COMP-INTER-003-007.

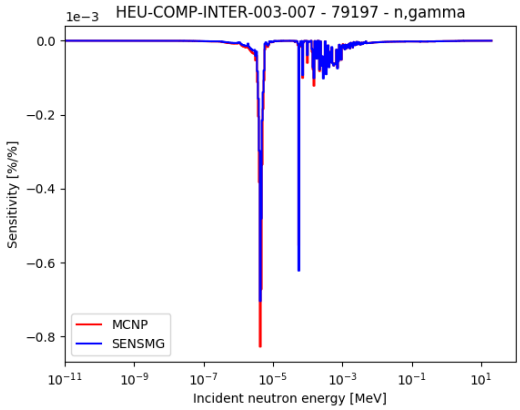

Figure 5.213: Sensitivity profiles for Au197 in HEU-COMP-INTER-003-007.

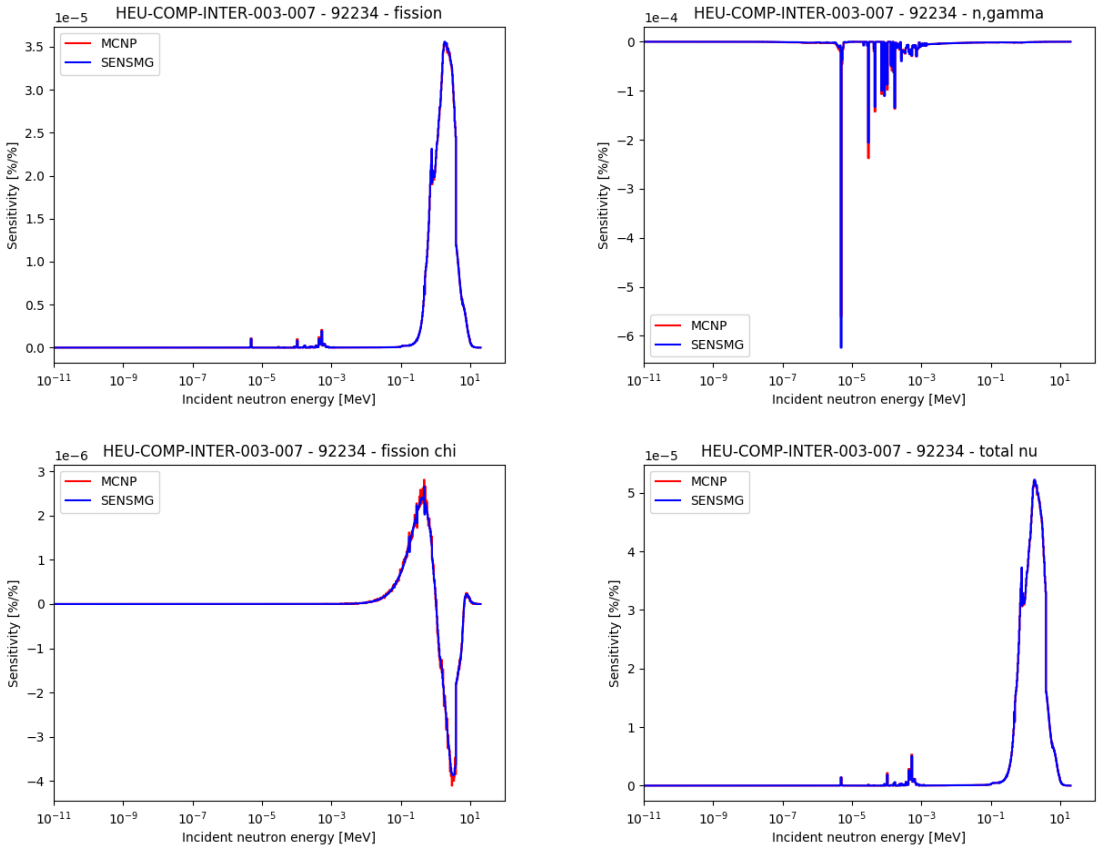

Figure 5.214: Sensitivity profiles for U234 in HEU-COMP-INTER-003-007.

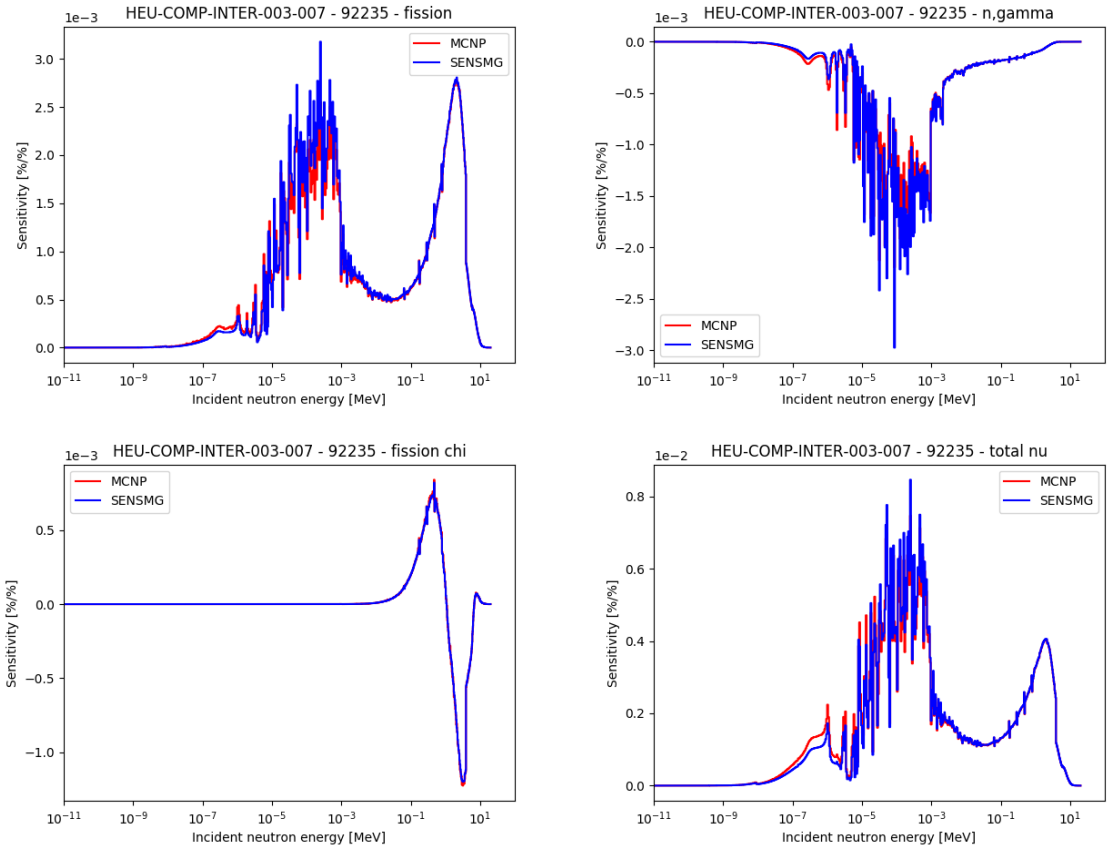

Figure 5.215: Sensitivity profiles for U235 in HEU-COMP-INTER-003-007.

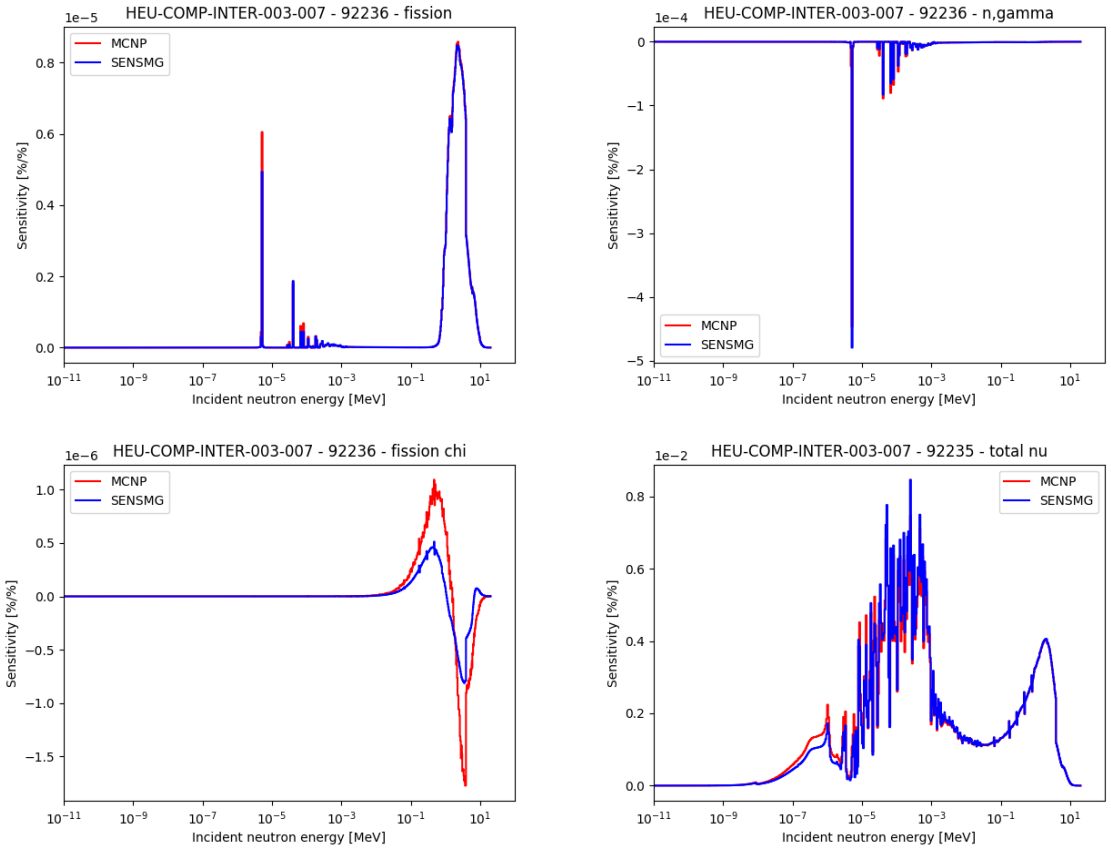

Figure 5.216: Sensitivity profiles for U236 in HEU-COMP-INTER-003-007.

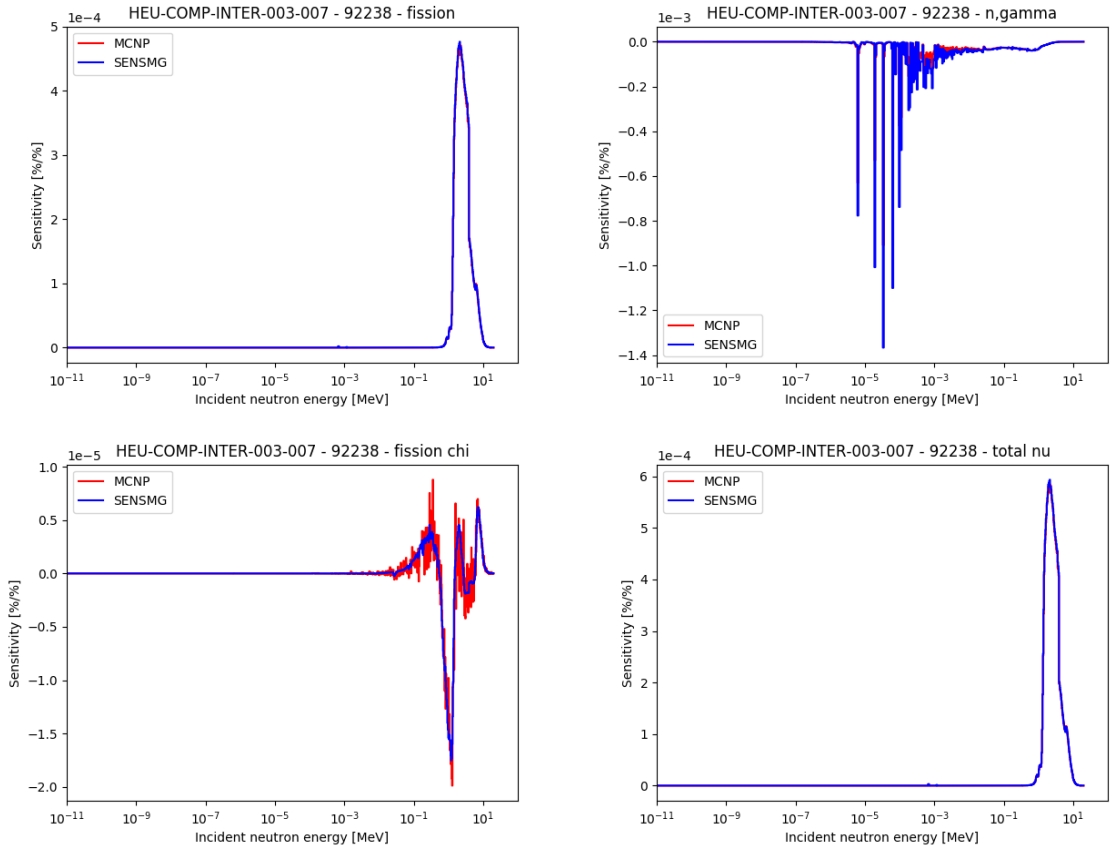

Figure 5.217: Sensitivity profiles for U238 in HEU-COMP-INTER-003-007.

Chapter 6

Conclusions

In this report, results for the effective multiplication factor and sensitivity profiles calculated with MCNP, PARTISN and SENSMG have been reported for four fast spectrum spherical benchmarks (HEU-MET-FAST-001, HEU-MET-FAST-032, HEU-MET-FAST-041 and HEU-MET-FAST-085) and one intermediate spectrum cylindrical benchmark (HEU-COMP-INTER-003) for a total of 24 cases.

For the effective multiplication factors, the MCNP results compare well with the experimental values. All calculations are within 3 sigma of the experimental values, as expected. The PARTISN calculated effective multiplication factors using standard (not self-shielded) cross sections are very close to the ones calculated with MCNP with the exception of some of the heavy reflector cases in the spherical benchmark (Cu, Fe and Ni-Cu-Zn) and the cylindrical benchmarks (excluding one case with an iron inner reflector). These discrepancies can be solved by applying Bondarenko self-shielded cross sections instead. In this last case, all PARTISN calculated effective multiplication factors are also within 3 sigma of the experimental values while following closely the calculated MCNP results.

Sensitivity profiles calculated by MCNP and SENSMG (using PARTISN) have also been reported in this report. The sensitivity profiles obtained through SENSMG correspond very well with the ones obtained with MCNP, with the exception of the U236 fission spectra sensitivity profiles. Some profiles like the neutron capture profiles exhibit some differences (small to large differences depending on the case) in the lower energy part of the profiles, most likely due to the difference in self-shielding between MCNP and SENSMG (which uses the standard not self-shielded cross sections for PARTISN).

References

[1] D. B. Pelowitz, A. J. Fallgren, G. E. McMath, "MCNP6 User's Manual - Code Version 6.1.1beta", LA-CP-14-00745 Rev. 0, Los Alamos National Laboratory, USA (2014)

[2] R. E. Alcouffe, R. S. Baker, J. A. Dahl, S. A. Turner, R. C. Ward, "PARTISN: A Time-Dependent, Parallel Neutral Particle Transport Code System", LA-UR-08-07258 Rev. November 2008, Los Alamos National Laboratory, USA (2008)

[3] I. I. Bondarenko, "Group Constants for Nuclear Reactor Calculations", Consultants Bureau, New York (1964)

[4] T. G. Saller, R. S. Baker, J. A. Dahl, "On-The-Fly Multigroup Weighting in PARTISN", M&C 2017 Conference, Korea, April 16-20, 2017

[5] J. A. Favorite, "SENSMG: First-Order Sensitivities of Neutron Reaction Rates, Reaction-Rate Ratios, Leakage, keff and α Using PARTISN", XCP-3:17-009 - LA-UR-16-28943 Rev. 3, Los Alamos National Laboratory, USA (2017)